The regulation of gp130 surface expression on monocytes – implications in chronic inflammation

Von der Fakultät für Mathematik, Informatik und Naturwissenschaften der RWTH Aachen University zur Erlangung des akademischen Grades einer Doktorin der Naturwissenschaften genehmigte Dissertation

vorgelegt von

Diplom-Biologin

Nora Honke

aus Wuppertal

Berichter: Privatdozent Dr. med. Klaus Tenbrock
Universitätsprofessor Dr. rer. nat. Rainer Fischer

Tag der mündlichen Prüfung: 15.11.2013

Table of contents

Summary

The glycoprotein 130 (gp130) is the signal transducing element common to all interleukin (IL)-6 type cytokines. Signals mediated by gp130 are involved in several biological processes such as hematopoiesis, cell differentiation and immune reactions. To initiate downstream signaling, a complex of gp130 and the ligand-specific α-receptor chain needs to be formed. Pathways activated by gp130-mediated signaling include the Janus kinase/signal transducer and activator of transcription (JAK/STAT) and the Src homology 2-domain containing tyrosine phosphatase/extracellular signal-regulated kinase (SHP2/ERK) cascade.

While gp130 is found on most cells, expression of ligand-binding receptor chains is restricted to particular cell types. It has therefore long been assumed that the expression pattern of α-receptors determines the sensitivity of cells to IL-6 type cytokines. However, depending on the regulatory state of a cell, expression of gp130 may vary and thus alter responsiveness. The importance of strictly regulated gp130 surface expression is further underlined by the fact that the soluble α-receptor of IL-6, sIL-6R, can replace the membrane-bound receptor and induce signaling in cells expressing only gp130.

In hepatocytes, a rapid downregulation of gp130 surface expression by pro-inflammatory cytokines has been described. This downregulation was mediated by the stress-induced mitogen-activated protein kinase (MAPK) p38, phosphorylation of serine 782 within the cytoplasmic tail of gp130 and its subsequent internalization and degradation. The reduced availability of the receptor on the cell surface restricted IL-6-induced STAT3 activation. Since IL-6 plays an important role in several immune reactions, we asked whether this regulatory mechanism might be of relevance in human monocytes. Different approaches confirmed that gp130 was internalized in response to the pro-inflammatory stimulus IL-1β. Internalization of gp130 was dependent on p38 and stimulation of monocytes with IL-1β led to an increased phosphorylation of serine 782. Furthermore, downstream signaling of IL-6 was affected by IL-1β, which again depended on p38.

To study these regulatory effects *in vivo*, two transgenic mouse lines were generated. Overexpression of gp130-wildtype (wt) or gp130-mutant (mut) was restricted to hematopoietic cells. In gp130-mut mice serine residues in the cytoplasmic domain were mutated to alanine to create non-phosphorylatable residues, which was assumed to prevent internalization and stabilize gp130 surface expression in response to stress stimuli. Two preliminary findings might support our expectations: 1) IL-1β had a stronger inhibitory effect on gp130 surface expression on cluster of differentiation (CD)11b^{+} splenocytes from gp130-wt mice compared to gp130-mut animals. 2) In a model of leukocyte infiltration into the peritoneal cavity more cells were recruited in gp130-mut than in gp130-wt mice. Given the

known role of IL-6 in migration, this supports the assumption that the altered stability of gp130 surface expression influences cell behavior.

A particular role in chronic inflammation is attributed to IL-6. Raised serum levels of IL-6 and sIL-6R have been associated with different chronic inflammatory disorders such as inflammatory bowel disease (IBD) or juvenile idiopathic arthritis (JIA). In this study gp130 surface expression on peripheral monocytes from pediatric IBD patients was shown to be increased compared to healthy controls. This was reflected in the level of downstream signaling. Specifically, monocytes from IBD patients displayed enhanced STAT3 phosphorylation. The clinical and pathophysiologic significance of this differential regulation remained unclear. However, these findings were reproduced in a murine model of chronic colitis, thus presenting a platform for future analyses.
Reduced gp130 surface expression was found on synovial fluid (SF) monocytes compared to peripheral blood (PB) monocytes in JIA patients. By incubating healthy peripheral blood mononuclear cells (PBMCs) with SF biochemical abnormalities of SF monocytes were partially reproduced. This included gp130 downregulation, which depended on p38.

In summary, in the framework of this thesis it was shown that gp130 surface expression on human monocytes is regulated by the pro-inflammatory cytokine IL-1β, which impairs IL-6-mediated downstream signaling. This mechanism might be of relevance in inflammatory conditions exemplified by inflamed joints of JIA patients. The herein generated transgenic mice may be of value for future investigations of the role of crosstalk regulation in chronic inflammatory situations.

Zusammenfassung

Das Glycoprotein 130 (gp130) ist das gemeinsame Signalübertragungselement aller Interleukin (IL)-6 Typ Zytokine. Gp130-vermittelte Signale spielen eine wichtige Rolle in unterschiedlichen biologischen Prozessen wie beispielsweise der Hämatopoese, in Zelldifferenzierungen und Immunreaktionen. Um Signale in die Zelle weiterzuleiten, muss zunächst ein Komplex aus gp130 und der Liganden-spezifischen α-Rezeptorkette gebildet werden. Signalwege, die durch gp130 induziert werden, umfassen die „Janus kinase/signal transducer and activator of transcription“ (JAK/STAT) und die „Src homology 2-domain containing tyrosine phosphatase/extracellular-regulated kinase“ (SHP2/ERK) Kaskade. Während gp130 auf den meisten Zellen gefunden wird, ist die Expression der Liganden-bindenden Rezeptorketten auf einige Zelltypen beschränkt. Aus diesem Grund wurde lange Zeit angenommen, dass das Expressionsmuster der α-Rezeptoren die Sensitivität von Zellen für IL-6 Typ Zytokine bestimmt. Die Expression von gp130 kann jedoch abhängig vom regulatorischen Status einer Zelle variieren. Die Bedeutung einer streng regulierten gp130 Oberflächenexpression wird außerdem dadurch verstärkt, dass der lösliche IL-6 α-Rezeptor, sIL-6R, den membrangebundenen Rezeptor ersetzen und so Signale in Zellen auslösen kann, die nur gp130 exprimieren.

In Leberzellen wurde eine schnelle Herunterregulation der gp130 Oberflächenexpression durch pro-inflammatorische Zytokine beschrieben. Diese Herunterregulation war durch die stress-induzierte Kinase p38, die Phosphorylierung von Serin 782 in der zytoplasmatischen Domäne von gp130 und eine nachfolgende Internalisierung und den Abbau des Rezeptors vermittelt. Die reduzierte Verfügbarkeit des Rezeptors an der Zelloberfläche beeinträchtigte die IL-6 induzierte STAT3 Aktivierung. Da IL-6 eine wichtige Rolle in verschiedenen Immunreaktionen spielt, sollte in dieser Arbeit ermittelt werden, ob der in Leberzellen gezeigte regulatorische Mechanismus in humanen Monozyten von Bedeutung sein könnte. Mit Hilfe unterschiedlicher experimenteller Ansätze konnte bestätigt werden, dass gp130 nach der Stimulation mit pro-inflammatorischem IL-1β internalisiert wurde. Diese Internalisierung war abhängig von p38 und die Stimulation von Monozyten mit IL-1β führte zu einer verstärkten Phosphorylierung von Serin 782. Weiterhin war die IL-6 induzierte Signalübertragung durch IL-1β beeinträchtigt, was wiederum auf der Wirkung von p38 beruhte.

Um diese regulatorischen Mechanismen *in vivo* untersuchen zu können, wurden im Rahmen der Arbeit zwei transgene Mauslinien generiert. Die Überexpression von gp130-Wildtyp (Wt) oder einer gp130-Mutante (Mut) war unter Kontrolle des VAV-Promoters auf hämatopoetische Zellen beschränkt. In gp130-Mut Tieren wurden Serinreste in der

zytoplasmatischen Domäne zu Alaninen mutiert, so dass diese nicht mehr phosphoryliert werden können. Es wurde angenommen, dass dies die Internalisierung als Reaktion auf Stress vermindern und damit die gp130 Oberflächenexpression erhöhen sollte. Zwei erste Beobachtungen haben die Erwartungen teilweise bestätigt: 1) IL-1β hatte einen stärkeren inhibitorischen Effekt auf die gp130 Oberflächenexpression auf cluster of differentiation (CD)11b^{+} Splenozyten von gp130-Wt Mäusen im Vergleich zu gp130-Mut Tieren. 2) In einem Modell zur Untersuchung von Leukozyteninfiltration in die Bauchhöhle wurden mehr Zellen in gp130-Mut als in gp130-Wt Mäusen rekrutiert. Aufgrund der bekannten Rolle, die IL-6 bei Migrationsprozessen spielt, können diese Ergebnisse die Annahme bestätigen, dass eine veränderte Stabilität der gp130 Oberflächenexpression das migratorische und inflammatorische Verhalten der Zellen beeinflusst.

IL-6 wird eine besondere Rolle in chronischen Entzündungssituationen zugeschrieben. Erhöhte Serum Level von IL-6 und seines löslichen Rezeptors werden mit verschiedenen inflammatorischen Krankheiten assoziiert. Darunter fallen chronisch entzündliche Darmerkrankungen (CED) oder die juvenile idiopathische Arthritis (JIA). In dieser Arbeit wurde gezeigt, dass im Vergleich zu gesunden Kontrollen die gp130 Oberflächenexpression auf peripheren Monozyten von Kindern mit CED erhöht war. Dies spiegelte sich auch in der Signaltransduktion wider. Hier wiesen Monozyten von CED Patienten eine verstärkte STAT3 Phosphorylierung auf. Die klinische und pathophysiologische Bedeutung dieser differentiellen Regulation wurde noch nicht aufgeklärt. Allerdings konnten die Ergebnisse der CED Patienten in einem Mausmodell mit chronischer Kolitis reproduziert werden, was eine Basis für weitere Untersuchungen darstellt.
Bei JIA Patienten wurde eine verringerte gp130 Oberflächenexpression auf Monozyten aus Synovialflüssigkeit (SF) im Vergleich zu Monozyten aus Peripherblut (PB) gefunden. Indem mononukleäre Zellen aus PB von gesunden Probanden mit SF stimuliert wurden, konnten Teile der biochemischen Veränderungen von SF Monozyten reproduziert werden. Dies schloss die Herunterregulation von gp130 ein, welche abhängig von p38 war.

Zusammenfassend wurde im Rahmen dieser Arbeit gezeigt, dass die gp130 Oberflächenexpression auf humanen Monozyten durch das pro-inflammatorische Zytokin IL-1β reguliert wird, was als Konsequenz die IL-6 abhängige Signaltransduktion beeinträchtigt. Wie am Beispiel von entzündeten Gelenken von JIA Patienten dargestellt, könnte dies für chronisch inflammatorische Erkrankungen von Bedeutung sein. Die generierten transgenen Mäuse können in Zukunft dazu beitragen, die Rolle dieser Regulationsmechanismen in entzündlichen Situationen weiter zu untersuchen.

Abbreviations

°C	Degree Celsius
µ-	Micro-
AIA	Antigen-induced arthritis
APC	Allophycocyanin
APP	Acute phase protein
BSA	Bovine serum albumin
CD	Cluster of differentiation
CD	Crohn's disease
cDNA	Complementary DNA
CIA	Collagen-induced arthritis
CLC	Cardiotrophin-like cytokine
CNTF	Ciliary neurotrophic factor
ct	Cycle threshold
CT-1	Cardiotrophin-1
Da	Dalton
DC	Dendritic cell
dd H_2O	Double distilled H_2O
DMSO	Dimethylsulfoxide
DNA	Desoxyribonucleic acid
DSS	Dextrane sodium sulfate
DTT	Dithiotreitol
ECL	Enhanced chemiluminescence
E. coli	*Escherichia coli*
EDTA	Ethylene diamine tetraacetic acid
e.g.	For example
ERK	Extracellular signal-regulated kinase
EtOH	Ethanol
FACS	Fluorescence activated cell sorting

FCS	Fetal calf serum
FITC	Fluorescein
g	Gram
g	Gravitational acceleration (9.81 m/s^2)
GFP	Green fluorescent protein
gp80	Glycoprotein 80
gp130	Glycoprotein 130
h	Hour(s)
HRP	Horseradish peroxidase
HS	Human serum
IBD	Inflammatory bowel disease
IL	Interleukin
IL-1Ra	Interleukin-1 receptor antagonist
IL-6R	Interleukin-6 receptor
i.p.	Intraperitoneal
IP	Immunoprecipitation
IgG	Immunglobulin G
IL	Interleukin
JAK	Janus kinase
JIA	Juvenile idiopathic arthritis
kDa	Kilo Dalton
l	Liter
LIF	Leukemia inhibitory factor
LP	Lamina propria
LPS	Lipopolysaccharide
m	Milli-
M	Molar
MAPK	Mitogen-activated protein kinase
M-CSF	Macrophage colony-stimulating factor

M-CSFR	Macrophage colony-stimulating factor receptor
MEF	Murine embryonal fibroblast
MFI	Meanfluorescence intensity
min	Minute(s)
MK2	Mitogen-activated protein kinase-activated kinase 2
mRNA	Messenger RNA
NF- κB	Nuclear factor-κB
NP	Neuropoeitin
ns	not significant
ON	Overnight
OSM	Oncostatin M
PB	Pacific blue
PB	Peripheral blood
PBMCs	Peripheral blood mononuclear cells
PBS	Phosphate buffered saline
PCR	Polymerase chain reaction
PE	Phycoerythrin
Pen/Strep	Penicillin/Streptomycin
PFA	Paraformaldehyde
PI3K	Phosphatidyl-inositol-3-kinase
PIAS	Protein inhibitors of activated STAT
p-STAT	Phosphorylated STAT
PVDF	Polyvinyliden fluorid
R	Receptor
RA	Rheumatoid arthritis
RANKL	Receptor activator of nuclear factor-κB ligand
RNA	Ribonucleic acid
RPL13A	Ribosomal protein L13A
RPMI	Roswell Park Memorial Institute
RT	Room temperature
RT-PCR	Real time polymerase chain reaction

SCID	Severe combined immunodeficiency
SDS	Sodium dodecylsulfate
SDS-PAGE	SDS-polyacrylamid gelelectrophoresis
sec	Second(s)
SF	Synovial fluid
SFMCs	Synovial fluid mononuclear cells
sgp130	Soluble gp130
sIL-6R	Soluble IL-6R
SH2	Src homology 2
SHP2	SH2-domain containing protein tyrosine phosphatase 2
STAT	Signal transducer and activator of transcription
TBE	Tris-buffered saline electrophoresis buffer
TBS-T	Tris-buffered saline containing 0.05% (v/v) tween-20
TEMED	N,N,N',N'-tetramethylen-ethylendiamin
TG	Transgenic
TGF	Transforming growth factor
Th	T helper
TNFα	Tumor necrosis factor-α
Treg	Regulatory T cell
Tyr	Tyrosine
UC	Ulcerative colitis
v/v	Volume per volume
WB	Western blot
WT	Wild type
w/v	Weight per volume

1 INTRODUCTION

1.1 The signal transducer gp130

The glycoprotein 130 (gp130, CD130) is the signal transducing element common to all interleukin (IL)-6 type cytokines. It mediates several different, in part redundant, biological activities. Gp130 plays an essential role in developmental processes, which is critically demonstrated by the lethality observed in gp130 knockout mice. These animals display hypoplasia of the ventricular myocardium and severe defects in hematopoiesis, resulting in perinatal death (Yoshida et al., 1996). Postnatal deletion of gp130 in hematopoietic stem cells, endothelial and liver cells by conditional knockout leads to several disorders affecting the heart, brain, liver and lung. Furthermore, abnormalities in hematopoiesis and immune response to pathogens have been observed (Betz et al., 1998).

Apart from IL-6 itself, the IL-6 cytokine family comprises IL-11, IL-27, IL-31, oncostatin M (OSM), leukemia inhibitory factor (LIF), cardiotrophin-1 (CT-1), ciliary neurotrophic factor (CNTF), cardiotrophin-like cytokine (CLC) and neuropoeitin (NP) (Diveu et al., 2004). To exert their effects on target cells the cytokines use different complexes of α- and β-receptors. While IL-6 and IL-11 signal via a homodimer of the β-receptor gp130 combined with their respective non-signaling α-receptor subunits, all other members use heterodimers of gp130 and one of the other β-receptors LIF receptor (LIFR), OSM receptor (OSMR) or IL-27 receptor (IL-27R/WSX-1). An exception is the cytokine IL-31, which binds to a heterodimer of OSMR and the gp130-like protein IL-31 receptor A (Garbers et al., 2012).

Activation of gp130 triggers three different signaling cascades, most prominently the Janus kinase/signal transducer and activator of transcription (JAK/STAT) pathway. JAKs are constitutively associated with the cytoplasmic tail of gp130 and become activated upon ligand-induced complex building (Stahl et al., 1994). This leads to phosphorylation of specific receptor tyrosine residues, which serve as docking sites for Src homology 2-domain containing tyrosine phosphatase (SHP2) and STAT proteins, respectively. Once recruited, STATs are phosphorylated on a single tyrosine, build dimers and translocate to the nucleus, where they bind to their target gene promoters. Within the STAT family, comprising seven members, signaling through gp130 typically activates STAT3, to a minor extent STAT1 and in some cases STAT5 (Heinrich et al., 2003). Both of the other gp130-mediated signaling pathways start with recruitment of the adapter protein SHP2 to the receptor. Like STAT proteins, SHP2 is phosphorylated after binding to gp130. It interacts with several other proteins, resulting in the activation of the extracellular signal-regulated kinase (ERK) 1/2 and

phosphatidyl-inositol-3-kinase (PI3K) (Eulenfeld et al., 2012). Figure 1-1 illustrates the different cascades initiated by IL-6-mediated gp130 activation.

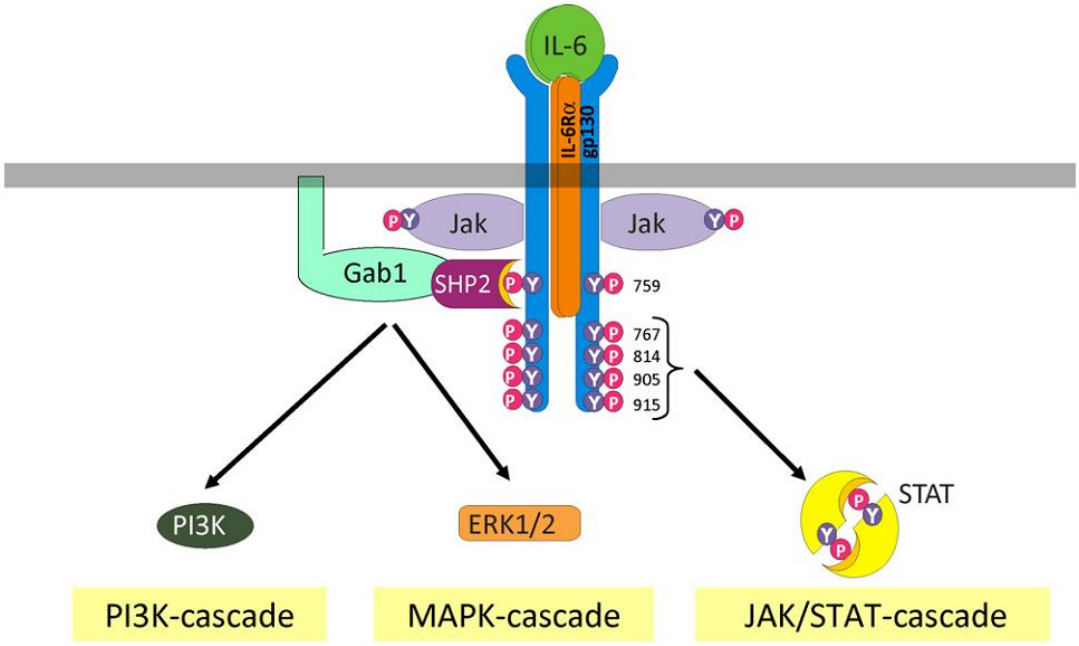

Figure 1-1: Signaling pathways activated by IL-6
Binding of IL-6 to IL-6Rα triggers the association of a hexameric signaling complex, composed of two IL-6Rα subunits and a gp130 homodimer. Constitutively associated JAKs are activated upon complex building and phosphorylate specific tyrosine residues within the cytoplasmic domain of gp130, which serve as docking sites for SHP2 and STAT. Binding to the receptor results in phosphorylation and activation of STAT and SHP2, subsequently leading to the initiation of dimerization and translocation to the nucleus and of the PI3K- and mitogen-activated protein kinase (MAPK)-cascade, respectively. [From (Eulenfeld et al., 2012)]

Endocytosis of the complex formed by ligand binding of IL-6 to its receptor has been observed in various cell lines, and is dependent on di-leucine motifs within the cytoplasmic tail of gp130 (Dittrich et al., 1994). It became clear that no signal is necessary for the internalization of gp130, but that instead it is internalized in a constitutive manner (Thiel et al., 1998b).

While the expression of cytokine-specific receptor chains is restricted to particular cell types, chiefly hepatocytes, monocytes/macrophages, neutrophils and some lymphocyte subsets, gp130 is ubiquitously expressed. Since none of the IL-6-type cytokines can signal through gp130 alone, it has long been widely assumed that the expression of cytokine-specific receptors determines the responsiveness of target cells. In 1992, a soluble form of the IL-6Rα (sIL-6R) was detected in human plasma of healthy individuals (Honda et al., 1992).

This soluble receptor binds to IL-6 with similar affinity as the membrane-bound IL-6R and the complex formed this way is able to associate with gp130 and to stimulate target cells. Thus, binding of IL-6 to sIL-6R renders cells that express gp130 but not IL-6R responsive, a process called trans-signaling (Rose-John and Heinrich, 1994) (figure 1-2 B). Soluble IL-6R can be derived either by alternative splicing or by enzymatic shedding from cell membranes. Although recombinant soluble receptors of other IL-6-type cytokines have been studied *in vitro*, IL-6 is the only cytokine of the family that uses classical and trans-signaling *in vivo* (Garbers et al., 2012).

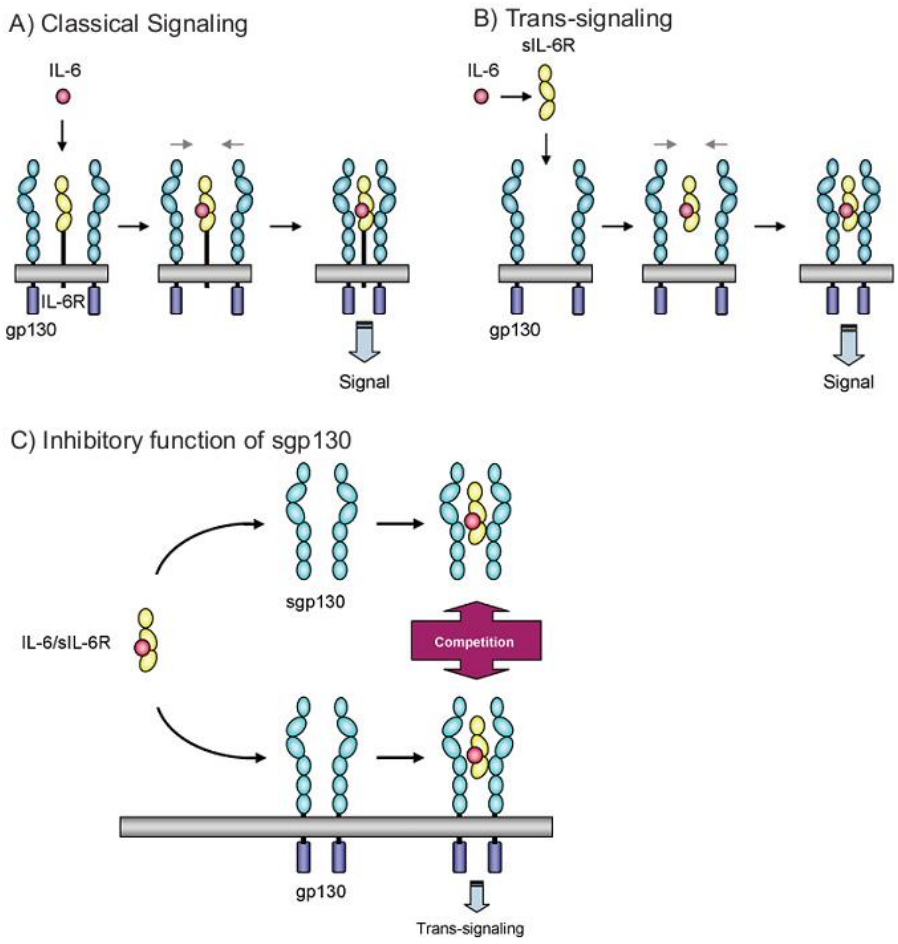

Figure 1-2: Classical IL-6 signaling vs. trans-signaling and the antagonistic function of sgp130
A) Classical signaling is initiated by the binding of IL-6 to its membrane-bound IL-6R, which leads to the recruitment of two gp130 molecules and to signal transduction. B) Trans-signaling begins with the binding of IL-6 to its soluble receptor sIL-6R. The complex formed interacts with gp130 on target cells, which again initiates homodimerization of gp130 and signaling. C) Soluble gp130 (sgp130) competes with the membrane-bound receptor for IL-6/sIL-6R complexes. Due to absence of an IL-6 binding site within gp130, the interaction is possible only with IL-6 bound to its α-receptor. The antagonistic effect of sgp130 is restricted to trans-signaling, since its connection with membrane-bound IL-6/IL-6R is inhibited by steric hindrance. [Modified from (Mitsuyama et al., 2006)]

In contrast to sIL-6R, sgp130, derived by differentially spliced mRNA, has an antagonistic effect. Interestingly, sgp130 turned out to inhibit only IL-6 trans-signaling but not classical signaling, i.e. responses via membrane-bound IL-6R (Jostock et al., 2001). This is explained by the fact that IL-6 does not bind directly to gp130 but that instead the two forms of gp130 compete for IL-6/sIL-6R complexes (figure 1-2 C). It was therefore proposed that sgp130 acts as a natural inhibitor of IL-6 trans-signaling.

1.2 Regulation of IL-6 signaling

Since dysregulation of gp130-mediated signaling leads to severe autoimmune diseases such as inflammatory bowel disease (IBD) or rheumatoid arthritis (RA), a tight control of cytokine action is indispensable. Different mechanisms of regulation, especially of the JAK/STAT pathway, have been identified, which can be divided into classical regulatory mechanisms and control by cytokine crosstalk. All of the mechanisms mentioned in this chapter are summarized in figure 1-3.

1.2.1 Classical regulators

An important role as inhibitors of gp130-mediated signaling has been attributed to the 8-member family of suppressors of cytokine signaling (SOCS): cytokine-inducible SH2 protein (CIS) and SOCS1-7. Acting as classical feedback inhibitors, SOCS proteins are synthesized in response to the JAK/STAT cascade and potently inhibit STAT-mediated as well as SHP2-mediated signal transduction (Wormald and Hilton, 2004). The mechanisms by which SOCS proteins inhibit cytokine signaling vary among family members. While SOCS1 has been found to bind to proteins of the JAK family, thereby inhibiting their catalytic function, SOCS3 interacts directly with gp130 and impedes JAK activity as well. This inhibitory effect seems to be based on a combination of kinase inhibition by kinase inhibitory region and targeting of the interacting protein to proteasomal degradation (Sasaki et al., 2000; Zhang et al., 1999). SOCS3 is the suppressor crucial for the regulation of IL-6-induced STAT3 activation and shares its interaction site tyrosine 759 (tyrosine 757 in mice) of gp130 with SHP2 (figure 1-1). Mice with a mutated tyrosine 757 show abolished SHP2- and SOCS3-binding resulting in impaired MAPK-signaling and enhanced activation of STAT, which is not sensitive to SOCS3 regulation anymore. Phenotypically the shift in equated STAT- and MAPK-signaling is manifested by gastric adenomas and splenomegaly (Tebbutt et al., 2002). Thus, tyrosine 757/9 determines the balance between STAT- and MAPK-pathways with important (patho-) physiological impact.

Apart from its function as an adaptor protein contributing to the activation of the MAPK- and

PI3K-cascades, an inhibitory function on IL-6 signaling has been described for SHP2. It has been shown that overexpression of dominant negative SHP2 mutants leads to enhanced phosphorylation of gp130, JAK, STAT and SHP2 (Lehmann et al., 2003). As a tyrosine phosphatase, SHP2 may dephosphorylate different elements of the gp130-JAK signaling axis. Other protein tyrosine phosphatases (PTPs) have been reported to be involved in the regulation of JAK/STAT signaling (Tanuma et al., 2001), but the physiological relevance and impact of PTPs on IL-6-induced signaling *in vivo* remains to be elucidated.
Protein inhibitors of activated STAT (PIAS) are constitutively expressed and interfere with STAT-mediated gene transcription by different molecular mechanisms. The first member PIAS1 was found to specifically inhibit STAT1, while the later identified PIAS3 exclusively interacts with STAT3 (Chung et al., 1997) (figure 1-3). Both of them bind to the dimeric but not the monomeric form of STATs and block their DNA binding activity.

1.2.2 Crosstalk regulation

In physiological conditions, where the impact of many different cytokines needs to be orchestrated in a way that generates an appropriate biological response, cytokine crosstalk is of particular importance.
The two major pro-inflammatory cytokines IL-1β and tumor necrosis factor (TNF)-α are secreted by blood monocytes and macrophages upon activation and are found at most sites of inflammation. They induce the release of several other cytokines and chemokines like IL-6 and IL-8 from tissue cells, monocytes or macrophages. Different crosstalk mechanisms between IL-6 and the pro-inflammatory mediators IL-1β and TNF-α have been described, including synergistic as well as antagonistic interactions.

Due to its crucial role in the acute phase response, crosstalk regulation of IL-6 signaling has been studied extensively in hepatocytes. The first hints of an inhibitory effect of IL-1β on IL-6-dependent acute phase protein (APP) production were discovered in the late 1980s (Andus et al., 1988). While these suppressive actions concern class II APPs, an enhanced expression of class I APPs has been described in response to IL-1β and IL-6. Mechanistically, both effects seem to involve nuclear factor (NF)-κB induced by IL-1β. A physical interaction between phosphorylated (p-)STAT3 and NF-κB can either function as transcriptional enhancer or repressor depending on the gene (Bode et al., 2012; Yoshida et al., 2004) (see figure 1-3).

In addition to these effects on late phase STAT3 activation an immediate inhibition on IL-6-induced STAT3 phosphorylation not only by IL-1β but also by other pro-inflammatory

stimuli, such as TNF-α and LPS, has been reported by different groups.

In primary and cell culture macrophages TNF-α and LPS have been shown to induce SOCS3 expression and thereby inhibit IL-6-triggered STAT3 phosphorylation. The stress-dependent MAPK p38 was hypothesized to be involved especially in the suppression mediated by TNF-α (Bode et al., 1999). Ehlting *et al.* have reported that TNF-α enhances SOCS3 expression by mRNA stabilization (Ehlting et al., 2007). This stabilization and the basal SOCS3 expression are impaired in fibroblasts and macrophages deficient for the p38 downstream target MAPK-activated kinase 2 (MK2). An IL-1β-dependent stabilization of *SOCS3* mRNA has been shown as well (Yang et al., 2004) (figure 1-3).

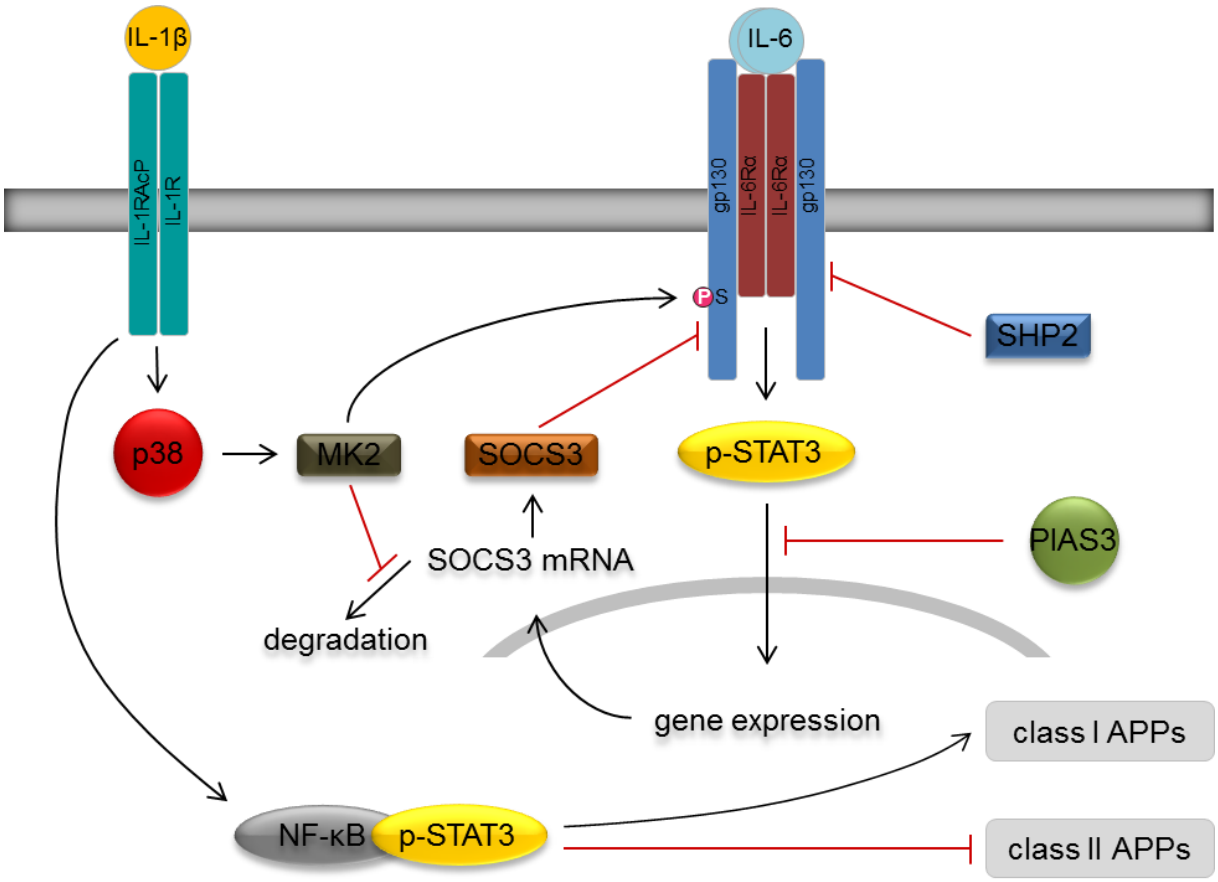

Figure 1-3: Regulation of IL-6 signaling

After initiation of the JAK/STAT cascade, p-STAT3 induces the feedback inhibitor SOCS3, which interferes with JAK activity. Other classical inhibitors are represented by the constitutively expressed PIAS and the protein phosphatase SHP2. Binding of IL-1β to its receptor complex leads to the activation of NF-κB, which can associate with p-STAT3 and enhance or repress the activation of class I and class II APPs, respectively. The MAPK p38, activated in response to IL-1β, phosphorylates MK2 and thereby affects IL-6 signaling by two mechanisms: 1) it stabilizes *SOCS3* mRNA by inhibiting its degradation and 2) it phosphorylates serine 782 in gp130, followed by internalization and degradation of the receptor. [Adapted from (Garbers et al., 2012)]

P38 turned out to be a key molecule in the crosstalk inhibition of IL-6 signaling, accounting for further observed effects, such as TNF-α-induced SHP2 recruitment to gp130 (Bode et al., 2003). Another influence of p38 on IL-6 signaling in response to pro-inflammatory cytokines and stress stimuli was shown by Radtke *et al.* in hepatocytes. Here, p38-dependent activation of MK2 leads to phosphorylation of gp130 on serine 782, located upstream of the di-leucine internalization motif, followed by increased internalization and degradation of the receptor (figure 1-3). The authors conclude that serine 782 is a stress sensor responsible for limitation of gp130 signaling. The loss of cell surface-bound gp130 results in impaired IL-6-induced STAT3 phosphorylation (Radtke et al., 2010). In line with these observations it has previously been suggested that the rapid inhibition of IL-6 signaling by pro-inflammatory cytokines in macrophages depends on a target within the cytoplasmic region of gp130 (Ahmed and Ivashkiv, 2000). These authors and others have also described the crosstalk inhibition as being independent of *de novo* protein synthesis, and thus of SOCS3, but instead dependent on p38. A decrease of gp130 levels in primary mouse macrophages in response to LPS and TNF-α has been suggested as well (Kiu et al., 2007).

1.3 Functions of IL-6 signaling

The most prominent member using gp130 as the signaling subunit of its receptor complex is IL-6. IL-6 is a pleiotropic cytokine, which can be secreted by different lymphoid and non-lymphoid cells and is involved in a wide range of biologic activities on various target cells. These include hematopoietic functions, immune regulation, inflammation, antibody production and oncogenesis (Naka et al., 2002). Some aspects of the involvement of IL-6 in inflammation, cell differentiation and bone metabolism will be discussed in this chapter.

1.3.1 Inflammation

IL-6 is a cytokine with pro- and anti-inflammatory properties. Its protective role in a septic shock model or in liver injury is countered by its detrimental activity in chronic disease, which has been demonstrated by the resistance of IL-6 deficient mice to a number of experimental chronic inflammatory conditions (Barton and Jackson, 1993; Klein et al., 2005; Ohshima et al., 1998). Moreover, the therapeutic application of an anti-IL-6R antibody has proven beneficial in various inflammatory disorders (Choy, 2012; Ito et al., 2004).

Inflammatory reactions occur in response to infection or tissue injury and are part of the normal healing process. IL-6 is one of the first cytokines to be produced in the early stages of inflammation and it is the main inducer of the acute phase response, stimulating hepatocytes to produce a set of plasma proteins, the APPs. These proteins are important components of

the innate immune response and some of them are used frequently as diagnostic markers (Gabay and Kushner, 1999). The successful resolution of an inflammatory condition leads to restoration of normal tissue architecture and is dependent on the transition from innate to adaptive immunity. This progression is characterized by a precise regulation of leukocyte recruitment and clearance. IL-6 plays an important role in both of these processes. IL-6 trans-signaling in particular seems to contribute to the recruitment of leukocytes by inducing chemokine secretion from resident tissue cells (Hurst et al., 2001). In addition to these indirect effects on leukocyte migration, IL-6 has been shown to directly mediate migration of human T cells and monocytes (Clahsen and Schaper, 2008; Weissenbach et al., 2004). The clearance of neutrophils, which predominantly account for the initial infiltrate in acute inflammation, is critical for the resolution of inflammation. IL-6 may be involved in this process by provoking apoptosis of neutrophils (Afford et al., 1992). Conversely, IL-6-mediated STAT3 activation induces the expression of anti-apoptotic regulators *in vitro* and in some murine models of chronic disease (Atreya et al., 2000; Teague et al., 1997). Whereas in the former case IL-6 is beneficial for the transition from innate to adaptive immunity, the inability of T cells to enter apoptosis results in their retention within the affected tissue and in further promotion of inflammation. Other examples of anti-inflammatory actions of IL-6 are the induction of IL-1 and TNF antagonists. In patients receiving recombinant IL-6, plasma levels of IL-1 receptor antagonist (IL-1Ra) and the soluble TNF receptor p55 have been found to be increased. Moreover, monocyte-derived macrophages produce IL-1Ra upon stimulation with IL-6 (Tilg et al., 1994).

How IL-6 balances these pro- and anti-inflammatory effects remains to be clarified. It has been proposed that in acute inflammation the anti-inflammatory properties of IL-6 are dominant, whereas in chronic conditions its effects are more deleterious to the organism (Jones, 2005). An important factor influencing this balance seems to be sIL-6R. While classical signaling seems to occur predominantly on the periphery, trans-signaling is upregulated during chronic disease and found mostly at the site of inflammation (Scheller et al., 2011).

1.3.2 Cell differentiation

IL-6 is relevant for cell differentiation processes such as B cell differentiation or the lineage commitment of T cells. In particular the question of whether a naïve $CD4^+$ T cell differentiates into a T helper (Th)17 or a regulatory T cell (Treg) depends essentially on IL-6. Th17 cells are often associated with autoimmunity and tissue injury. However, Tregs suppress the proliferation of activated T cells and help to maintain self-tolerance. The cytokine

transforming growth factor (TGF)-β is needed for the development of both of the T cell subsets but the additional presence of IL-6 shifts the differentiation towards Th17 cells (Bettelli et al., 2006).
Another cell differentiation process influenced by IL-6 is the decision whether monocytes give rise to dendritic cells (DCs) or to macrophages. Upon having crossed the endothelial barrier, monocytes are activated and differentiate depending on local cytokines. *In vitro* studies have shown that after contact with monocytes, fibroblasts secret IL-6, which in turn up-regulates the expression of macrophage colony-stimulating factor (M-CSF) receptors on monocytes. This enables them to consume their autocrine M-CSF and to skew differentiation towards a macrophage phenotype (Chomarat et al., 2000).

1.3.3 Bone metabolism

Bone homeostasis is characterized by a strictly regulated balance of bone-forming osteoblasts and bone-resorbing osteoclasts (Kwan Tat et al., 2004). IL-6 has been shown to promote osteoclastogenesis by different mechanisms. In addition to a direct effect on osteoclast precursors (Kudo et al., 2003), IL-6 and other pro-inflammatory cytokines mediate the upregulation of receptor activator of nuclear factor-κB ligand (RANKL) (O'Brien et al., 1999). In association with M-CSF RANKL induces osteoclast formation from $CD14^+$ precursors (Nicholson et al., 2000; Quinn et al., 1998).

1.4 Gp130 in inflammation and autoimmunity

Regulation of inflammation is mainly controlled by cytokines and an imbalance between pro- and anti-inflammatory cytokines may lead to autoimmunity and chronic inflammation. Under these conditions the natural course of the inflammatory response is lost, which can lead to tissue damage and disease progression rather than resolution. The growing number of cytokine-targeting therapies reflects their importance during the development and perpetuation of chronic inflammatory diseases.

Among the cytokines signaling via gp130, IL-6 plays a unique role in inflammation and autoimmunity. The resistance of IL-6 knockout mice to several inflammatory conditions has not been found for other IL-6-type cytokines. IL-27, for instance, has been reported to suppress collagen-induced arthritis (CIA) and mice deficient in IL-11Rα and OSM-Rβ have shown a susceptibility towards antigen-induced arthritis (AIA) similar to that found in wildtype mice (Niedbala et al., 2008; Wong et al., 2006b). Furthermore, recombinant IL-11 has a protective effect in animal models of colitis, as well as in patients with IBD (Mitsuyama et al.,

2006). Increased levels of IL-6 and sIL-6R in patients suffering from chronic inflammatory disorders have been reported in several studies, further underlining the crucial role played by gp130-mediated IL-6 signaling (Jones et al., 2001).

1.4.1 Inflammatory bowel disease

Crohn's disease (CD) and ulcerative colitis (UC) are the two major types of inflammatory bowel diseases and are characterized by chronic recurrent inflammation of the gastrointestinal tract. IBD pathogenesis is complex, involving genetic factors, innate and adaptive immune responses, the intestinal microbial flora and epithelial barrier function (Murphy et al., 2012). A range of locally produced cytokines leads to inflammation and damage of intestinal epithelial cells (IECs).

IL-6 has been found to be elevated in serum and colonic tissue of IBD patients and its levels correlate with disease activity (Mitsuyama et al., 1991). Studies using dextrane sodium sulfate (DSS)-induced colitis in mice have reported an increased production of IL-6, while IL-6 deficient mice show limited pathological signs of experimental colitis, thus confirming the crucial role of the cytokine (Suzuki et al., 2001).

Consistent with enhanced IL-6 levels, the downstream signal molecule STAT3 has been highlighted as a major player in IBD with different biological functions. While many studies have explored the role of p-STAT3, less interest has been focused on SHP2-mediated signals. Increased STAT3 activation has been described for cells of the lamina propria (LP) and IECs in human IBD and in different murine colitis models, where a correlation with disease severity has been reported (Mudter et al., 2005; Suzuki et al., 2001). However, other investigators have reported evidence of a protective effect of STAT3 phosphorylation in IECs of DSS-treated mice and development of spontaneous chronic enterocolitis with age in macrophage- and neutrophil-specific STAT3 knockout mice (Grivennikov et al., 2009; Takeda et al., 1999). This phenotype closely resembles that of IL-10 deficient mice, reflecting the anti-inflammatory effects of p-STAT3 in response to cytokines of the IL-10 family. One member of this family, IL-22, has been shown to be an important inducer of STAT3 phosphorylation in IECs during colitis, being responsible for the expression of anti-apoptotic and pro-proliferative genes, which contribute to resolution of inflammation and wound healing (Neufert et al., 2010). In contrast, STAT3 activity in T cells of the lamina propria perpetuates chronic inflammation. A study using a murine experimental colitis model mediated by Th1 cells has reported an enhanced resistance of mucosal T cells to apoptosis, which was ascribed to IL-6-mediated STAT3 activation. Interestingly, most of these T cells do not express IL-6R on their surface, pointing to IL-6 trans-signaling as the pivotal pathway.

Indeed, treatment with a gp130-Fc fusion protein that mimics sgp130 and thereby specifically inhibits IL-6 trans-signaling has been shown to suppress colitis activity in mice (Atreya et al., 2000). Since a large amount of IL-6 in the circulation of IBD-patients is found in a complex with sIL-6R, treatment with gp130-Fc might represent a promising therapeutic approach. First clinical trials are planned for 2013 (Rose-John, 2012). In contrast to tocilizumab, an antibody against IL-6R, which is commonly used as a treatment of IBD, gp130-Fc can be expected to produce fewer side-effects and a more specific efficacy, because not all IL-6 functions are blocked.

The ambiguous role of STAT3 in IBD is further supported by studies in mice deficient in IL-6 and those with disrupted gp130-mediated STAT-signaling. Both of them show impaired gastrointestinal wound healing, possibly due to reduced survival and proliferation of IECs (Ernst et al., 2001; Kopf et al., 1994). On the other hand, a conditional gp130 knockout protects against DSS-induced colitis and gp130 deficiency in neutrophils and macrophages delays and reduces disease activity (Sander et al., 2008). Thus, concerning the role of STAT3, it is important to distinguish between different cell populations and origins of signaling. I.e. mice unable to produce gp130-mediated STAT3 signaling in neutrophils and macrophages are still capable of activating STAT3 in response to IL-10, while those with an STAT3 deficiency in the same cell types cannot do so. Whereas in the former the missing STAT3 signal has a protective effect regarding colitis induction, in the latter the lack of anti-inflammatory IL-10 signaling seems to overcome the protective effects.

In line with increased levels of IL-6 and activated STAT3 in IBD, the negative feedback inhibitor SOCS3 is augmented. However, its expression may not be sufficient to shut off STAT3 activity (Li et al., 2012). This could be due to the extremely high IL-6 levels or to posttranslational modifications of SOCS3, impairing its function. Mice expressing a dominant negative SOCS3 mutant were more susceptible to DSS-induced colitis than their wildtype littermates suggesting its involvement in pathogenesis (Suzuki et al., 2001).

A loss of SOCS3 in IECs has been described in colorectal cancer, the risk of which is increased in IBD. This may further promote the anti-apoptotic and pro-proliferative role attributed to p-STAT3 in such conditions.

Other cytokines raised during initial inflammation and shown to be key players in IBD are the pro-inflammatory cytokines IL-1β and TNF-α, the expression of which is increased in IBD patients and in different mouse models of colitis. The pivotal role of TNF-α in the pathogenesis of IBD is reflected in the clinical use of different anti-TNF agents. Interestingly, the efficacy of these substances differs among patients (Horiuchi et al., 2010).

1.4.2 Juvenile idiopathic and rheumatoid arthritis

Rheumatoid and juvenile idiopathic arthritis (JIA) refer to a group of chronic arthritic disorders in adult- and childhood, respectively. JIA is the most common pediatric rheumatic condition, defined by an onset before the age of 16 years and persistence for at least 6 weeks. Of 7 differentiated subtypes, the highest frequency is found for oligoarthritis, followed by polyarthritis and systemic-onset arthritis (Ravelli and Martini, 2007). Both of the conditions, RA and JIA, are characterized by chronic recurrent inflammation targeting mainly the synovial membrane, cartilage and bone resulting in joint effusion, swelling, pain, restriction of physical activity and systemic complications. The pathogenesis is multifactorial, involving genetic and environmental factors, a breakdown of self-tolerance, innate and adaptive immune responses. Different cytokines and chemokines can be detected at high levels within serum and synovial fluid (SF) and an imbalance between pro- and anti-inflammatory factors is a key feature of the disease (Kutukculer et al., 1998; McInnes and Schett, 2007).

RA and JIA go along with increased levels of IL-6 and sIL-6R. An association between IL-6 levels in the SF and markers of inflammation has been reported for RA, while for systemic JIA levels of circulating IL-6 correlate with disease activity (Gabay and Kushner, 1999). IL-6 deficient mice are largely resistant to the induction of experimental arthritis. This is accompanied by reduced synovial infiltration, lower IL-17 levels and fewer osteoclasts, which promote bone destruction. The administration of IL-6 to IL-$6^{-/-}$ mice is not sufficient to restore disease. However, the sIL-6R-IL-6 fusion protein (HYPER-IL-6) reconstitutes AIA and sgp130 alleviates disease in wildtype animals, emphasizing the importance of IL-6 trans-signaling in arthritis (Nowell et al., 2003). Thus, the decreased synovial infiltration seen in sgp130-treated wildtype mice compared to non-treated mice after induction of arthritis is consistent with the idea that IL-6 trans-signaling plays a major role in the recruitment of mononuclear cells to areas of inflammation. Furthermore, the role of IL-6 in bone metabolism is represented by reduced numbers of osteoclasts in IL-6 deficient mice after the induction of AIA. Destruction of articular cartilage and bone is a hallmark in JIA and RA (Gravallese et al., 1998).

The anti-apoptotic and pro-proliferative properties of p-STAT3 have been highlighted to contribute essentially to pathogenesis of RA. Hyperplasia of the synovial membrane is a characteristic feature of arthritis and synovial fibroblasts show a number of abnormalities in RA patients, such as resistance to the induction of apoptosis and elevated proliferation. Overexpression of dominant negative Stat3 in RA synovial fibroblasts leads to increased apoptosis and reduced proliferation (Krause et al., 2002). In addition to these functions of p-STAT3 in synovial fibroblasts, similar effects have been observed in T cells at sites of

inflammation. IL-6 thereby contributes to synovial infiltration not only by recruiting mononuclear cells but also by promoting their maintenance at the site of inflammation. In accordance with the pro-inflammatory role of p-STAT3, mice with a mutation of the shared binding site for SHP2 and SOCS3 within the cytoplasmic domain of gp130 spontaneously develop inflammatory joint disease similar to RA. These mice display enhanced STAT and especially STAT3 activation due to the missing counterregulation by SOCS3 and SHP2 (Atsumi et al., 2002). On the other hand, RA-like joint pathology has been reported for mice with disrupted STAT-binding sites of gp130 as well. Overactivation of SHP2/ERK, caused by the missing feedback inhibition by SOCS proteins, leads to increased proliferation of synovial fibroblasts and chondrocytes (Ernst et al., 2001). Mice lacking SOCS3 in the hematopoietic and endothelial cell compartment show more severe joint inflammation after the induction of experimental arthritis compared to wildtype animals, indicating an important role in the regulation of gp130-mediated signaling (Wong et al., 2006a). This is further supported by the observation of enhanced SOCS3 expression in synovial tissues of mice during experimental arthritis and RA patients. As in the case of IBD, the levels of SOCS3 might still not be sufficient to counteract STAT3 activation or it could be that the feedback inhibitor is modified or rapidly degraded (Shouda et al., 2001).

Much attention has been paid to the balance between pro-inflammatory Th17 cells and anti-inflammatory Tregs in RA and JIA. Several studies indicate high numbers of Tregs within inflamed joints despite persisting inflammation, which has raised the question of whether the suppressive capacity of these Tregs or the responsiveness of effector T cells is impaired. Suppression assays with Tregs isolated from arthritic joints have shown even higher activity than their counterparts derived from peripheral blood (van Amelsfort et al., 2004). However, effector T cells from SF of RA and JIA patients show resistance to inhibition by functional Tregs (Haufe et al., 2011; van Amelsfort et al., 2004).

As in other chronic inflammatory conditions, high levels of the typical pro-inflammatory cytokines TNF-α and IL-1β can be found in arthritic patients and serve as therapeutic targets. The use of anti-TNF and -IL-6 agents has been shown to influence the Th17/Treg cell balance in the SF of RA patients. Interestingly, Tregs isolated from RA patients treated with the anti-TNF antibody adalimumab, but not etanercept, are able to regulate monocyte-derived IL-6 and thereby suppress Th17 cells (McGovern et al., 2012). The JAK inhibitor tofacitinib, which is reported to be effective in clinical studies with RA patients, seems to affect T cell responses by suppressing IL-17 and interferon γ production (Tanaka et al., 2012).

1.5 Aim of this study

IL-6 plays a crucial role in different immune reactions. Together with other IL-6-type cytokines, it shares the signal transducer gp130 as part of its receptor. Dysregulated IL-6 signaling leads to severe inflammatory disorders. One way to restrict cytokine signaling is by limiting the availability of their respective receptors on the cell surface. In contrast to the ligand-binding α-chain of the IL-6 receptor complex, which is present on few cell types, gp130 is ubiquitously expressed. Thus, a strictly regulated surface expression is indispensable.

Previous work has shown that gp130 surface expression on hepatocytes is negatively regulated by pro-inflammatory stimuli, which affect downstream signaling.
The first important aim of this study was therefore to elucidate potential crosstalk regulation of IL-6 signaling in immune cells. Since human monocytes express high levels of gp130, regulatory mechanisms of the pro-inflammatory cytokine IL-1β were studied in this cell type.
The objective in the second part of the thesis was to generate transgenic mice that would enable crosstalk regulation of gp130-mediated signaling to be explored *in vivo*. The vav promoter was used to drive overexpression stably throughout the hematopoietic compartment. One mouse line was generated, which overexpresses a serine-mutated gp130 that was assumed to impair crosstalk-mediated internalization of gp130. These mice were compared to a second mouse strain overexpressing the gp130 wildtype protein.

IL-6 signaling is of utmost importance in chronic inflammatory disorders. This is exemplified by the successful clinical use of an anti-IL-6R antibody and by the resistance of IL-6 deficient mice to disease in several inflammatory models. However, the role of IL-6 in inflammation is sometimes contradictory and is not completely understood. Thus, the aim in the third part of the study was to investigate the expression levels of the IL-6 signaling molecule gp130 in chronic inflammatory conditions like IBD and JIA. The identification of regulatory mechanisms that control gp130 surface expression and downstream signaling in chronic inflammation could contribute to a better understanding and treatment of these diseases.

All essential steps are illustrated by the flow chart in figure 1-4.

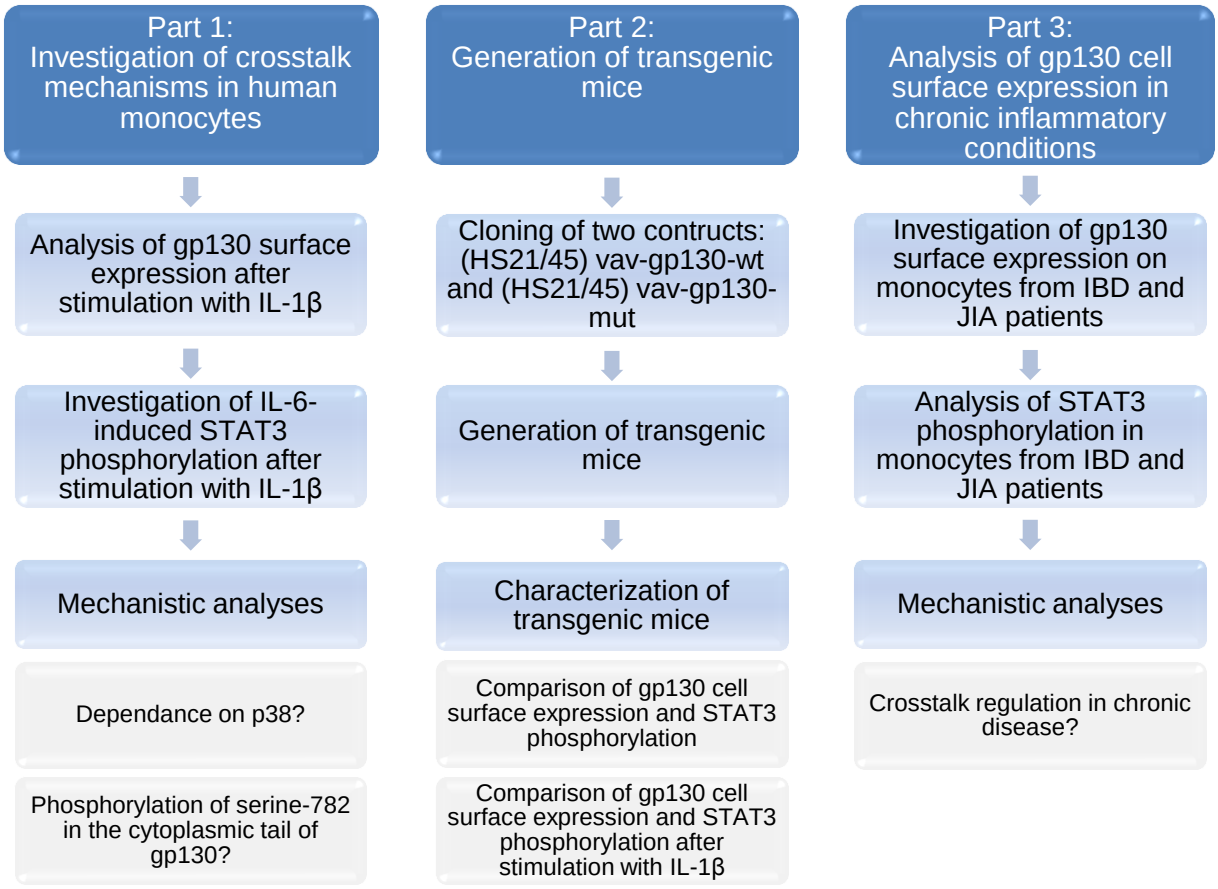

Figure 1-4: Flow chart showing the different parts of this PhD thesis.

2 MATERIALS AND METHODS

2.1 Materials

2.1.1 Consumables and chemicals

Consumables were purchased from:

BD Biosciences (Heidelberg), BD Microlance (Ireland), Eppendorf (Hamburg), Greiner Bio-One (Solingen), Miltenyi Biotec GmbH (Bergisch Gladbach), Peqlab (Erlangen), Schleicher&Schuell (Dassel), Starlab GmbH (Ahrensburg), Terumo Europe N.V. (Belgium).

Laboratory chemicals were purchased from:

Applichem (Darmstadt), Bio-Rad (Munich), eBioscience (Frankfurt), GE Healthcare (Munich), Invitrogen (Karlsruhe), Merck (Darmstadt), Macherey-Nagel (Düren), Millipore (Eschborn), MP Biomedicals (USA), Qiagen (Hilden), Roth (Karlsruhe), Sigma Aldrich (Steinheim), Thermo Fisher Scientific (Schwerte), Zymo Research (USA).

2.1.2 Equipment

Table 2-1: Used equipment

Equipment	Manufacturer
7300 Real Time PCR System	Applied Biosciences (Darmstadt)
Analytical Balance	Sartorius AG (Göttingen)
Bio Photometer	Eppendorf(Wesseling)
FACS CANTOII	BD Biosciences (Heidelberg)
Hera Cell Incubator	Thermo Fischer Scientific (Schwerte)
Heraeus Multifuge 3SR+	Thermo Fischer Scientific (Schwerte)
Heraeus Pico 17 Centrifuge	Thermo Fischer Scientific (Schwerte)
Microcentrifuge	Thermo Fischer Scientific (Schwerte)

Lapdancer Digital	VWR International GmbH (Darmstadt)
LAS 3000, Image Reader	Fujifilm (Düsseldorf)
Nano Drop ND 1000 Spectrophotometer	PEQLAB Biotechnologie GmbH (Erlangen)
Opera High Content Screening System	PerkinElmer (USA)
Pipetboy Acu	IBS Integra Biosciences (Fernwald)
Laminar Flow Hood	Thermo Fisher Scientific (Schwerte)
Mini-PROTEAN® 3 Electrophoresis System	BIO-RAD (Munich)
Semi-Dry Transfer Cell	BIO-RAD (Munich)
Thermomixer Compact	Eppendorf (Hamburg)
Transfer Pipettes S	Brand (Wertheim)
Ultrasonic Sonicator	Hielscher (Teltow)
Ultraviolet Sterilizing PCR Workstation	PEQLAB Biotechnologie GmbH (Erlangen)

2.1.3 Reaction kits

Table 2-2: Used reaction kits

Kit	Manufacturer
First Strand cDNA Synthesis Kit	Fermentas (St. Leon-Roth)
NucleoBond® PC500	Macherey-Nagel (Düren)
qPCR Master Mix for SYBR Green I	Eurogentec GmbH (Cologne)
RNAse free DNAse Set	Qiagen (Hilden)
RNeasy® Mini Kit	Qiagen (Hilden)
TopTaq DNA Polymerase	Qiagen (Hilden)

Wizard® SV Gel and PCR Clean-Up System	Promega (Mannheim)
Zippy Plasmid Miniprep Kit	Zymo Research (USA)

2.1.4 Oligonucleotides and plasmids

Table 2-3: Used oligonucleotides

Gen	Sequence 5' → 3'
Human RPL13A	for: AGGTATGCTGCCCCACAAAAC rev: TGTAGGCTTCAGACGCACGAC
Human SOCS3	for: CACCTGGACTCCTATGAGAAAGTCA rev: GGGGCATCGTACTGGTCCAGGAA
Murine β-actin	for: ACTATTGGCAACGAGCGGTTC rev: TTACGGATGTCAACGTCACACTTC
Murine gp130 for RT-PCR	for: ATAGTCGTGCCTGTGTGCTTAGC rev: GGTGACCACTGGGCAATATGA
Murine gp130 for genotyping	for: CGGCTCATATGGAAGGCACTGCC rev: CGCGGCCATTCGGACCATGT

All primers were ordered from VBC Biotech (Switzerland).

Table 2-4: Used plasmids

Plasmid	Description
vav hematopoietic vector	pIC-19H vav-hCD4
SW213	pcDNA3.1 mugp130 wt
SW214	pcDNA3.1 mugp130 SS/AA
Vav-gp130wt	pIC-19H vav mugp130 wt

Vav-gp130mut	pIC-19H vav mugp130 SS/AA

2.1.5 Antibodies

Table 2-5: Used antibodies

Antibody	Clone	Manufacturer	Application
Mouse α-human CD14, APC/FITC-conjugated	MEM-18	Immunotools (Friesoythe)	FC, FM
Mouse α-human IL-6R, PerCP-eFluor® 710-conjugated	47.7G7.1F2	eBioscience (Frankfurt)	FC
Mouse α-human IL-6R, APC-conjugated	17506	R&D Systems	FC
Mouse α-human gp130, FITC-conjugated	B-R3	Abcam (UK)	FC, FM
Mouse α-human gp130, PE-conjugated	AM64	BD Biosciences (Heidelberg)	FC
Mouse α-human/mouse STAT3 (pY705), Alexa Fluor® 647-conjugated	4/P-STAT3	BD Biosciences (Heidelberg)	FC
Mouse α-human/mouse p38 MAPK (pT180/pY182), Alexa Fluor® 488-conjugated	36/p38 (pT180/pY182)	BD Biosciences (Heidelberg)	FC
Armenian Hamster α-mouse CD3, PE/APC-conjugated	145-2C11	eBioscience (Frankfurt)	FC
Rat α-mouse CD11b, eFluor® 450-conjugated	M1/70	eBioscience (Frankfurt)	FC

Rat α-mouse CD19, FITC-conjugated	eBio1D3	eBioscience (Frankfurt)	FC
Rat α-mouse F4/80, APC-conjugated	BM8	eBioscience (Frankfurt)	FC
Rat α-mouse gp130, APC-conjugated	KGP130	eBioscience (Frankfurt)	FC
Mouse α-human gp130-pSer782		BD Biosciences (Heidelberg)	WB
Rabbit α-human/mouse gp130	M-20	Santa Cruz Biotechnology (USA)	IP, WB
Rabbit α-human/mouse phospho-STAT3 (Tyr705)		Cell Signaling Technology (USA)	WB
Mouse α-human/mouse STAT3	84/Stat3	BD Biosciences (Heidelberg)	WB
Goat α-rabbit immunoglobulins, HRP-conjugated	Polyclonal	DakoCytomation (Denmark)	WB

2.1.6 Cytokines

Table 2-6: Used cytokines

Cytokine	Concentration	Manufacturer
Human IL-1β	20 ng/ml	PeproTech (Hamburg)
Human IL-6	20 ng/ml	MiltenyiBiotec GmbH (Bergisch Gladbach)
Human IL-10	20 ng/ml	PeproTech (Hamburg)
Murine IL-1β	20 ng/ml	PeproTech (Hamburg)
Murine IL-6	20 ng/ml	MiltenyiBiotec GmbH (Bergisch Gladbach)

2.1.7 Inhibitors

Table 2-7: Used inhibitors

Inhibitor	Concentration	Manufacturer
SB202190	1-5 µM	Calbiochem (Darmstadt)
Actinomycin D	5 µg/ml	Sigma Aldrich (Steinheim)

2.1.8 Buffers and media

Table 2-8: Used buffers and formulation

Buffer	Formulation
Blocking Buffer	TBS-T 10% (w/v) BSA
Blot Buffer	25 mM Tris Base 192 mM Glycine 0.1% (w/v) SDS 20% (v/v) Methanol
FACS Buffer	PBS 0.5% (w/v) BSA
RIPA Buffer	10 mM Tris-HCL, pH 7,4 150 mM NaCl 1% (v/v) NP40 1% (w/v) Sodium desoxycholate 0.1% (w/v) SDS
SDS Running Buffer	25 mM Tris base 192 mM Glycine 2% (w/v) SDS
SDS Sample Buffer (2x)	100 mM Tris-HCl, pH 6,8 4% (w/v) SDS

	0.2% (w/v) Bromophenol blue 20% (v/v) Glycerol 200 mM β-Mercaptoethanol
Separating Gel, 7.5%	50% (v/v) Distilled water 25% (v/v) Separating Gel Tris Solution (4x) 25% (v/v) Acrylamide 4K Solution (30%), Mix 37.5:1 0.1% (w/v) APS 0.1% (v/v) TEMED
Separating Gel, 12%	35% (v/v) Distilled Water 25% (v/v) Separating Gel Tris Solution (4x) 40% (v/v) Acrylamide 4K Solution (30%), Mix 37.5:1 0.1% (w/v) APS 0.1% (v/v) TEMED
Separating Gel Tris Solution (4x)	1.5 M Tris-HCL, pH 8,8 0.4% (w/v) SDS
Stacking Gel	65% (v/v) Distilled Water 25% (v/v) Stacking Gel Tris solution (4x) 10% (v/v) Acrylamide 4K Solution (30%), Mix 37.5:1 0.1% (w/v) APS 0.1% (v/v) TEMED
Stacking Gel Tris Solution (4x)	0.5 M Tris-HCL 0.4% (w/v) SDS pH 6.8
Stripping Buffer	200 mM Glycine 0.1% (w/v) SDS 1% (v/v) Tween-20 pH 2.2
TBS-T Buffer	20 mM Tris-HCL, pH 7.6

	137 mM NaCl 0.05% (v/v) Tween-20
TE Buffer	10 mM Tris Base 1 mM EDTA

Table 2-9: Used media

Medium	Formulation	Manufacturer
Complete RPMI	RPMI 1640 10% (v/v) FCS 1% (v/v) Pen/Strep	Invitrogen (Darmstadt) Gibco (Eggenstein) Invitrogen (Darmstadt)
Cell medium for microscopy	RPMI 1640, no Phenol Red 10% (v/v) FCS	Invitrogen (Darmstadt) Gibco (Eggenstein)
LB medium	2% (w/v) LB-Broth (Lennox)	Roth (Karlsruhe)

2.1.9 Prokaryotic cells

Table 2-10: Used bacteria

Bacterial strain	Description	Manufacturer
E. coli DH5 α	deoR endA1 hsdR17 (rk-, mk+) supE44 thi-1 recA1 ∆(argFV169-LacZYA) U169 Φ80lacZ∆M15 F- λ-	Invitrogen (Darmstadt)

2.2 Methods

2.2.1 Animal studies

2.2.1.1 Generation of transgenic mice

Transgenic mice are widely used in laboratory research carried out to elucidate the physiological functions of gene products and their implications in human diseases.

For the generation of transgenic mice two different vectors were cloned as described in 2.2.4.10. All further processes were carried out in the animal facility of Universitätsklinikum Aachen, Pauwelsstr. 30. Briefly, DNA was directly injected into the pronuclei of fertilized oocytes. These oocytes were then implanted into the ovary ducts of pseudo-pregnant mice. Genomic DNA was isolated from tails of the offspring and transgenic integration was confirmed by PCR (2.2.4.8).

2.2.1.2 Laboratory animals

Table 2-11: Used mice

Name	Genetic background	Age	Genetic properties
gp130-wt	B6-Mix	8-16	Overexpression of gp130 in the haematopoetic compartment under control of the vav promoter. Control mice for gp130-mut.
gp130-mut	B6-Mix	8-16	Overexpression of a mutated version of gp130 in the haematopoetic compartment under control of the vav promoter: Serine 778 and 780 were exchanged for alanine residues to produce a non-phosphorylatable mutant, which might be impaired in its internalization.
Wt	B6	8-16	Wildtype mice without genetic modification.

All animals were housed in temperature-controlled rooms on a 12-hour light/dark cycle in the animal facility of Universitätsklinikum Aachen, Pauwelsstr. 30. Standard diet and water were

given *ad libitum*. All animal experiments were conducted in agreement with German animal protection law and were approved by the local animal care committee (file reference: 50.203.2 AC; 8.87-50.10.35.09.035).

2.2.1.3 DSS induced chronic colitis

The oral administration of dextran sodium sulphate (DSS) is a well-established model for the induction of colitis, which shows several similarities to human IBD. Inflammation is usually restricted to the colon and clinical symptoms include diarrhea, weight loss and occult blood in stools. Depending on the DSS concentration, frequency and duration of its administration colitis can be developed in an acute or chronic manner (Solomon et al., 2010). Mice were fed with 2.5% (w/v) DSS in their drinking water for 1 week followed by 1 week without DSS. These cycles were repeated until day 37, when the animals were sacrificed. Control mice were included, which were fed with normal drinking water throughout the experiment. Weight of the animals was determined every other day.

2.2.1.4 Zymosan induced peritonitis

The intraperitoneal (i.p.) injection of zymosan is a well-established model to study the infiltration of leukocytes into the peritoneal cavity. Zymosan is a polysaccharide cell wall component from *Saccharomyces cerevisiae* and its injection results in self-resolving acute inflammation (Cash et al., 2009).

2.2.2 Immunological methods

2.2.2.1 Isolation of PBMCs from peripheral blood

PBMCs were isolated from buffy coats, provided by the local blood bank (Transfusionsmedizin, UK Aachen, Germany), or from peripheral blood obtained from healthy volunteers. The blood was diluted with PBS at a ratio of 1:1 and layered onto 14 ml of Ficoll Histopaque. After centrifugation (950 g, 15 min, RT, without brake in a swing-out rotor) mononuclear cells were separated from plasma and erythrocytes. PBMCs formed a distinct layer at the plasma-interface and could be transferred with a Pasteur pipette into a new tube. The cells were washed two times, counted in a Neubauer haemocytometer and used for further analysis.

2.2.2.2 Isolation of monocytes from peripheral blood

For the isolation of monocytes, PBMCs were prepared from peripheral blood as described under 2.2.2.1. The separation of monocytes from lymphocytes was performed according to Repnik *et al.* with two different Percoll gradients (Repnik et al., 2003). In the first step monocytes were separated from lymphocytes by hyperosmotic Percoll density gradient centrifugation (580 g, 15 min, RT, without brake in a swing-out rotor). In the second step, dead cells and thrombocytes were removed from monocytes by an isosmotic Percoll density gradient centrifugation (350 g, 15 min, RT, without brake in a swing-out rotor). After gradient centrifugations cells were washed and counted. The final purity of monocytes was examined by flow cytometry (2.2.2.4).

2.2.2.3 Isolation of cells from spleen and lymph nodes

Mice were sacrificed by CO_2 inhalation and cervical dislocation and the spleen and lymph nodes were removed. Organs were collected in tubes containing T cell medium. To prepare a single cell suspension, organs were meshed through a 50 µm cell strainer with the stamp of a syringe. Red blood cells were lysed with erythrocyte lysis buffer according to the manufacturer's instructions. Cell number was defined with a Neubauer haemocytometer.

2.2.2.4 Flow cytometry

Flow cytometry is a laser-based technology, which allows the analysis of multiple parameters of individual cells. Single cell suspensions are hydrodynamically focused within a flowing sheath fluid before they pass by a laser beam. The scatter light produced by a single cell as it passes through the laser beam is collected by different detectors. While forward scatter (FSC) gives information about the size, side scatter (SSC) determines the granularity of the cell. In addition to these parameters, different lasers can excite a range of fluorophores and the emitted light is received by detectors. Fluorophore-labeled antibodies against cell surface molecules or intracellular proteins are useful tools to study individual cellular characteristics within a heterogeneous population.

Flow cytometric analysis was performed on BD FACS Canto II (BD Biosciences), while data was evaluated usind FCS Express or Flowing Software. Isotype controls or unstained samples were used for the determination of quadrants within dot plots.

2.2.2.4.1 Detection of cell surface proteins

5 x 10^5 to 1 x 10^6 cells were incubated with fluorescent dye-coupled antibodies against specific cell surface epitopes for 20 min on ice. After washing with FACS buffer, cells were subjected to analysis.

2.2.2.4.2 Detection of intracellular phospho-proteins

1 x 10^6 cells were fixed in 1.5% (w/v) paraformaldehyde (PFA) for 10 min at RT. After centrifugation, cells were resuspended in 1 ml ice-cold methanol and either incubated on ice for 10 min or stored at -20°C for up to 3 days. Cells were washed two times with FACS-buffer and incubated with antibodies against specific phosphorylated proteins and against cell surface epitopes for 30 min at RT. Cells were washed and analyzed.

2.2.2.4.3 Flow cytometric analyses from whole blood

A minimum sample of 40 µl was washed once with the same volume of PBS. 1 volume of 2% (w/v) PFA was added and incubated for 15 min at RT. After washing, the pellet was resuspended in 1 ml of erythrocyte lysis buffer and incubated for 15 min at RT. Cells were washed and either cell surface staining was performed and continued as described in 2.2.2.4.1 or 1 ml ice-cold methanol was added and continued as described in 2.2.2.4.2.

2.2.2.5 Confocal fluorescence microscopy

Confocal microscopy was performed on Opera High Content Screening System (PerkinElmer). This automated system allows fast confocal imaging of cell samples. Temperature and CO_2 control units enable live cell experiments to be carried out under physiological conditions.

1500 PBMCs per well were seeded onto poly-L-lysine coated 96-well plates and left to settle down ON. Non-adhered lymphocytes were removed by washing with PBS and the cells were incubated with fluorophore-coupled antibodies for 30 min on ice. Cells were washed with PBS to remove non-bound antibody and cell medium for microscopy with or without IL-1β was added prior to microscopy.
Images were acquired automatically from 10 positions per well and using a 40x air objective. The images were blinded and cells assessed based on the following scoring system:

Table 2-12: Internalization score

Score	Description
0	No internalization: staining localized only at the membrane
0.5	Early internalization: appearance of some rafts
1	Medium internalization: appearance of many rafts
1.5	Late internalization: appearance of many rafts and intracellular staining

2.2.3 Proteinchemical methods

2.2.3.1 Preparation of cell lysates

4 to 5 x 10^6 cells were lysed in 200 µl of RIPA buffer containing protease-inhibitors (complete mini). Lysates were incubated on ice for 15 min. For homogenization and to shear the high molecular weight DNA, lysates were passed 15 to 20 times through a 19G needle attached to a 1 ml syringe. Cell debris was pelleted at 17000 x g for 20 min at 4°C and the supernatant transferred to a new Eppendorf tube. Clarified lysates were subjected to further analysis or stored at -20°C.

2.2.3.2 Bradford

For the determination of protein concentrations the classic method of Bradford (Bradford, 1976) was used. 2 µl of clarified cell lysates were mixed with 798 µl dd H_2O and 200 µl of Bradford reagent. Following 10 min of incubation at RT, absorption at 595 nm was measured and the protein concentration calculated based on a calibration line generated for BSA.

2.2.3.3 SDS-polyacrylamide gelelectrophoresis (SDS-PAGE)

The denaturing SDS-PAGE allows the separation of proteins according to their molecular weight. The anionic detergent SDS binds quantitatively to the linearized protein and generates a negative net charge. During their electrophoretically driven movement towards the anode through a polyacrylamide gelmatrix the proteins are separated.

The discontinuous SDS-PAGE was performed according to Laemmli (Laemmli, 1970) with a 5% stacking gel and a 7.5-12% separating gel. A prestained protein ladder served as molecular marker for the determination of protein size. The electrophoresis was carried out at 150 V.

2.2.3.4 Western blot and immunodetection

Proteins separated by SDS-PAGE were transferred to a polyvinylidene difluoride (PVDF) membrane in an electrophoretic semi-dry blotting chamber. After transfer the membrane was incubated with blocking buffer for 45 to 60 min at RT. For the immunodetection of specific proteins the membrane was incubated with a suitable antibody at 4°C ON. After several wash steps a secondary, HRP-coupled antibody, which binds to the primary antibody was added for 45 to 60 min at RT. Following another 3 to 5 washes the membrane was incubated with ECL solution, containing an HRP-substrate. Under emission of chemiluminescence this substrate is turned over by the enzyme and the signal can be detected with a computer-assisted camera system (LAS4000, Fuji).

2.2.3.5 Immunoprecipitation

By the use of an antibody against a specific protein of interest, an immunoprecipitation can serve to concentrate this protein in a cellular extract. Protein-G coupled beads bind to the antibody-protein complex and can subsequently be isolated from the lysate. The precipitated protein is detected in a western blot.

4×10^7 monocytes with a minimum purity of 70% were lysed in 500 µl RIPA buffer containing protease inhibitors. Protein concentration of clarified lysates (2.2.3.1) was measured by Bradford (2.2.3.2) and 2 to 2.5 mg of protein were incubated with 1 µg of antibody at 4°C ON. After addition of protein G coupled beads samples were incubated for another 4 hours at 4°C. Immune complexes were washed, mixed with 10 µl of 2x sample buffer and boiled for 5 min at 96°C followed by SDS PAGE and western blot.

2.2.3.6 Blot stripping

The treatment of PVDF membranes, which have already been subjected to immunodetection, with stripping buffer allows a new incubation with antibodies and detection of another protein of interest.

For stripping of antibodies the membrane was incubated with stripping buffer for 30 min. The solution was then changed, followed by another 30 min incubation. The membrane was

washed several times and the blocking step was repeated before the treatment with the suitable antibody and immunodetection (2.2.3.4).

2.2.4 Work with nucleic acids

2.2.4.1 DNA preparation

DNA was extracted from transformed bacteria according to the manufacturer's instructions using the NucleoBond® PC500 kit (Macherey-Nagel) for preparative purposes and the Zippy Plasmid Miniprepkit (Zymo Research) for small-scale preparations.

2.2.4.2 RNA preparation

Total RNA was extracted from primary cells using the RNeasy Mini Kit (Qiagen) following the manufacturer's instructions.

2.2.4.3 cDNA synthesis

Extracted RNA was transcribed to cDNA using the First Strand cDNA Synthesis Kit (Fermentas) according to the manufacturer's instructions.

2.2.4.4 Enzymatic manipulation of plasmid DNA

Plasmid DNA was digested in 25 µl reaction volume using restriction enzymes (Fermentas) with appropriate buffers for 1 h to overnight at the denoted temperature.

DNA was ligated using T4 Ligase (Fermentas). Sticky end ligations were carried out for 1 to 2 h at RT, blunt end ligations ON at 16°C.

2.2.4.5 Determination of concentration and purity of DNA and RNA

The concentration of DNA and RNA was measured on a photospectrometer where the absorption of the nucleic acid at 260 nm was determined. The purity was determined by the ratio $OD_{260\ nm}/OD_{280\ nm}$.

2.2.4.6 Agarose gel electrophoresis

The electrophoretic separation of DNA fragments was performed as described (Sambrook et al., 1989) in 0.5-2% (w/v) agarose gels.

2.2.4.7 Gel extraction

DNA was recovered from agarose gels using the Wizard SV Gel and PCR Clean-Up System (Promega) according to the manufacturer's instructions.

2.2.4.8 Polymerase chain reaction (PCR)

For the enzymatic amplification of DNA fragments suitable primers were used, which flanked the respective regions.

For PCR reactions with analytical purposes TopTaq DNA Polymerase (Qiagen) was used, while for reactions where the products were to be further utilized for cloning Phusion Polymerase (Finnzymes) was used.

2.2.4.9 Quantitative real time polymerase chain reaction (RT-PCR)

As with the conventional PCR reaction in quantitative real time PCR, specific nucleic acid fragments are amplified with the help of oligonucleotides flanking the suitable regions. The use of DNA intercalating fluorescent dyes or labeled probes allows the additional quantification of the generated products. In each cycle the increase of fluorescence is measured, which rises in proportion to the number of PCR-products. The cycle threshold (ct)-value describes the cycle where the number of copies rises exponentially and was used for analysis of the results.

Quantitative RT-PCR was carried out on a TaqMan 7900 (Applied Biosystems) using the intercalating dye SYBR green, included in the quantitative RT-PCR Master Mix for SYBR Green I (Eurogentec GmbH). 7000 System SDS Software was used for data evaluation. Housekeeping genes were analyzed for normalization and calculation of relative expression.

2.2.4.10 Cloning

Cloning of the vectors for gp130 transgenic mice was performed according to Ogilvy *et al.* (Ogilvy et al., 1999). The vav haematopoetic vector was digested with the restriction enzymes SfiI and NotI to remove the hCD4 sequences. PCR products with appropriate SfiI and NotI specific overhangs were generated from SW213 and SW214, kindly provided by the Department of Biochemistry (UK Aachen). After digestion of the PCR products, they were subcloned into the vav haematopoetic vector.

2.2.4.11 Sequencing

All cloned vectors were controlled by sequencing (Eurofins MWG). Samples were prepared according to the sample submission guide of the company.

2.2.5 Work with prokaryotic cells

2.2.5.1 Transformation

100 µl competent bacteria (*E. coli* DH5α) were thawed on ice and mixed with 50-500 ng plasmid DNA. After up to 30 min incubation on ice, bacteria were subjected to heat-shock for 45 sec at 42°C and immediately placed back on ice. 900 µl of LB medium were added and the tube was incubated for 1 h at 37°C. Bacteria were pelleted by centrifugation, resuspended in 100 µl of LB medium and plated on LB agar plates containing the appropriate antibiotics. Plates were incubated ON at 37°C.

3 RESULTS

3.1 Crosstalk inhibition of IL-6 signaling in human monocytes

3.1.1 Effect of IL-1β on gp130 surface expression

Previous studies with hepatocytes have shown a crosstalk inhibition of IL-6 signaling by pro-inflammatory cytokines and stress stimuli. This inhibition was mediated by phosphorylation and subsequent internalization and degradation of the IL-6 receptor subunit gp130 (Radtke et al., 2010). Other groups demonstrated a negative influence of pro-inflammatory cytokines on STAT3 phosphorylation, also in other cell types such as macrophages, but the precise mechanism remained unclear (Ahmed and Ivashkiv, 2000).
Since IL-6 signaling plays a major role in different immune reactions and is implicated in the pathogenesis of chronic inflammatory disorders, we decided to investigate whether the mechanism discovered in hepatocytes can be found in immune cells as well.

In human peripheral blood almost all monocytes display a high expression of gp130 (Oberg et al., 2006). As shown in figure 3-1, these observations could be confirmed by our own flow cytometric analyses. PBMCs were isolated from healthy donors and stained for gp130 and the monocyte marker CD14. The gate was set to $CD14^+$ cells and gp130 expression within the monocyte population was analyzed. Approximately 95% of the monocytes displayed cell surface expression of gp130.

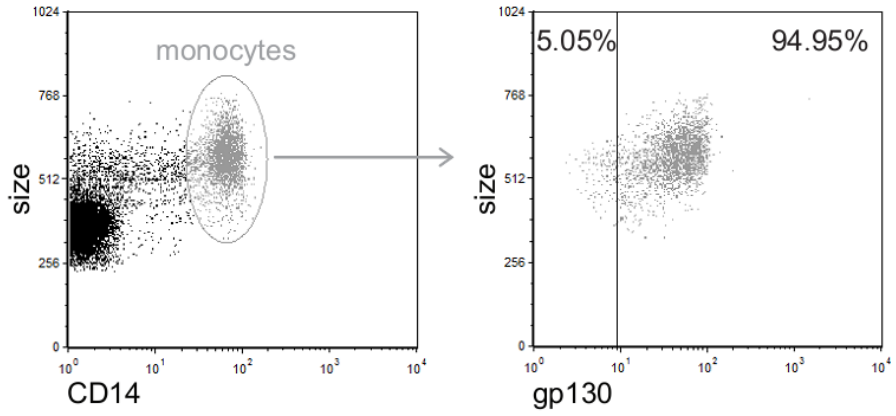

Figure 3-1: Cell surface expression of gp130 on monocytes.
FACS analysis (2.2.2.4.1) of human PBMCs. Cells were isolated and incubated with antibodies against CD14 and gp130. The gate was set on $CD14^+$ cells (left dotplot) and monocytes were classified as $gp130^-$ or $gp130^+$ based on isotype control. Representative plots are shown.

We therefore focused on this population and performed live-cell imaging to investigate the influence of IL-1β on gp130 surface expression. After isolation PBMCs were allowed to settle down. A reduction of lymphocytes and an enrichment of adherent monocytes was achieved by washing the cells stringently. The cells were labeled with antibodies against gp130 and CD14 and analyzed by confocal fluorescence microscopy. Figure 3-2 A shows representative images of cells left untreated (upper panel) compared to samples stimulated with recombinant IL-1β (lower panel). Pictures were taken immediately after subjecting the samples to microscopy and every 10 min. While a localization of the gp130-staining could be detected mainly at the cell membrane in untreated cells, monocytes exhibited less clear membrane staining in the presence of IL-1β. Instead, gp130 was distributed throughout the cell and some rafts were visible (see arrowheads). In figure 3-2 B a statistical analysis of two individual microscopy experiments can be seen. According to the degree of internalization, cells were assessed based on a scoring system (table 2-12). There was a certain rate of constitutive internalization during the experiment, which explains how the internalization score had reached almost 0.5 at time point 2 min and rose further even in the absence of IL-1β. However, in the presence of IL-1β internalization was significantly higher compared to untreated cells.

To confirm these findings, gp130 surface expression was measured by flow cytometry after stimulation with IL-1β and compared to non-stimulated cells. PBMCs were gated on $CD14^+$ cells and mean fluorescence intensity (MFI) of gp130 within the monocyte population was examined. Figure 3-2 C shows a small but reproducible downregulation of gp130 surface expression after 20 min of stimulation with IL-1β.

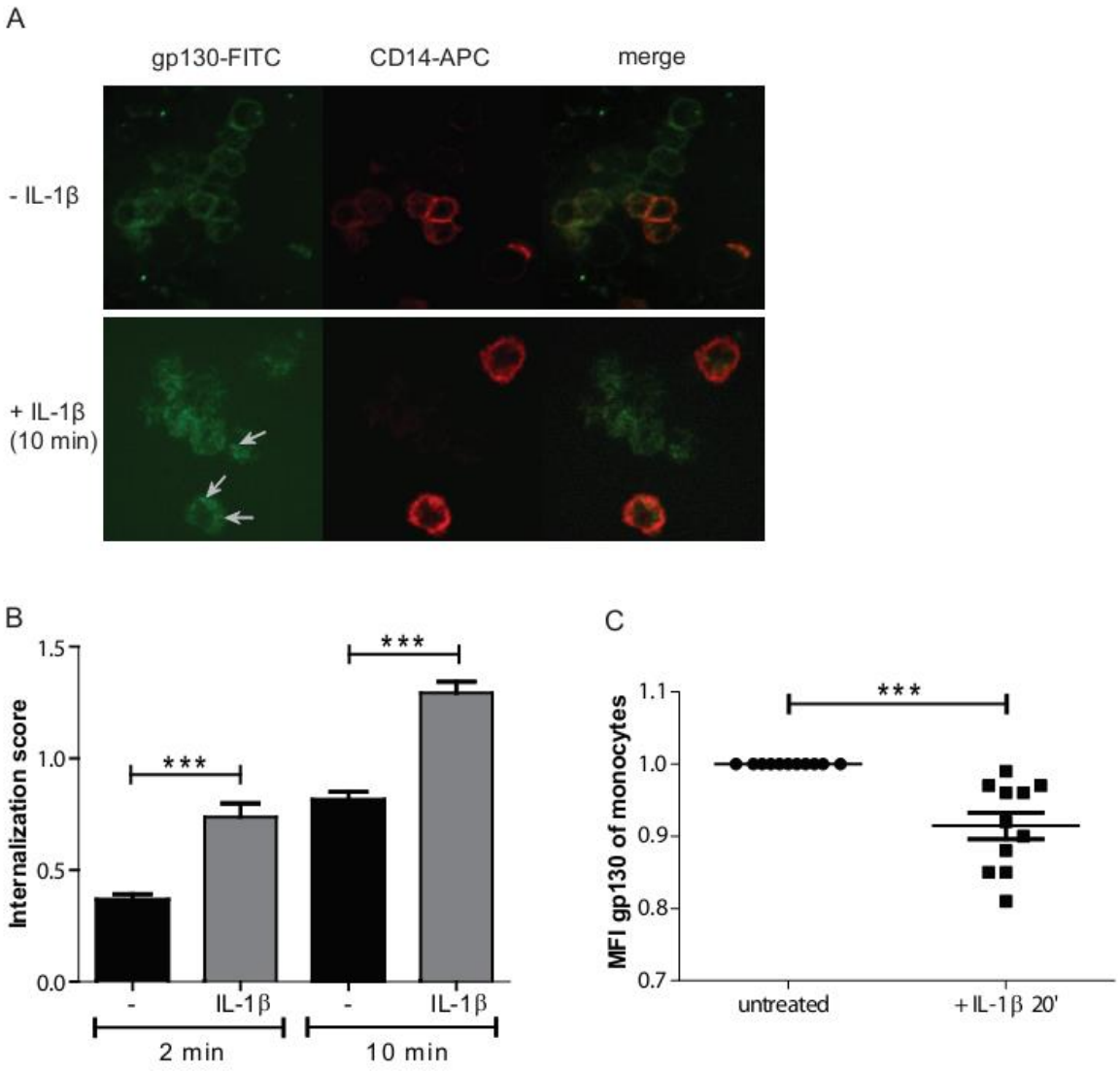

Figure 3-2: Effect of IL-1β on gp130 cell surface expression on CD14$^+$ human monocytes.

A) Confocal fluorescence microscopy (2.2.2.5). PBMCs were labeled with α-gp130-FITC and α-CD14-APC for 30 min on ice. Medium with or without IL-1β (20 ng/ml) was added to the cells after washing and the plate was subjected immediately to live-cell imaging at 37°C. 10 pictures per well were taken every 10 min. Representative images are shown. B) Statistical analysis of microscopy (based on table 2-12). Bars represent mean values plus SEM (n = 231 for untreated, n = 61 or n = 46 for treated cells); *** $p<0.001$ (one-way ANOVA with Dunn's Multiple Comparison Test). C) FACS analysis (2.2.2.4.1) of human PBMCs. Cells were stimulated with IL-1β (20 ng/ml) for 20 min and gp130 expression on the cell surface was determined by FACS analysis. CD14 was co-stained and 5000 CD14$^+$ cells were recorded. MFI values measured for untreated cells were set to 1. Horizontal lines represent mean values plus SEM (n=11); *** $p<0.001$ (one sample t-test).

In summary, the pro-inflammatory stimulus IL-1β had a significant influence on gp130 surface expression on human monocytes. Enhanced internalization of the receptor was observed within minutes of stimulation. While the internalization score, determined by

confocal microscopy, rose by more than 60%, gp130 cell surface expression, measured by flow cytometry, was reduced by approximately 10%.

3.1.2 Influence of IL-1β on STAT3 activation

As a consequence of diminished gp130 expression on the cell surface downstream signaling was assumed to be affected. To test this hypothesis, PBMCs were stimulated with IL-1β or left untreated before IL-6 was added for different periods of time. Cells were lysed and phosphorylation of STAT3 was detected in a western blot. Figure 3-3 A shows a clear induction of p-STAT3 after stimulation with IL-6 for 10 or 30 min. Pre-incubation of the cells with IL-1β for 15 min resulted in a reduction of phosphorylated protein. The amount of non-phosphorylated STAT3 remained constant as illustrated in the lower panel. Flow cytometric analyses confirmed an inhibitory effect of IL-1β on IL-6-induced STAT3 phosphorylation, as demonstrated in figure 3-3 B. Cells were stimulated as described for A and based on the surface marker CD14 only the MFI of monocytes is shown in the representative histogram. Basal STAT3 phosphorylation of non-stimulated cells is shown in black. The red line indicates STAT3 activation induced by IL-6 while the blue histogram represents MFI of p-STAT3 after pre-incubation with IL-1β and subsequent IL-6 stimulation. Although pre-incubation with IL-1β did not reduce STAT3 phosphorylation to baseline level, a clear reduction could be monitored. To exclude the possibility that the observed effects on STAT3 activation were mediated by co-stimulation of other cell types contained in PBMCs, monocytes were purified from PBMCs by gradient density centrifugation. Isolated monocytes with a minimum purity of 70%, as determined by flow cytometry, were stimulated in the same manner as described for PBMCs. Figure 3-3 C shows histograms of p-STAT3 MFI, analogous to figure 3-3 B. As illustrated by the histograms, inhibition of IL-6-mediated STAT3 phosphorylation by IL-1β was comparable in isolated monocytes to PBMCs.

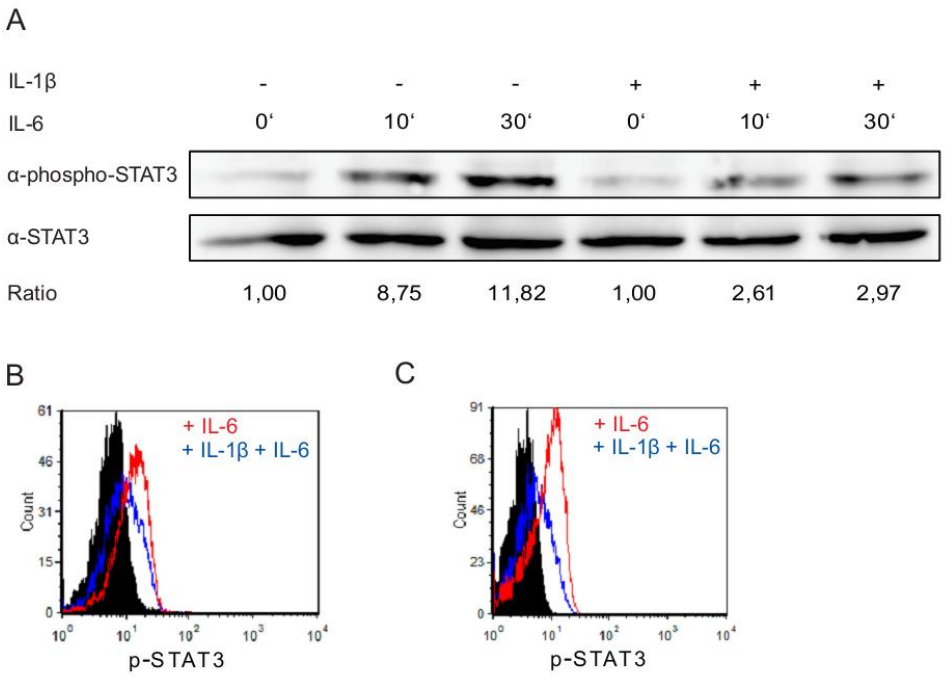

Figure 3-3: STAT3 phosphorylation after stimulation with IL-1β.
A) Western Blot (2.2.3.4) of PBMCs. 3 x 10^6 cells were stimulated with IL-6 (20 ng/ml) for the indicated times. For co-stimulation IL-1β (20 ng/ml) was added 15 min prior to the addition of IL-6. Cells were lysed and separated in a 12% SDS-PAGE (2.2.3.3). Phosphorylated STAT3 was detected in a western blot, membrane was stripped (2.2.3.6) and re-probed with an antibody against STAT3. Quantification of protein amounts is shown as ratio of p-STAT3:STAT3. Ratios of untreated cells were set to 1. B) and C) Flow cytometric analysis of STAT3 phosphorylation (2.2.2.4.2). 1 x 10^6 PBMCs (B) or monocytes (C) were stimulated as described in A. After 10 min of IL-6 stimulation, cells were fixed, lysed and stained for p-STAT3. CD14 was co-stained and 5000 $CD14^+$ cells were recorded. Histograms show MFI for p-STAT3 within the $CD14^+$ population. A filled histogram illustrates untreated cells as a control, the red line represents MFI after IL-6 stimulation and the blue line after co-stimulation with IL-1β. One representative experiment out of 5 is shown.

As demonstrated by different approaches, IL-1β diminished STAT3 phosphorylation mediated by IL-6. To clarify that this effect was not a result of IL-6-induced feedback inhibition, the influence of SOCS proteins was investigated by two different methods. Figure 3-4 A shows that the addition of actinomycin D, an inhibitor of protein synthesis and thus of SOCS expression, had no impact on IL-1β-mediated reduction of STAT3 phosphorylation after IL-6 stimulation. The pre-incubation of PBMC cultures with IL-1β led to decreased levels of p-STAT3 in response to IL-6, independent of *de novo* protein synthesis. A more specific verification was carried out by quantitative RT-PCR where the expression level of *SOCS3* was determined after addition of IL-1β, IL-6, or a combination of both cytokines. The incubation of PBMCs with IL-6 for 1 h was used as positive control and revealed a clear induction of *SOCS3* expression compared to the untreated sample, as shown in figure 3-4 B.

A slight increase of *SOCS3* expression could be noted after IL-6 stimulation for 10 min. This was not further enhanced by pre-treatment of IL-1β nor did IL-1β alone lead to a significant induction of *SOCS3* compared to untreated cells.

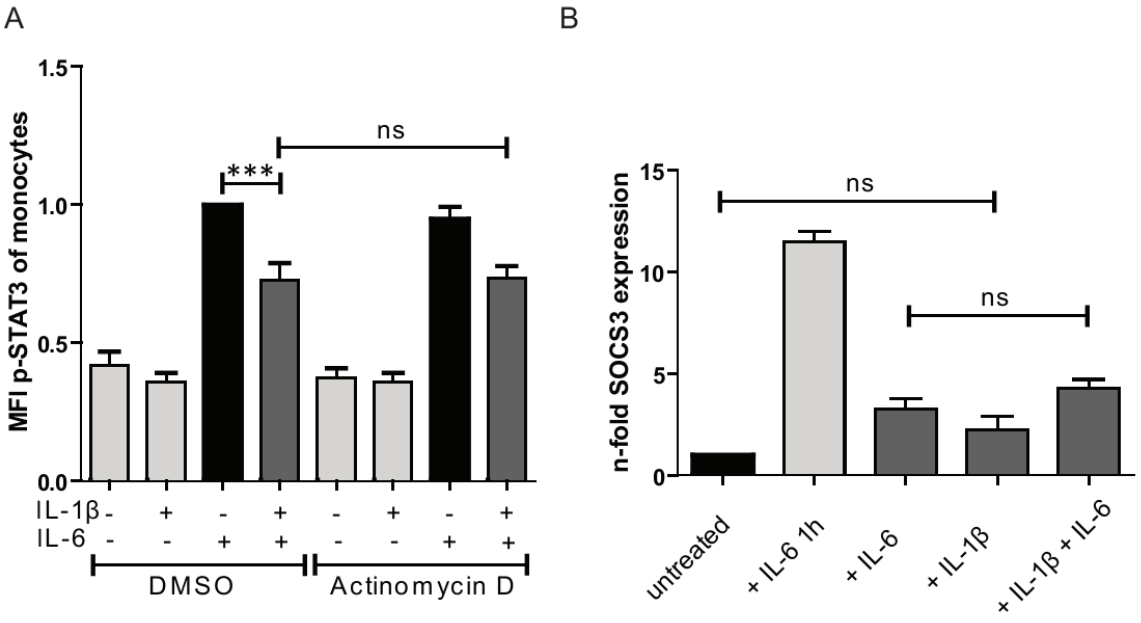

Figure 3-4: Influence of SOCS on IL-1β-mediated inhibition of STAT3 phosphorylation.
A) FACS analysis of STAT3 phosphorylation (2.2.2.4.2). After incubation with actinomycin D (5 µg/ml) or the carrier DMSO for 30 min, PBMCs were stimulated with IL-6 (20 ng/ml) for 10 min. For co-stimulation IL-1β (20 ng/ml) was added 20 min prior to the addition of IL-6. Cells were fixed and permeabilized followed by the incubation with antibodies against p-STAT3 and CD14. FACS analysis was performed and 5000 $CD14^+$ cells were recorded. MFI of p-STAT3 within the $CD14^+$ population was used for statistical analysis and values measured for IL-6-treated cells, pre-incubated with DMSO, were set to 1. Bars represent mean values plus SEM (n = 5); ns = not significant; *** $p<0.001$ (one-way ANOVA with Bonferroni's Multiple Comparison Test). B) Quantitative RT-PCR (2.2.4.9). PBMCs were incubated with IL-6 (20 ng/ml) for 1 h as positive control, or for 10 min. IL-1β (20 ng/ml) was added 20 min prior to IL-6 for co-stimulation. RNA was isolated (2.2.4.2) and transcribed to cDNA (2.2.4.3) before being used for quantitative RT-PCR. The expression of *SOCS3* was adjusted to expression of the housekeeping gene *RPL* and values for untreated cells were set to 1. Bars represent mean values of n-fold *SOCS3* expression plus SEM (n = 4); ns = not significant (one-way ANOVA with Bonferroni's Multiple Comparison Test).

Taken together, the results show that IL-1β exerted an inhibitory effect on IL-6-induced STAT3 activation. This effect was independent of protein synthesis and thus of the feedback inhibitor SOCS3.

3.1.3 The role of p38 in crosstalk inhibition of IL-6 signaling

It has been described earlier that feedback inhibition in hepatocytes and macrophages depends on the MAPK p38 (Ahmed and Ivashkiv, 2000; Radtke et al., 2010). We therefore investigated the role of p38 in our model. First of all, the induction of p38 phosphorylation by IL-1β was tested by flow cytometry after different periods of time. CD14 was co-stained and the MFI for p-p38 within the monocyte population was determined. As shown by the black histogram in figure 3-5, p38 was activated after 10 min of IL-1β stimulation. At the 20 min time point the amount of phosphorylated p38 was slightly decreased again and after 30 min it had almost reached baseline levels. Barely any p-p38 was measurable after 45 min of stimulation.

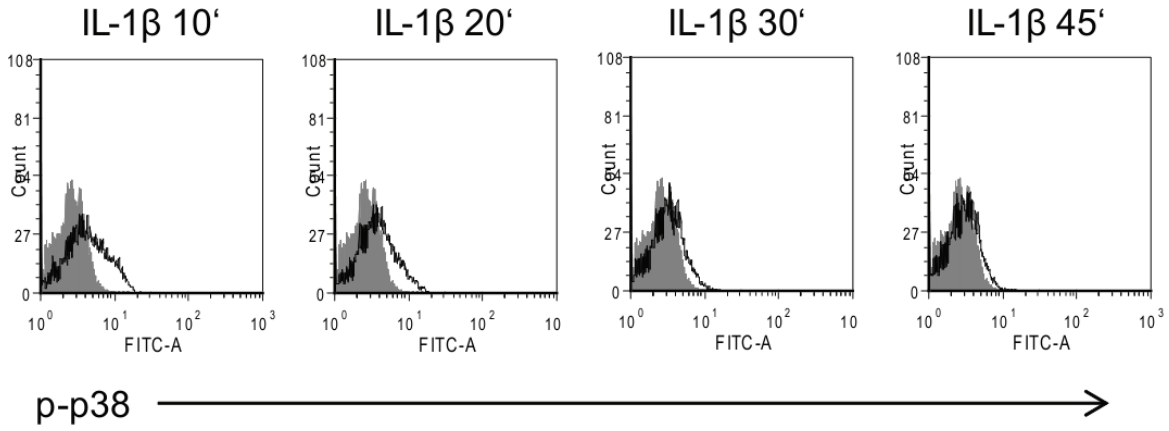

Figure 3-5: Activation of p38 after IL-1β stimulation.
FACS analysis of p38 phosphorylation (2.2.2.4.2). PBMCs were incubated with IL-1β (20 ng/ml) for 10, 20, 30 or 45 min, fixed, permeabilized and incubated with antibodies against p-p38 and CD14. 5000 $CD14^+$ cells were recorded and expression of p-p38 within the monocyte population is shown. Filled histograms represent MFI of untreated cells, black lines of stimulated cells. One representative experiment out of 3 is shown.

In the next experiments, the influence of a p38-specific inhibitor on gp130 surface expression and IL-6-induced STAT3 phosphorylation after IL-1β treatment was examined by flow cytometry. PBMCs were incubated with IL-1β in the presence or absence of the p38 inhibitor SB202190 and gp130 expression on $CD14^+$ cells was measured. Figure 3-6 A shows that inhibition of p38 rescued the decreased gp130 expression after stimulation with IL-1β. To investigate whether this restored cell surface expression was reflected in the level of STAT3 phosphorylation, PBMCs were stimulated with IL-1β or left untreated before the addition of IL-6. Duplicates of each sample were prepared and pre-stimulated with SB202190 or DMSO

as control, respectively. As indicated by figure 3-6 B, IL-6-induced STAT3 phosphorylation was reduced by IL-1β in DMSO-treated cells by approximately 60%. However, in cells stimulated with SB202190 the inhibitory effect of IL-1β was absent.

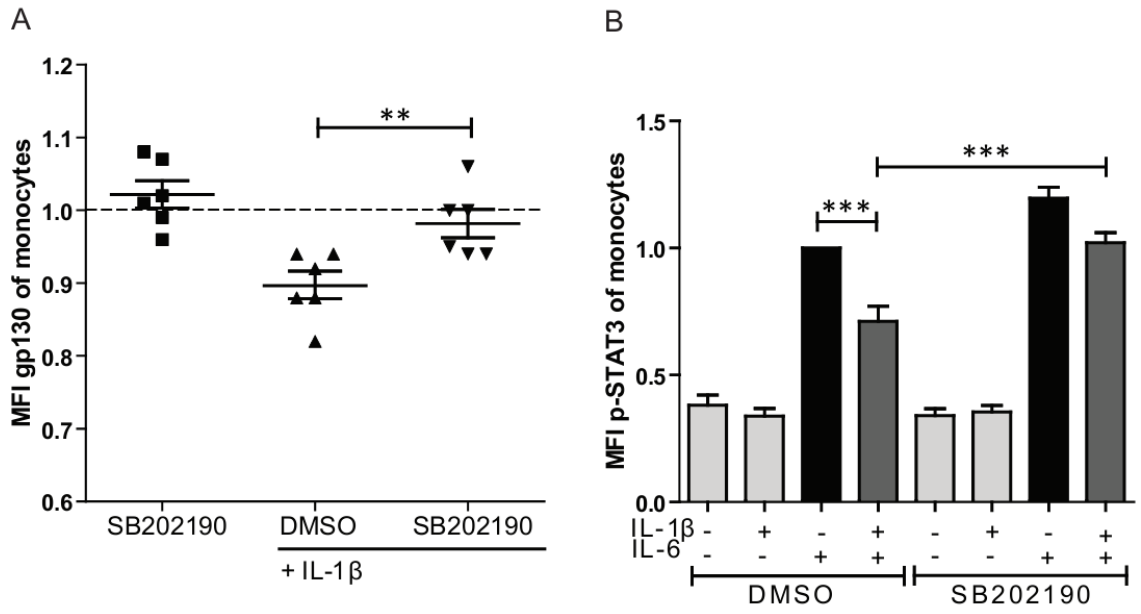

Figure 3-6: Influence of SB202190 on crosstalk inhibition by IL-1β.
A) FACS analysis of cell surface gp130 expression (2.2.2.4.1). After incubation with SB202190 (1 µM) or DMSO for 30 min, PBMCs were stimulated with IL-1β (20 ng/ml) for 20 min or left untreated. PBMCs were stained with antibodies against gp130 and CD14 and 5000 $CD14^+$ cells were recorded. MFI values of untreated monocytes were set to 1. Symbols indicate individual values and horizontal lines represent mean plus SEM (n = 6); ** $p<0.01$ (two-tailed, paired t-test). B) FACS analysis of p-STAT3 (2.2.2.4.2). PBMCs were pre-treated with SB202190 (1 µM) or DMSO for 30 min followed by stimulation with IL-6 (20 ng/ml) for 10 min. For co-stimulation IL-1β (20 ng/ml) was added 20 min prior to the addition of IL-6. Cells were fixed and permeabilized followed by the incubation with antibodies against p-STAT3 and CD14. FACS analysis was performed and 5000 $CD14^+$ cells were recorded. MFI of p-STAT3 within the $CD14^+$ population is shown and values measured for DMSO- and IL-6-treated cells were set to 1. Bars represent mean values plus SEM (n = 5); *** $p<0.001$ (one-way ANOVA with Bonferroni's Multiple Comparison Test).

3.1.4 Influence of IL-1β on phosphorylation of serine 782

Different studies have shown that the internalization of gp130 is dependent on a di-leucine motif within its cytoplasmic domain (Dittrich et al., 1994). It was suggested that serine 782, located in close proximity to the di-leucine motif, serves as a stress sensor, regulating the internalization process and thus the availability of gp130 on the cell surface (Gibson et al., 2000; Radtke et al., 2010). Phosphorylation of this residue was therefore examined in response to IL-1β in monocytes. PBMCs were derived from human blood and monocytes

were isolated from PBMCs. Monocytes were at least 70% pure, as determined by FACS analysis shown in figure 3-7 A. Cells were stimulated with IL-1β or left untreated and this was followed by cell lysis and immunoprecipitation of gp130. Phosphorylation of serine 782 was detected in a western blot, illustrated by figure 3-7 B. After stimulation with IL-1β a slightly stronger phosphorylation was observed compared to untreated cells. The blot was stripped and re-probed with an antibody against gp130 to exclude the possibility that the total amount of gp130 differed between treated and non-treated cells. As the lower panel illustrates, the quantity of gp130 was unaffected.

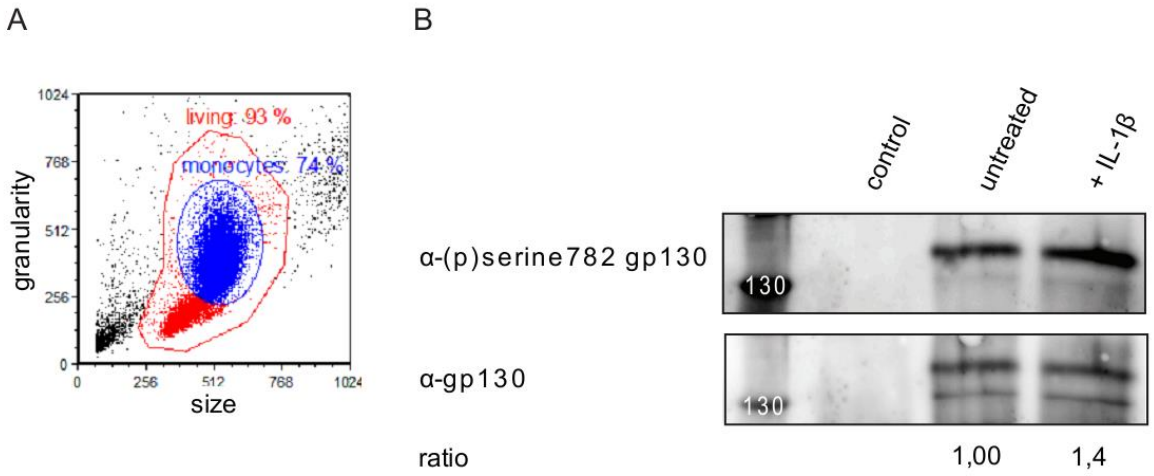

Figure 3-7: Phosphorylation of serine 782 after IL-1β treatment.
A) Monocytes were isolated (2.2.2.2) and properties of size and granularity were analyzed by FACS analysis. The gating for this population of monocytes was based on their well-characterized size and granularity. B) Immunoprecipitation (2.2.3.5). Monocytes (purity 70-80%) were stimulated with IL-1β (20 ng/ml) for 20 min or left untreated. Cells were lysed with RIPA buffer and clarified lysates or RIPA buffer alone were incubated with α-gp130 and protein G beads. Serine phosphorylation of immunoprecipitated gp130 was monitored by immunoblotting. The blot was stripped and re-probed with an antibody against gp130 to ensure equal loading. One representative experiment out of 5 is shown. Quatification is shown as ratio of phosphorylated:unphosphorylated protein and was set to 1 for untreated cells.

Compared to untreated monocytes, phosphorylation of serine 782 in the cytoplasmic tail of gp130 was enhanced after stimulation with IL-1β.

3.2 *In vivo* relevance of receptor internalization – a mouse model

To investigate whether the observed crosstalk mechanism in human monocytes is of relevance *in vivo*, we decided to generate transgenic mice with alterations of gp130 serine phosphorylation sites. The vav promoter was used to drive overexpression stably throughout the hematopoietic compartment. Vav is expressed in all hematopoietic cells but is hardly found in other cell types (Ogilvy et al., 1999). According to figure 3-8, two different constructs were cloned. In the first one, gp130 wildtype was included (transgenic mice are referred to as gp130-wt). This strain was supposed to serve as control for the second mouse line to be established where a mutated gp130 was inserted (referred to as gp130-mut).

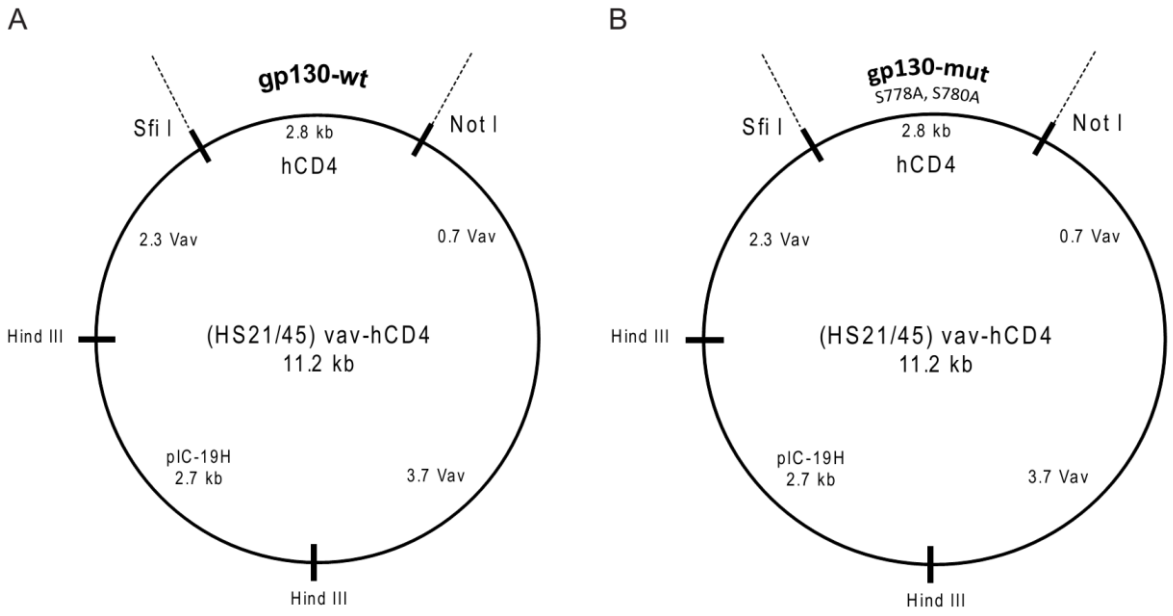

Figure 3-8: Constructs used to establish two trangenic mouse strains.
HS21/45 vav-hCD4 vector was digested with the restriction enzymes Sfi I and Not I to remove hCD4 element and insert gp130-wt (A) or gp130-mut (B).

The mutation changes serine 778 and serine 780 to alanines. These residues, analogous to serine 780 and serine 782 in the human receptor (figure 3-9), might be critical for internalization in response to stress stimuli. Since alanine prevents phosphorylation, the mutation should inhibit potential crosstalk regulation of IL-6 signaling in gp130-mut mice.

Figure 3-9: Protein alignment of cytoplasmic fragment of human and murine gp130.
One letter code for amino acids is shown. Section contains the di-leucine internalization motif in blue and the two upstream serine residues are shown in red.

3.2.1 Determination of gp130 expression and STAT3 phosphorylation

After generation of the two transgenic mouse lines the animals were analyzed. No phenotypic differences were observed in any of them compared to mice without transgene (referred to as wt). Quantitative RT-PCR from splenocytes was performed to investigate mRNA levels of *gp130* in transgenic mice compared to wt mice. As shown in figure 3-10, transgenic mice displayed increased levels of *gp130* mRNA. Approximately 4-fold levels were found in splenocytes of gp130-wt mice, whereas in gp130-mut splenocytes 3-fold levels were detected compared to wt mice.

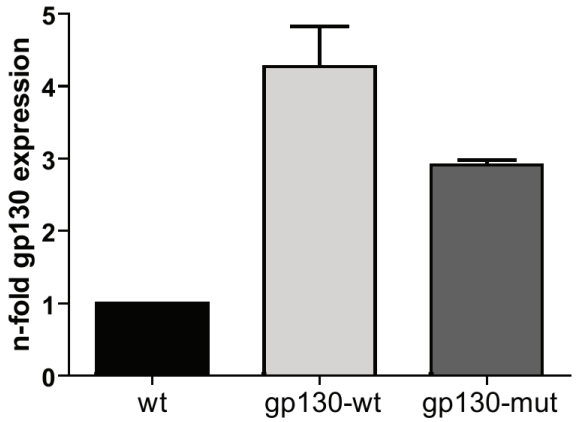

Figure 3-10: Expression of gp130 mRNA in wt and transgenic mice.
Quantitative RT-PCR (2.2.4.9) of splenocytes. Cells were isolated and RNA was prepared (2.2.4.2). After transcription to cDNA (2.2.4.3), quantitative RT-PCR was performed. The expression of *gp130* was adjusted to the housekeeping gene *actin*. Bars represent n-fold expression of *gp130* compared to expression level of wt splenocytes, which were set to 1. Bars show mean plus SEM (n = 3).

After confirmation that transgenes were present not only at the genomic level, but that also enhanced levels of gp130 mRNA could be found in splenocytes of transgenic animals, we investigated cell surface expression of gp130 on different hematopoietic cells. Since the aim of this mouse model was to find out whether the cell surface expression of gp130 was influenced by the mutation of serine 778/780, gp130-mut mice were compared to gp130-wt animals. Basal expression was analyzed in peripheral blood (PB) by flow cytometry. As shown in figure 3-11 A, gp130-mut animals exhibited significantly lower gp130 expression on whole living cells from PB compared to gp130-wt mice. To investigate in which leukocyte subset these changes were visible, different markers were co-stained. By gating to these populations, gp130 expression was analyzed on $CD3^+$ T cells, $CD19^+$ B cells and $CD11b^+$ myeloid cells. Values for gp130-wt mice were set to 1 and the expression on gp130-mut cells is shown in figure 3-11 B. Expression of gp130 differed on gp130-mut $CD19^+$ and $CD11b^+$ subsets where decreased amounts of the receptor on the cell surface were detected compared to gp130-wt cells. This tendency was also visible for T cells, however, the lowest expression level of gp130 compared to gp130-wt was determined for B cells.

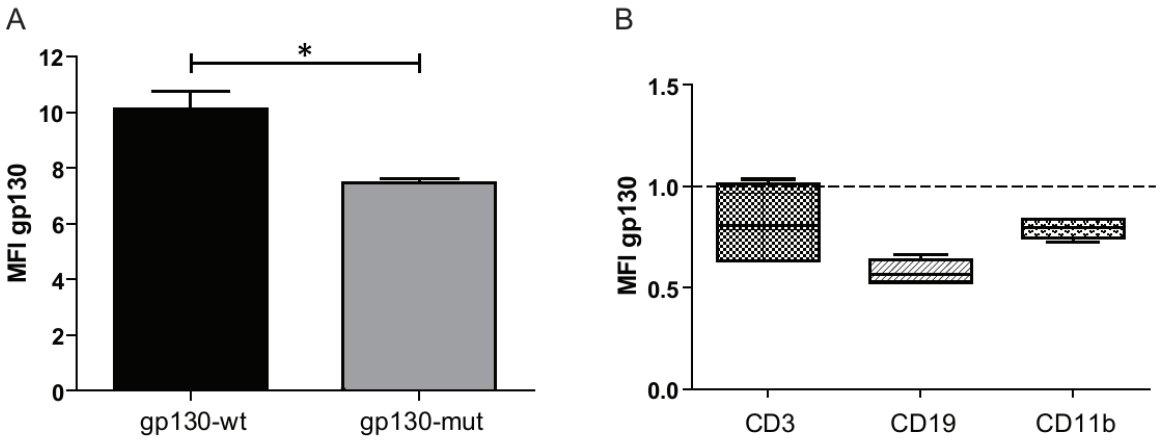

Figure 3-11: Expression of gp130 on different leukocyte subsets from PB.
Flow cytometric analysis of cell surface expression from whole blood (2.2.2.4.3). After fixation of cells with PFA, erythrocytes were lysed followed by incubation with antibodies against gp130, CD3, CD19 and CD11b. Gates were set to whole living cells (A), $CD3^+$, $CD19^+$ or $CD11b^+$ cells (B) and MFI of gp130 within the particular population was determined. A) Bars represent mean plus SEM (n = 7 for gp130-wt, n = 4 for gp130-mut); * $p<0.05$ (two-tailed, unpaired t-test). B) Values measured for gp130-wt splenocytes were set to 1. Boxes show MFI values for gp130 within the indicated cell populations from gp130-mut mice. Boxes and whiskers represent values from min to max, horizontal line represents mean (n = 7 for gp130-wt, n = 4 for gp130-mut).

To investigate whether the observed differences were visible on splenocytes as well, the same flow cytometric analysis was performed with this cell type. In contrast to PB cells,

gp130 expression on whole living splenocytes did not differ between gp130-wt and gp130-mut as can be seen in figure 3-12 A. Expression in subpopulations was determined to establish whether subtle differences were apparent on T cells, B cells or myeloid cells. Figure 3-12 shows the expression of gp130 on the indicated cell population isolated from gp130-mut in relation to gp130-wt. While slightly reduced expression levels on $CD3^+$ cells could be observed, no changes were detected for $CD19^+$ or $CD11b^+$ cells.

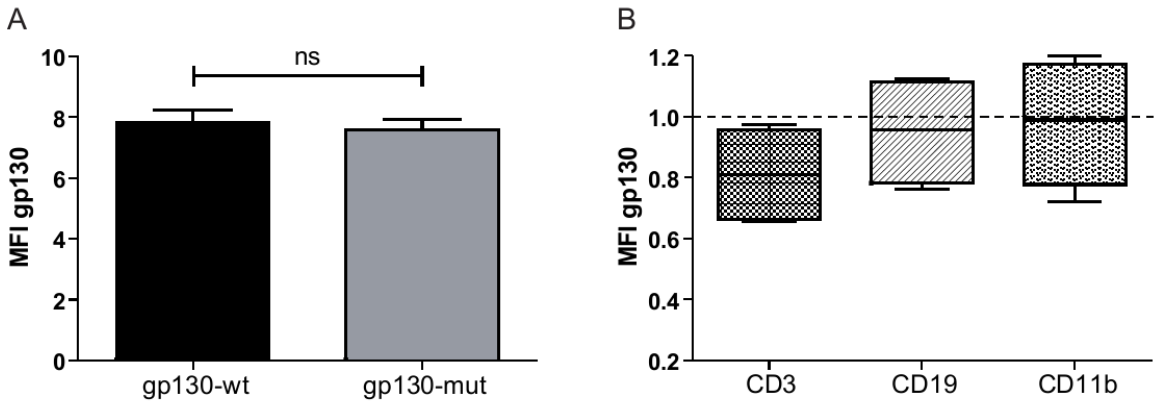

Figure 3-12: Expression of gp130 on different splenocyte subsets.
FACS analysis of cell surface expression (2.2.2.4.1). Cells were isolated from spleens and incubated with antibodies against gp130, CD3, CD19 and CD11b. Gates were set to whole living cells (A) $CD3^+$, $CD19^+$ or $CD11b^+$ (B) and gp130 expression within the different populations was determined as MFI. A) Bars represent mean plus SEM (n = 7 for gp130-wt, n = 4 for gp130-mut); ns = not significant (two-tailed, unpaired t-test). B) Values obtained for gp130-wt were set to 1. Boxes show MFI values for gp130 within the indicated cell populations from gp130-mut mice. Boxes and whiskers represent values from min to max, horizontal lines represent mean (n = 7 for gp130-wt, n = 4 for gp130-mut).

For further analyses we decided to use splenocytes, since they are easy to isolate and high numbers of cells can be recovered. STAT3 phosphorylation was determined at baseline and after stimulation with IL-6. Figure 3-13 A shows the amount of p-STAT3 in splenocytes isolated from gp130-mut mice in relation to cells from gp130-wt without any stimulation. MFI of p-STAT3 was determined within the indicated subpopulations and values for gp130-wt were set to 1. Basal STAT3 activation did not differ significantly in any of the three cell populations of gp130-mut mice compared to gp130-wt. However, after IL-6 stimulation STAT3 was activated significantly stronger in the T cell population of gp130-mut splenocytes compared to gp130-wt, as illustrated in figure 3-13 B. Values relative to basal STAT3 phosphorylation are shown. From figure 3-13 C and D it can be seen that STAT3 induction did not differ between gp130-mut and gp130-wt in $CD19^+$ and $CD11b^+$ cells, respectively.

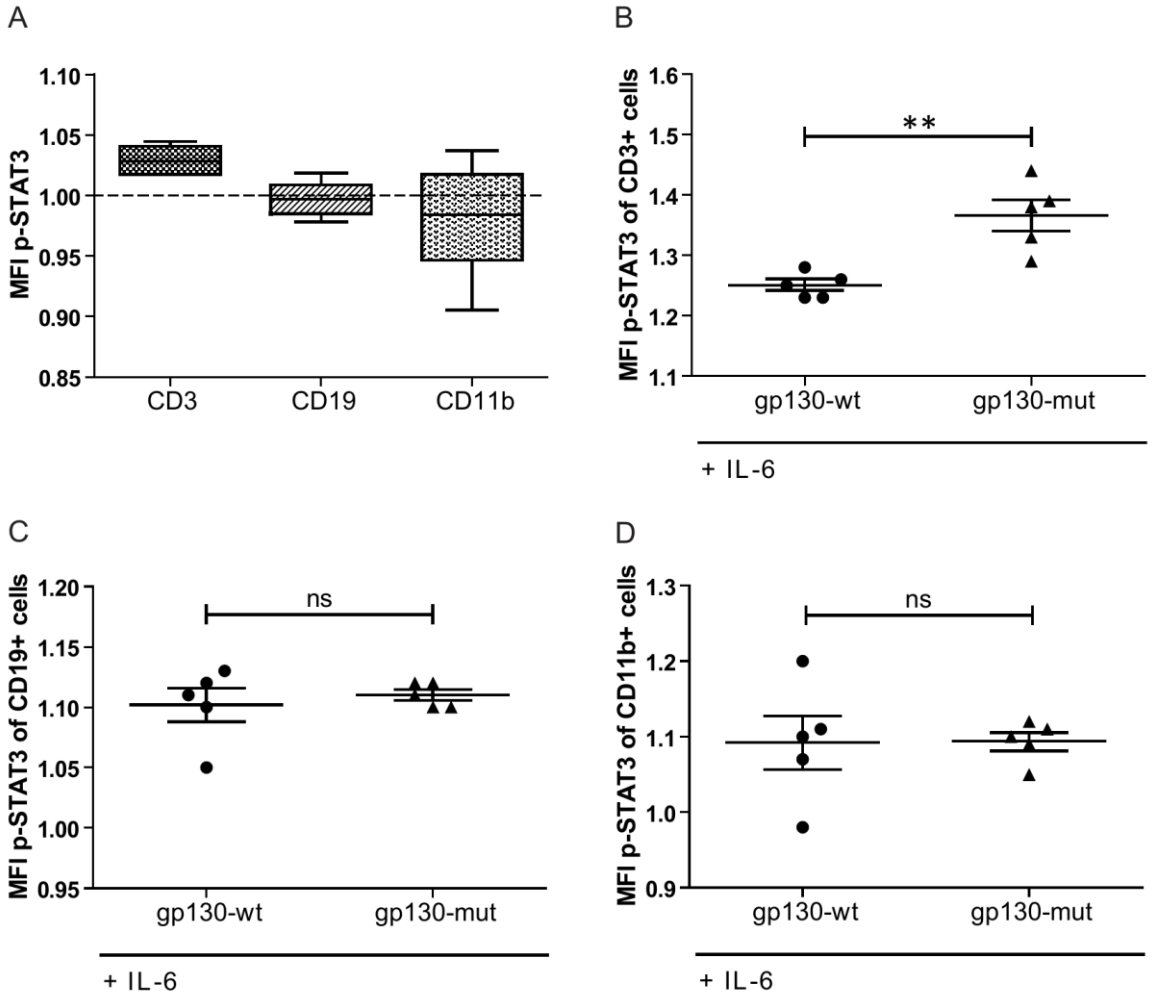

Figure 3-13: Expression of p-STAT3 in different leukocyte subsets from splenocytes.
FACS analysis of p-STAT3 (2.2.2.4.2). After fixation and permeabilization, cells were incubated with antibodies against p-STAT3, CD3, CD19 and CD11b. Gates were set to CD3, CD19 or CD11b and MFI values for p-STAT3 within the populations were determined. A) MFI values obtained for gp130-wt were set to 1. Boxes and whiskers show values from min to max, horizontal lines represent mean (n = 5). B-D) Prior to fixation cells were stimulated with IL-6 (20 ng/ml) for 10 min. MFI values measured for untreated cells were set to 1. Horizontal lines represent mean plus SEM (n = 5); ns = not significant (two-tailed, unpaired t-test); ** p<0.01 (two-tailed, unpaired t-test).

Taken together, an increased expression of *gp130* mRNA was observed for splenocytes from both mouse strains compared to wt animals. On the level of cell surface expression, no changes could be detected on different splenocytes subsets, while $CD19^+$ and $CD11b^+$ PB cells from gp130-mut mice displayed decreased gp130 surface expression in comparison to gp130-wt PB cells. STAT3 phosphorylation in response to IL-6 was stronger in $CD3^+$ splenocytes from gp130-mut mice than in those from gp130-wt animals.

3.2.2 Influence of IL-1β on gp130 expression and STAT3 activation

In human monocytes stimulation with IL-1β resulted in downregulation of gp130 surface expression and restriction of IL-6-induced STAT3 phosphorylation. These effects depended on the MAPK p38 and probably on the phosphorylation of serine 782 within the cytoplasmic tail of gp130. Since in the gp130-mut mice the analogous serine residues are mutated to alanine and should therefore prevent phosphorylation, in the next experiments the influence of IL-1β on gp130 cell surface expression and STAT3 phosphorylation was compared between the two mouse strains. Splenocytes were stimulated with IL-1β and gp130 expression was determined by flow cytometry. Figure 3-14 A shows gp130 expression on the surface of whole splenocytes from gp130-mut compared to gp130-wt. Values measured for untreated cells were set to 1. After stimulation with IL-1β a slight decrease of gp130 cell surface expression on gp130-wt splenocytes was observed, which was not apparent in cells from gp130-mut mice. To investigate whether this tendency was more pronounced within one distinct cell population, gp130 expression was again examined on T cells, B cells and myeloid cells after IL-1β stimulation. As can be seen in figure 3-14 B, $CD3^+$ T cells did not turn out to be the population that caused the tendency observed for total splenocytes. No downregulation of gp130 on T cells was visible after incubation with IL-1β, either in gp130-wt, or in gp130-mut T cells. In contrast, on B cells as well as on myeloid cells from gp130-wt animals, IL-1β caused a small decrease of gp130 surface expression as shown in figure 3-14 C and D, respectively. This decrease was, however, not detected in $CD19^+$ or $CD11b^+$ splenocyte subsets from gp130-mut mice.

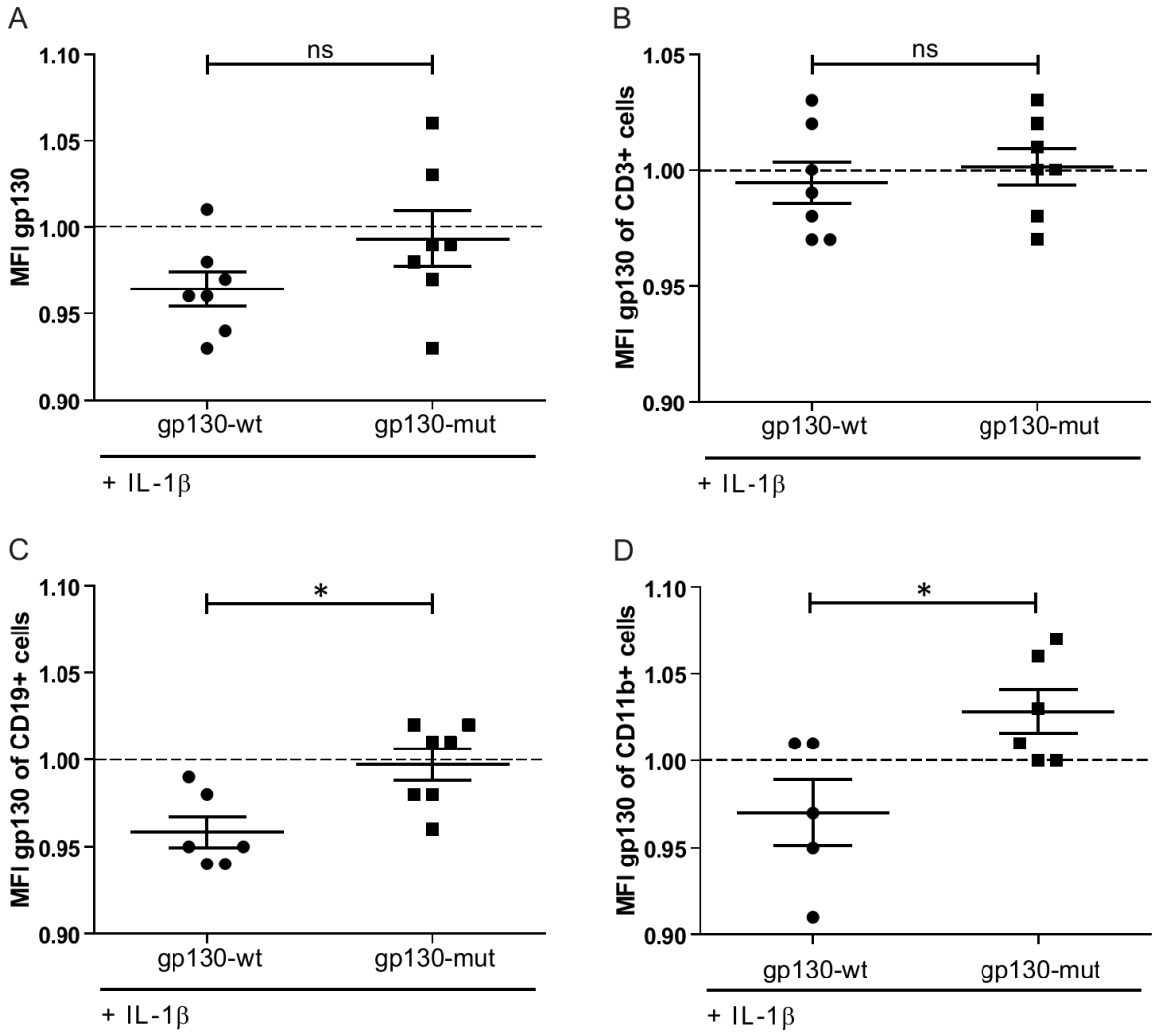

Figure 3-14: Influence of IL-1β on gp130 surface expression.
FACS analysis of cell surface expression (2.2.2.4.1). Splenocytes were stimulated with IL-1β (20 ng/ml) for 20 min or left untreated prior to staining with antibodies against gp130, CD3, CD19 and CD11b. Gates were set to total living cells (A), $CD3^+$ (B), $CD19^+$ (C) or $CD11b^+$ cells (D) and MFI of gp130 was determined. Values for untreated cells were set to 1. Horizontal line represents mean plus SEM (n = 7 for A and B, n = 6 for C and n = 5 for D); ns = not significant (two-tailed, unpaired t-test), * $p<0.05$ (two-tailed Mann Whitney test for C, two-tailed, unpaired t-test for D).

To investigate whether the changes of gp130 cell surface expression were reflected in downstream signaling, STAT3 phosphorylation was examined. Splenocytes were incubated with IL-1β prior to the addition of IL-6 and p-STAT3 was determined by flow cytometry. Control cells were stimulated with IL-1β alone. As shown in figure 3-15 A, an incubation with IL-1β did not have any influence on basal STAT3 phosphorylation, irrespective of the population being considered. Values for untreated cells were set to 1. In figure 3-15 B-D IL-6-induced STAT3 activation after pre-treatment with IL-1β is shown in relation to stimulation with IL-6 alone. No changes between gp130-wt and –mut could be observed in

T cells (figure 3-15 B). STAT3 phosphorylation was marginally reduced in gp130-mut compared to gp130-wt B cells (figure 3-15 C). A tendency was also observed for $CD11b^+$ splenocytes: IL-6-induced STAT3 activation was decreased in gp130-wt compared to gp130-mut, as shown in figure 3-15 D.

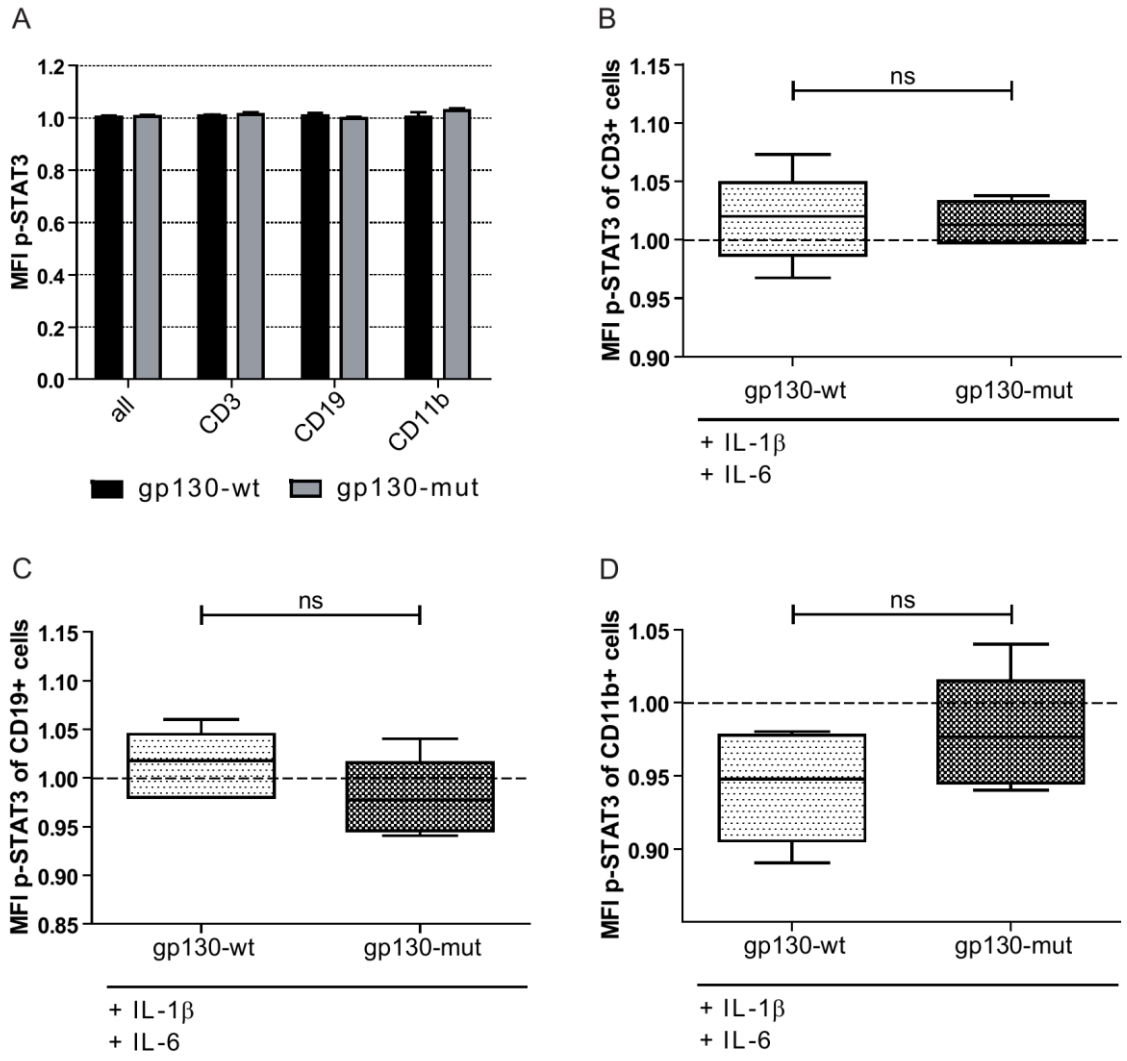

Figure 3-15: Influence of IL-1β on IL-6-induced STAT3 phosphorylation.
FACS analysis of p-STAT3 (2.2.2.4.2). A) Splenocytes were stimulated with IL-1β for 20 min or left untreated. Cells were fixed and permeabilized before the incubation with antibodies against p-STAT3, CD3, CD19 and CD11b. MFI values for p-STAT3 were determined within the indicated populations. Values for untreated cells were set to 1. Black bars represent mean plus SEM for gp130-wt (n = 5), grey bars show mean plus SEM for gp130-mut (n = 5). B-D) Splenocytes were stimulated with IL-6 (20 ng/ml) for 10 min to induce STAT3 phosphorylation. IL-1β (20 ng/ml) was added 20 min prior to the addition of IL-6. Cells were fixed and permeabilized before being stained with antibodies against p-STAT3, CD3, CD19 and CD11b. MFI of p-STAT3 was determined within gates set to $CD3^+$ (B), $CD19^+$ (C) or $CD11b^+$ cells (D). Values measured for cells treated with IL-6 were set to 1. Boxes and whiskers show values from min to max, horizontal lines show mean (n = 5); ns = not significant (two-tailed, unpaired t-test).

In summary, IL-1β induced a slight downregulation of gp130 surface expression on $CD19^+$ and $CD11b^+$ splenocyte subsets of gp130-wt mice. This downregulation, however, was not observed for the respective leukocyte subsets of gp130-mut mice. This resulted in significant differences between the two transgenic mouse strains regarding gp130 downregulation in response to IL-1β. T cells were resistant to regulation of gp130 surface expression by IL-1β in both mouse strains. This was reflected in the level of downstream signaling inasmuch as IL-1β did not have any influence on IL-6-induced STAT3 phosphorylation in T cells of gp130-wt or –mut mice. In contrast, the observed downregulation of gp130 on gp130-wt B cells in response to IL-1β was not translated to the level of STAT3 phosphorylation. In gp130-wt myeloid cells IL-6-induced STAT3 activation was slightly diminished after IL-1β stimulation, which was less pronounced in the respective cell population of gp130-mut mice.

3.2.3 Migration of leukocytes into the peritoneal cavity

In the human system IL-6 acts as a migration factor in $CD14^+$ monocytes by inducing upregulation of adhesion molecules and reorganization of the actin cytoskeleton (Clahsen and Schaper, 2008). Moreover, IL-6 knockout mice display impaired migration of leukocytes to sites of inflammation and mice deficient in gp130 likewise show reduced migration of myeloid cells (Romano et al., 1997; Sander et al., 2008). We therefore used a model of zymosan-induced peritonitis in gp130-wt and –mut mice to explore migration of myeloid cells into the peritoneal cavity. Animals were injected intraperitoneally with zymosan and cells were collected 24 h after injection from the peritoneal cavity. Total cell numbers were determined and quantities of myeloid cells were analyzed by flow cytometry. Figure 3-17 shows that in gp130-mut mice significantly increased cell numbers could be recovered compared to gp130-wt mice. Cells positive for the myeloid marker $CD11b^+$ but negative for the macrophage marker F4/80, i.e. neutrophils and monocytes, were found in enhanced numbers in peritoneal cavities of gp130-mut mice compared to gp130-wt. However, these changes were not significant. The quantity of macrophages, which are characterized by carrying CD11b and F4/80, was not altered between the two mouse strains.

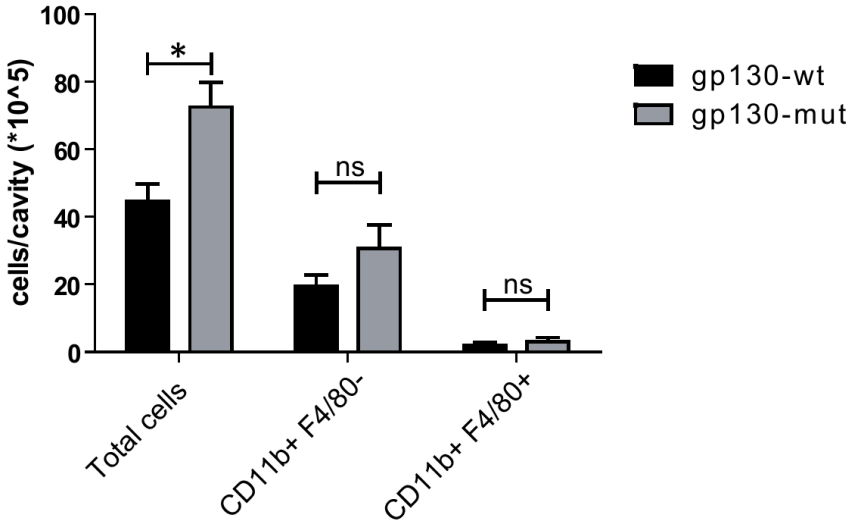

Figure 3-16: Migration of leukocytes into the peritoneal cavity after administration of zymosan. Mice were injected i.p. with 1 ml of zymosan and cells from peritoneal cavity were collected by lavage 24 h later (2.2.1.4). Cell numbers were determined by counting with a Neubauer haemocytometer. Subsequently, cells were incubated with antibodies against CD11b and F4/80 and analyzed by flow cytometry (2.2.2.4.1). Gates were set to $CD11b^{+}F4/80^{-}$ or $CD11b^{+}F4/80+$ and percentages of cells within the respective gates were related to the total cell number. Bars show mean plus SEM (n = 6 for gp130-wt and n = 3 for gp130-mut); ns = not significant (two-tailed, unpaired t-test), * $p<0.05$ (two-tailed, unpaired t-test).

In gp130-mut mice more cells, and by trends more $CD11^{+}F4/80^{-}$ cells, were collected from peritoneal cavities compared to gp130-wt animals. No changes were observed in the numbers of macrophages.

3.3 Regulation of gp130 signaling in chronic inflammation

Since IL-6 signaling plays an important role in different inflammatory disorders, we sought to examine the regulatory status of gp130 in children suffering from IBD and JIA. Both conditions are accompanied by increased serum levels of IL-6, TNF-α and IL-1β. Biologic agents have been developed against all these cytokines and are used clinically. Whereas some patients respond well, the same treatment is only partly effective if at all in others. Biological parameters to indicate responsiveness of patients, toxicity or prognosis are lacking and it is therefore difficult to choose a suitable medication (McInnes and Schett, 2011). The combined effects of different cytokines in chronic inflammatory situations create a complex network, and crosstalk between these cytokines most likely is of high relevance for the biological outcome. As cytokine crosstalk had been found to influence the expression of gp130 on human monocytes in *in vitro* experiments, we asked whether gp130 cell surface expression might be changed in patients with chronic inflammation and if downstream signaling might be altered.

3.3.1 Inflammatory bowel disease

3.3.1.1 Pediatric IBD patients

To investigate whether the cell surface expression of gp130 might be changed during the course of IBD, blood was taken from pediatric IBD patients during routine blood withdrawal. Blood from healthy donors was obtained as control. Gp130 expression on monocytes was compared between healthy controls and IBD patients by FACS analysis. Figure 3-17 A shows the gating on $CD14^{high}$ monocytes, exemplified by a representative dot plot. Histograms demonstrate upregulation of gp130 expression on monocytes derived from PB of IBD patients (lower panel) compared to those from healthy control (upper panel). This significant increase in gp130 measured on the cell surface is displayed as scatter plot for a total of 21 patients in figure 3-17 B. To examine whether the expression of the complete IL-6 receptor complex was changed, the level of IL-6R was analyzed on the cell surface of monocytes from IBD patients and healthy controls. Expression levels did not differ significantly between the two groups, as is clearly visible in figure 3-17 C.

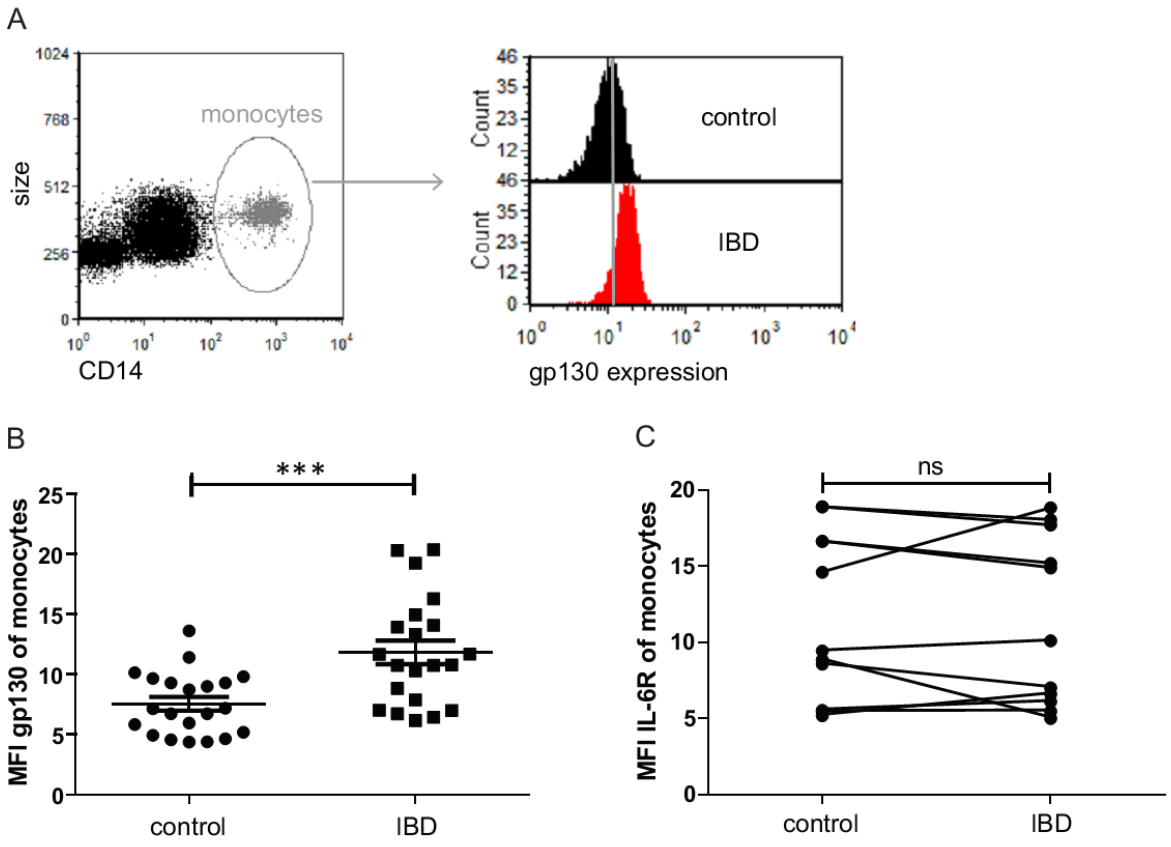

Figure 3-17: Cell surface expression of gp130 and IL-6R of PB monocytes from IBD patients compared to healthy controls.

FACS analysis of cell surface expression from whole blood (2.2.2.4.2). Cells were fixed with 1% (w/v) PFA and erythrocytes were lysed by incubation with lysis buffer prior to staining. Antibodies against gp130 and CD14 (A, B) or IL-6R and CD14 (C) were used. The gate was set to $CD14^+$ cells. A) Representative dot plot and histograms. Dot plot demonstrates gating to monocytes and stacked histograms show MFI of gp130 within the monocyte population of a healthy control (upper panel) and an IBD patient (lower panel). B) Symbols indicate MFI of gp130 within the monocyte population from individual donors and horizontal lines represent mean values plus SEM; *** $p<0.001$ (two-tailed Wilcoxon signed rank test; n = 21). C) Symbols show MFI of IL-6R within the monocyte population from individual donors. Horizontal lines represent mean values plus SEM; ns = not significant (two-tailed Wilcoxon signed rank test; n = 11).

We next asked whether downstream signaling was affected by the enhanced amount of gp130 on the cell surface and investigated STAT3 phosphorylation in PB monocytes of IBD patients in comparison to healthy controls. Enhanced STAT3 activation in monocytes of an IBD patient compared to a healthy control is shown in figure 3-18 A on the basis of representative dot plots. While only about 16% of the monocytes derived from control blood are positive for p-STAT3, approximately 54% of the monocytes from IBD blood show p-STAT3 staining. Figure 3-18 B illustrates the change of STAT3 activation in monocytes of

children with IBD compared to healthy controls summarized for 15 tested individuals. Differences are significant with p<0.01.

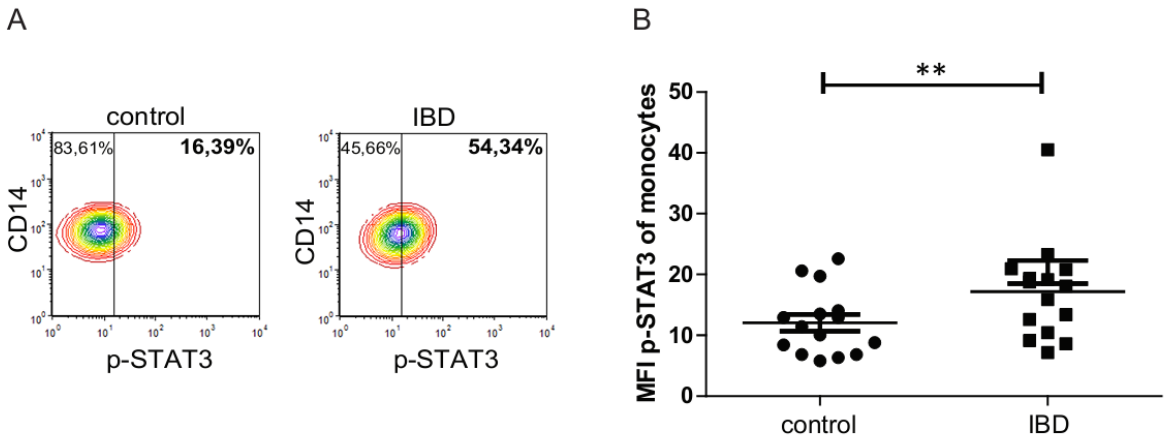

Figure 3-18: STAT3 phosphorylation in PB monocytes of IBD patients and healthy controls. FACS analysis of p-STAT3 from whole blood (2.2.2.4.3). Prior to staining with antibodies against p-STAT3 and CD14 cells were fixed with 1% (w/v) PFA, erythrocytes were lysed by incubation with lysis buffer and permeabilization was achieved by incubation with ice-cold methanol. The gate was set on $CD14^+$ cells. A) Representative dot plots showing the percentage of p-STAT3 expressing monocytes of healthy control (left) and IBD patient (right). Positive and negative cells were distinguished on the basis of unstained cells. B) Symbols indicate p-STAT3 MFI within the monocyte population of individual donors (n = 15). Horizontal lines represent mean values plus SEM; ** p<0.01 (two-tailed Wilcoxon signed rank test).

The use of biologic agents in the treatment of IBD has emerged as a standard therapeutic strategy in combination with conventional drugs. TNF-α plays a pivotal role in IBD and the first biological therapeutic agent to become available was a monoclonal antibody against this cytokine (Yang et al., 2012). To investigate whether anti-TNF-α therapy had an influence on gp130 expression levels and STAT3 activation in monocytes, PB was obtained from children with IBD before and after the treatment with the chimeric monoclonal anti-TNF-α antibody infliximab. Figure 3-19 A shows a slight, but reproducible, and thus significant downregulation of gp130 expression levels after treatment with infliximab. STAT3 activation was also significantly reduced after infliximab treatment as illustrated in figure 3-19 B.

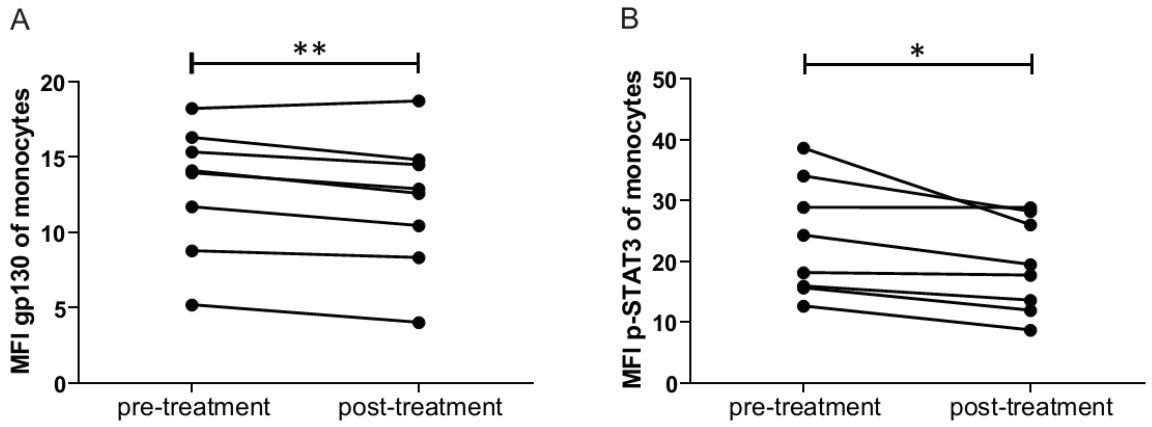

Figure 3-19: Expression of gp130 and p-STAT3 in monocytes from IBD patients before and after treatment with infliximab.

FACS analysis from whole blood (2.2.2.4.3). A) Prior to staining with antibodies against gp130 and CD14 cells were fixed with 1% (w/v) PFA and erythrocytes were lysed. The gate was set to $CD14^+$ cells and MFI of gp130 was determined. Symbols indicate individual patients (n = 8); ** $p<0.01$ (two-tailed, paired t-test). B) Cells were fixed with 1% (w/v) PFA, erythrocytes were lysed and permeabilization was achieved by incubation with ice-cold methanol. For staining, antibodies against p-STAT3 and CD14 were used and MFI of p-STAT3 was determined within $CD14^+$ gate. Symbols indicate individual patients (n = 8), * $p<0.05$ (two-tailed, paired t-test).

Taken together, PB monocytes of children with IBD displayed higher expression levels of gp130 and of p-STAT3. The treatment with an anti-TNF-α antibody resulted in a reduction of gp130 surface expression and STAT3 activation.

3.3.1.2 Chronic colitis in mice

Mouse models of colitis represent immunological models for human IBD. We decided to induce chronic colitis in wildtype mice to analyze cell surface expression of gp130 and downstream signaling. Colitis mediated by the administration of DSS is independent of T and B cells, as it can be established in severe combined immunodeficiency (SCID) mice, where these cell types are absent (Axelsson et al., 1996). To focus on innate immune cells such as monocytes, DSS colitis was chosen as model and to enhance the similarity to the situation in IBD patients the model was applied chronically. For this purpose mice were fed with water containing DSS for one week, followed by normal drinking water for another week. These cycles were repeated and mice were sacrificed on day 37. Throughout the experiment, the weight of the animals was determined every other day. Change of weight from the first day was calculated in %. The resulting curve can be seen in figure 3-20 and shows that control animals that had not received any DSS, gained weight continuously throughout the duration

of the experiment. In contrast, mice with DSS added to their drinking water lost weight after each cycle of DSS. At the end of the 37 days they weighed approximately 8% more than on the first day in comparison to control animals, that gained about 22% of weight.

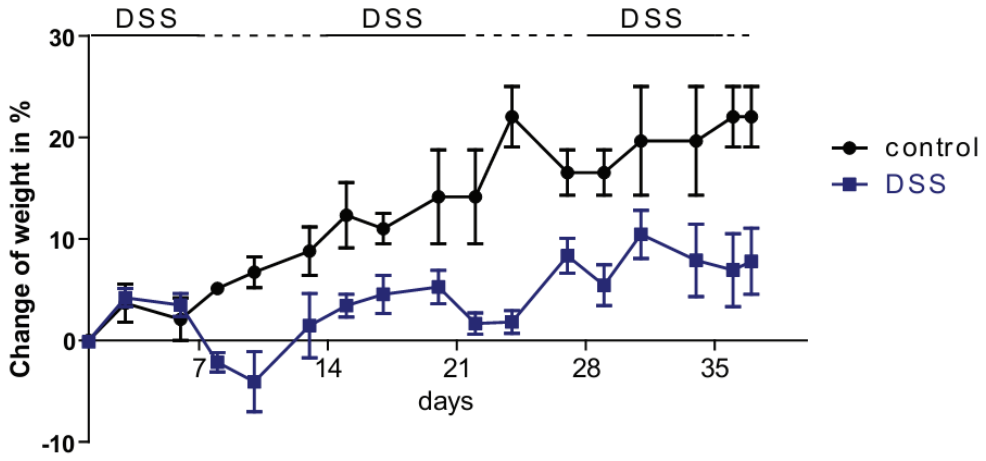

Figure 3-20: Change of weight during chronic colitis.
One group of wildtype mice (n = 6) was supplied with drinking water containing 2.5% (w/v) DSS for one week, followed by normal drinking water for the next week. Cycles were repeated until day 37 to induce chronic colitis (2.2.1.3). Another group of wildtype mice (n = 3) served as control and received normal drinking water throughout the duration of the experiment. Weight of animals was determined every other day and calculated as change in % referred to the weight at the starting day.

Blood was taken on day 1, before the administration of DSS was started, and on day 37. Expression of gp130 and STAT3 phosphorylation was determined by flow cytometry. MFI values of the DSS group were referred to MFI of control animals, which was set to 1. Expression strength was analyzed within the population of $CD11b^+$ myeloid cells. As illustrated in figure 3-21 A, expression of gp130 on $CD11b^+$ cells increased significantly during the course of DSS colitis compared to untreated control animals. Figure 3-21 B shows that downstream signaling, indicated by STAT3 activation, in this cell population was significantly higher on day 37 than on day 1 in comparison to control mice. While on day 1 the MFI values measured for p-STAT3 were identical to those of control mice, a 1.5-fold increase could be determined on day 37 in relation to STAT3 phosphorylation in control animals.

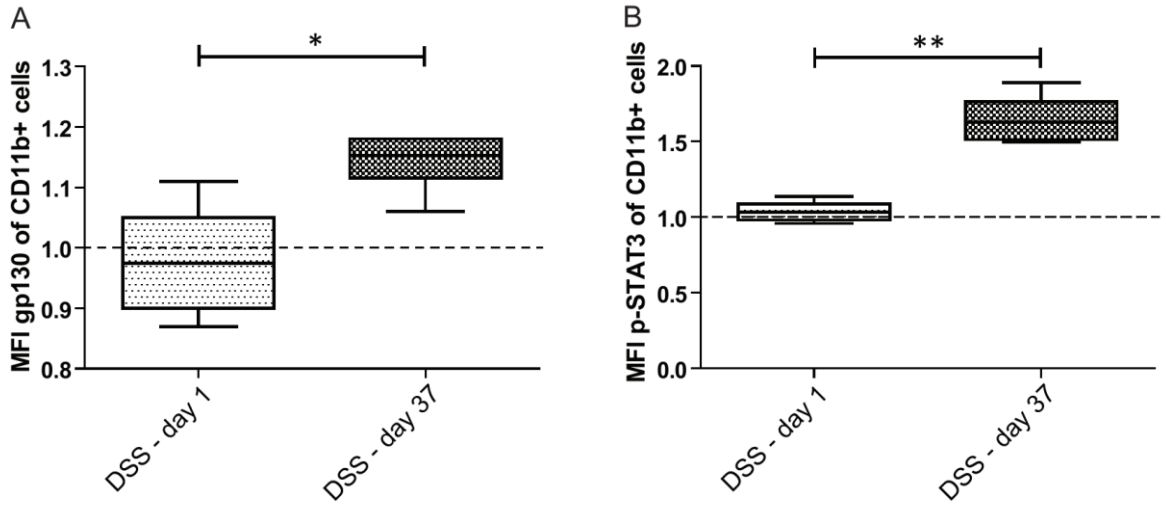

Figure 3-21: Expression of gp130 and p-STAT3 on day 1 and day 37 of chronic DSS colitis.
A) FACS analysis of gp130 from whole blood (2.2.2.4.3). Cells were fixed with 1% (w/v) PFA and erythrocytes were lysed by the addition of an appropriate lysis buffer. Antibodies against gp130 and CD11b were used for staining and samples were subjected to FACS analysis. The gate was set to $CD11b^+$ cells and MFI values of gp130 were determined. Values measured for control mice were set to 1. Boxes and whiskers show values from min to max, horizontal lines represent mean (n = 6 for day 1 and n = 5 for day 37); * $p<0.05$ (two-tailed, paired t-test). B) FACS analysis of p-STAT3 from whole blood (2.2.2.4.3). Cells were fixed and erythrocytes lysed as described for A. Cells were permeabilized and FACS staining was performed with antibodies against p-STAT3 and CD11b. The gate was set to $CD11b^+$ cells and values obtained for untreated control animals were set to 1. Boxes and whiskers show values from min to max, horizontal lines represent mean (n = 6 for day 1 and n = 5 for day 37); ** $p<0.01$ (two-tailed, paired t-test).

In order to determine whether the changes in gp130 expression and STAT3 activation were restricted to PB myeloid cells, mesenteric lymph nodes were prepared from mice on day 37. In contrast to the results from PB, the gp130 expression on $CD11b^+$ cells was significantly lower in DSS-treated animals as illustrated by figure 3-22 A. It was assumed that the downregulation of gp130 would result in a decreased IL-6 responsiveness. This was tested by stimulation with IL-6 and the subsequent analysis of STAT3 activation. Figure 3-22 B shows that in line with decreased levels of gp130, the potential of $CD11b^+$ cells from DSS-treated animals to activate STAT3 in response to IL-6 was diminished compared to control mice.

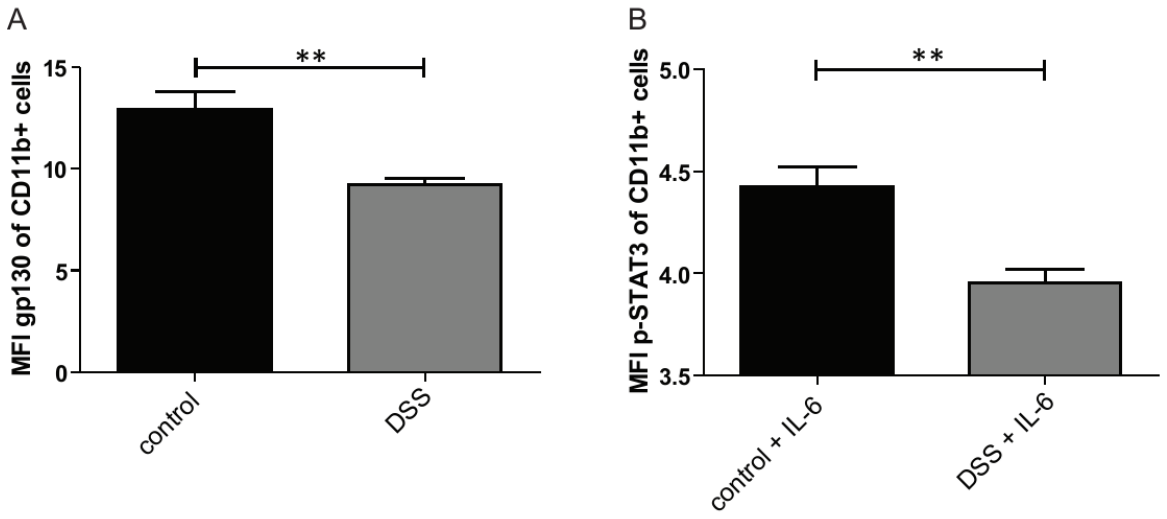

Figure 3-22: Expression of gp130 and p-STAT3 in CD11b+ cells of mesenteric lymph nodes.
A) FACS analysis of gp130 expression (2.2.2.4.1) on $CD11b^+$ cells isolated from mesenteric lymph nodes. Antibodies against gp130 and CD11b were used and the gate was set to $CD11b^+$ cells. MFI of gp130 within the gate was determined for control animals (black bar) and animals that received DSS (grey bar). Bars show mean plus SEM (n = 5); ** $p<0.01$ (two-tailed Mann Whitney test). B) FACS analysis of p-STAT3 (2.2.2.4.2) in cells isolated from mesenteric lymph nodes. Cells were stimulated with IL-6 (20 ng/ml) for 15 min prior to staining with antibodies against p-STAT3 and CD11b. MFI of p-STAT3 within $CD11b^+$ population was determined for control animals (black bar) and DSS-treated mice (grey bar). Bars represent mean plus SEM (n = 5); ** $p<0.01$ (two-tailed, unpaired t-test).

In summary, the characteristics of PB monocytes from pediatric IBD patients, i.e. increased gp130 and p-STAT3 levels, could in part be transferred to a model of chronic colitis in mice. After having received DSS for 3 cycles, PB $CD11b^+$ cells of animals displayed higher expression of gp130 and p-STAT3 than control mice. However, in mesenteric lymph nodes the situation was reversed and decreased gp130 surface expression on $CD11b^+$ cells was observed as well as diminished responsiveness to IL-6.

3.3.2 Juvenile idiopathic arthritis

3.3.2.1 Influence of synovial fluid on gp130 and IL-6R expression on monocytes

To investigate whether the inflammatory situation in the joints of JIA patients influenced the expression of the IL-6 receptor complex on monocytic cells, we compared PB monocytes to synovial fluid (SF) monocytes. As illustrated by representative histograms in figure 3-23 A, both components of the receptor complex were differentially expressed within the two compartments. On monocytes from SF (lower panel), significantly lower expression levels of gp130 (left) and IL-6R (right) were detected compared to PB monocytes (upper panel). A total of 18 and 15 patients were investigated for the expression of gp130 and IL-6R, respectively. This is displayed as scatter plots in figure 3-23 B and C.

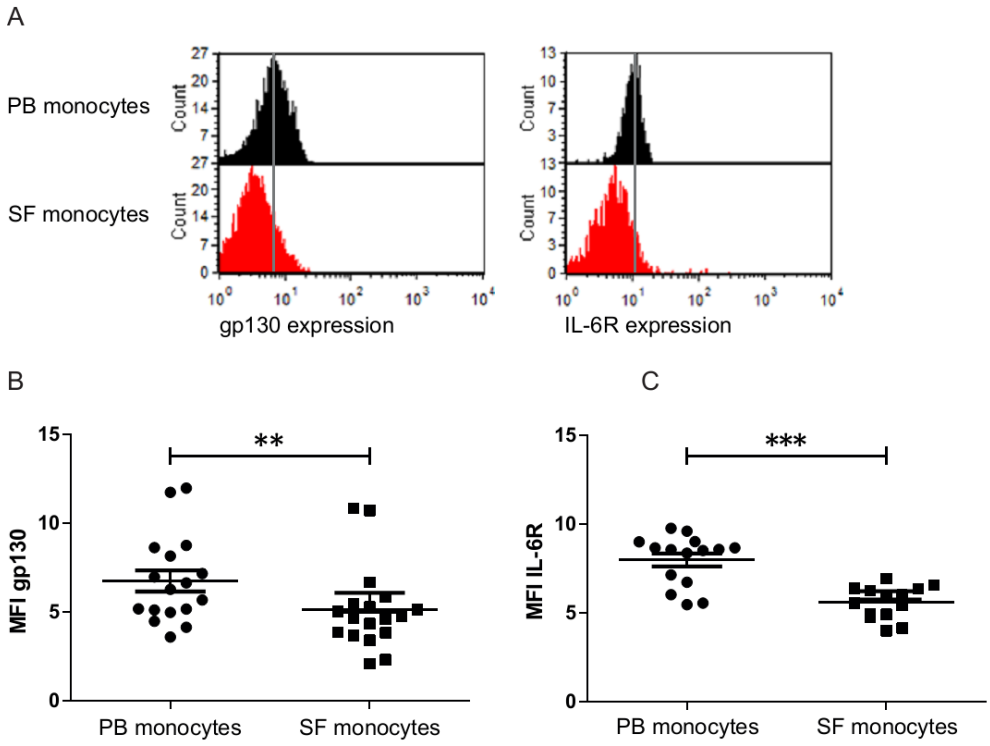

Figure 3-23: Expression of gp130 and IL-6R on PB and SF monocytes from JIA patients.
FACS analysis from whole blood and SF (2.2.2.4.3). Cells were fixed with 1% (w/v) PFA followed by incubation with lysis buffer to eliminate erythrocytes. FACS staining was performed with antibodies against gp130, IL-6R and CD14 and the gate was set to $CD14^+$ cells. A) Representative histograms of gp130 (left) and IL-6R (right) surface expression within the monocyte population. PB monocytes from JIA patient (upper panel) are compared to SF monocytes (lower panel) from the same patient. B) Symbols indicate MFI values of gp130 expression of individual patients (n = 18), horizontal lines represent mean plus SEM; ** $p<0.01$ (two-tailed Wilcoxon signed rank test). C) Symbols indicate MFI values of IL-6R expression of individual patients (n = 15), horizontal lines represent mean plus SEM; *** $p<0.001$ (two-tailed Wilcoxon signed rank test).

In the SF of patients with JIA many pro-inflammatory cytokines can be detected. Since we observed a reduction of gp130 surface expression on PB monocytes by the pro-inflammatory cytokine IL-1β, we hypothesized that soluble factors present in SF were responsible for the observed downregulation of gp130 and IL-6R. Synovial fluid mononuclear cells (SFMCs) were isolated from SF by density gradient centrifugation, incubated in RPMI with 10% (v/v) FCS and rested for up to 60 min. Gp130 and IL-6R expression levels were measured after different periods of rest. As shown in figure 3-24 A, the monocytic cell surface expression of gp130 increased significantly within 1 hour of culture, whereas IL-6R levels remained constant. We thus asked whether incubation with SF would again result in a downregulation of gp130 surface expression. We incubated PBMCs, which were isolated from healthy donors, with 10% SF in RPMI. As control, cells were stimulated with 10% (v/v) human serum (HS) in RPMI. MFI of gp130 was measured by flow cytometry and values for untreated cells were set to 1. Figure 3-24 B shows that the incubation of PBMCs with SF led to a significant downregulation of gp130 surface expression on monocytes. The expression of IL-6R after stimulation with SF was determined as well, which is illustrated by figure 3-24 C. Although the isolation of SFMCs from SF did not result in an increase of IL-6R expression within 1 hour of rest, SF induced downregulation of IL-6R. However, the statistical spread of MFI values measured after SF stimulation was much higher than that obtained with gp130.

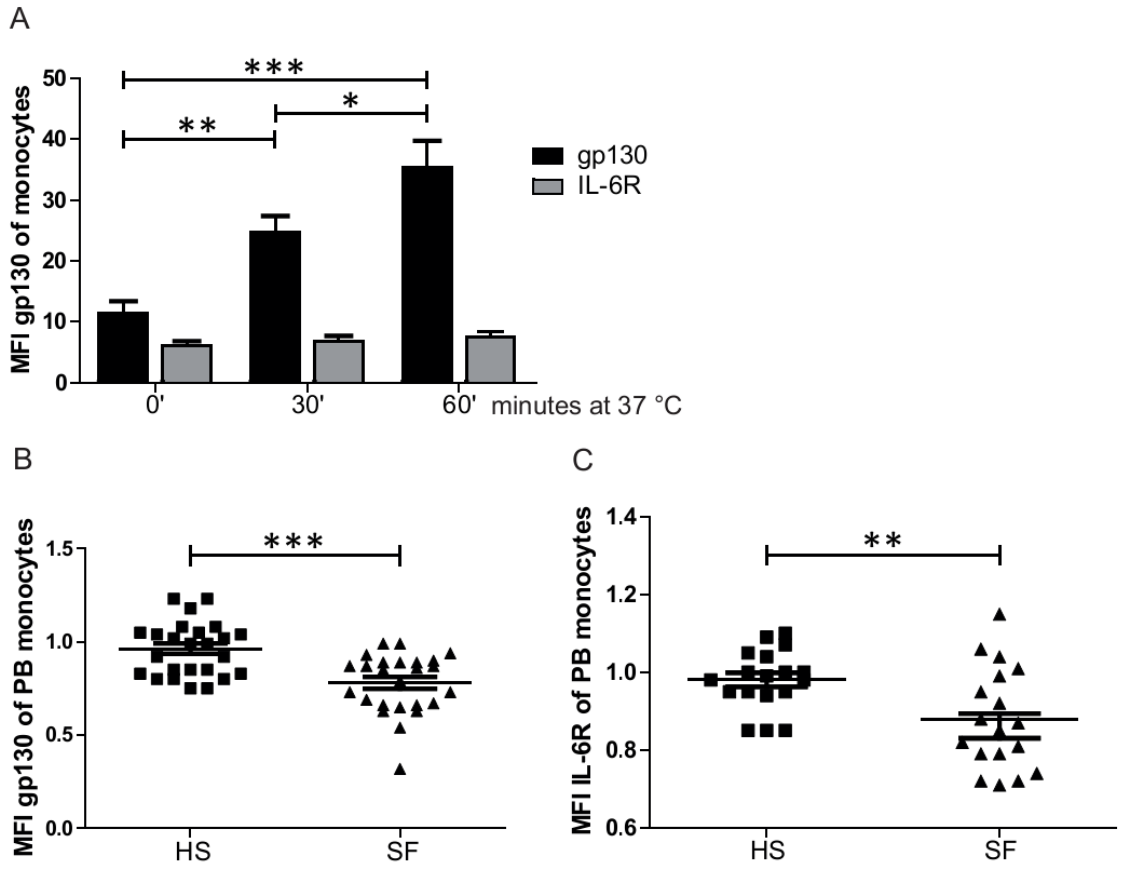

Figure 3-24: Effect of SF on IL-6 receptor surface expression.
FACS analysis (2.2.2.4.1) of SFMCs (A) or PBMCs (B and C). A) Cells were isolated and either immediately prepared for FACS analysis or cultured at 37°C and 5% CO_2 in RPMI supplemented with 10% (v/v) FCS for the indicated times prior to flow cytometry. Antibodies against gp130, IL-6R and CD14 were used. The gate was set to $CD14^+$ cells and MFI values for gp130 (black bars) and IL-6R (grey bars) were determined. Bars represent mean values plus SEM (n = 5 for gp130, n = 4 for IL-6R), * p<0.05, ** p<0.01, *** p<0.001 (one-way ANOVA with Tukey's Multiple Comparison Test) B and C) PBMCs were isolated and stimulated with 10% (v/v) SF or human serum (HS) as control for 20 min. Cells were stained for gp130 and CD14 (B) or IL-6R and CD14 (C) and analyzed by flow cytometry. $CD14^-$ cells were excluded by gating and untreated controls were set to 1. Symbols indicate MFI of paired samples of HS and SF. Horizontal lines represent mean plus SEM (n = 25 for B, n = 18 for C); *** p<0.001 (two-tailed Wilcoxon signed rank test), ** p<0.01 (two-tailed paired t-test).

Previous studies have shown a crosstalk regulation of IL-6 signaling dependent on the stress-induced MAPK p38, which was supported by our own findings that the IL-1β-induced internalization of gp130 in monocytes was dependent on p38 (figure 3-6 A). We therefore asked whether a blockade of p38 would prevent the downregulation of gp130 in PBMCs incubated with SF. PBMCs were pre-incubated with the p38-specific inhibitor SB202190 or the carrier DMSO, after which SF was added. As shown in figure 3-25 A, cell surface expression of gp130 on monocytes could partially be restored by pre-incubation with the p38

inhibitor. The same analysis was performed to investigate the effect of SB202190 on downregulation of IL-6R by SF. Figure 3-25 shows that inhibition of p38 could partially restore diminished expression of IL-6R after SF stimulation.

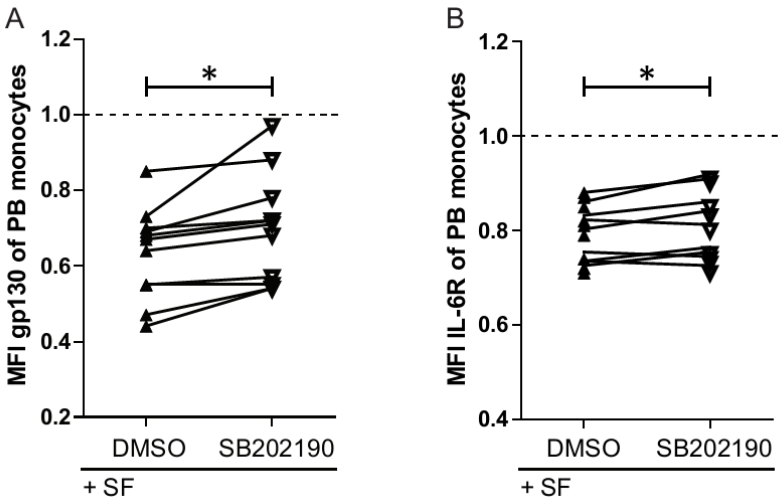

Figure 3-25: Influence of p38-inhibition on gp130 and IL-6R downregulation by SF.
Flow cytometric analysis of gp130 (A) or IL-6R (B) surface expression (2.2.2.4.1). PBMCs were incubated with DMSO or SB202190 (5 µM) 30 min prior to the addition of SF (10%, v/v) for 20 min. A) PBMCs were stained with antibodies against CD14 and gp130. MFI of gp130 measured within the $CD14^+$ population for untreated cells was set to 1. Symbols indicate individual values (n = 11); * $p<0.05$ (two-tailed, paired t-test). B) Cells were incubated with antibodies against CD14 and IL-6R. $CD14^-$ cells were excluded by gating and MFI of IL-6R determined for untreated cells was set to 1. Symbols indicate individual values (n = 9); * $p<0.05$ (two-tailed, paired t-test).

Taken together, soluble factors in the SF induced downregulation of gp130 and IL-6R surface expression on monocytes. This downregulation depended partially on the MAPK p38.

3.3.2.2 Influence of synovial fluid on STAT3 phosphorylation in monocytes

To investigate whether the downstream signaling in SF monocytes was affected by reduced expression levels of gp130 and IL-6R, basal STAT3 phosphorylation was determined and compared to PB monocytes. Unexpectedly, SF monocytes displayed significantly higher levels of phosphorylated STAT3 than PB monocytes (figure 3-26 A). This led us to analyze the IL-6 responsiveness of SF and PB monocytes. Cells were incubated with IL-6 for 15 min, fixed, and p-STAT3 levels were determined by flow cytometry. Basal STAT3 phosphorylation was set to 1. Figure 3-26 B shows that in PB monocytes of the 4 tested JIA patients stimulation with IL-6 resulted in a clear induction of p-STAT3, whereas in SF monocytes

STAT3 activation did not exceed baseline levels. These preliminary data demonstrate a definite tendency towards reduced IL-6 responsiveness in SF compared to PB monocytes.

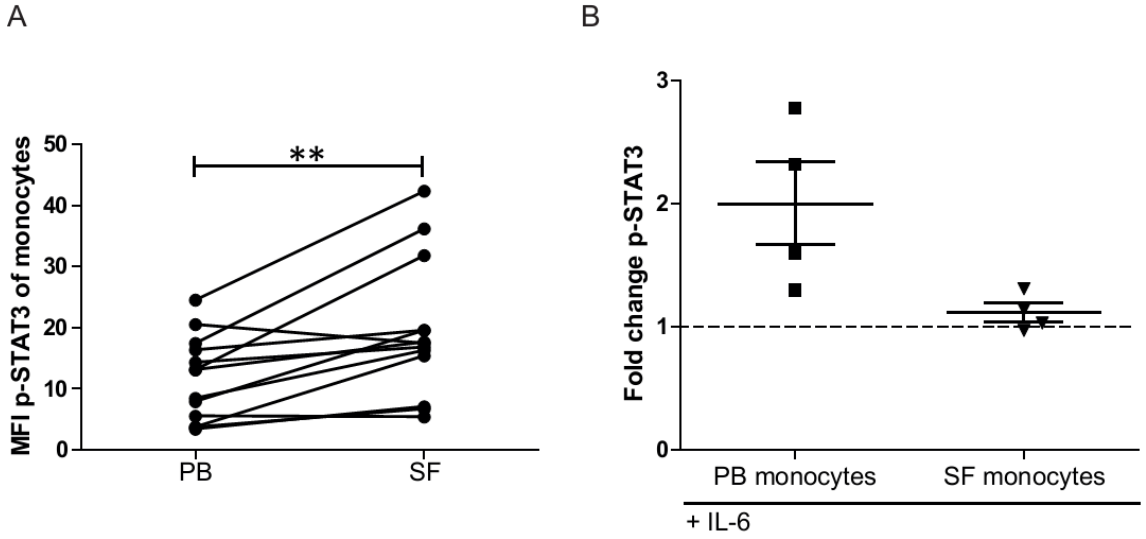

Figure 3-26: Basal STAT3 phosphorylation and IL-6 responsiveness in PB and SF monocytes.
A) Flow cytometry of p-STAT3 from PB and SF (2.2.2.4.3). Cells were fixed with 1% (w/v) PFA, erythrocytes were lysed and cells were permeabilized by the addition of ice-cold methanol prior to staining with antibodies against p-STAT3 and CD14. The gate was set on $CD14^+$ cells. Symbols indicate p-STAT3 MFI of individual donors (n = 14). Horizontal lines represent mean values plus SEM; ** $p<0.01$ (two-tailed, paired t-test). B) FACS analysis of p-STAT3 (2.2.2.4.2). Erythrocytes were lysed prior to incubation with IL-6 (20 ng/ml) for 15 min. Cells were fixed, permeabilized and stained with antibodies against p-STAT3 and CD14. $CD14^-$ cells were excluded by gating and MFI values of p-STAT3 measured in untreated cells were set to 1. Horizontal lines show mean plus SEM (n = 4).

In vitro stimulations with SF led to downregulation of gp130 on PB monocytes and could thus mimic the situation in the inflamed joint. Since SF monocytes displayed increased levels of activated STAT3 compared to PB monocytes, we investigated the potential of SF to induce STAT3 phosphorylation. PBMCs were incubated with SF or HS as control and STAT3 phosphorylation was determined. Samples were prepared in duplicate, one half being incubated with IL-6 20 min after the addition of SF or HS. As demonstrated by figure 3-27 A, the stimulation with SF resulted in a significant induction of p-STAT3. HS had no effect on STAT3 phosphorylation, independent of the presence or absence of IL-6. The additional incubation with IL-6 after stimulation with SF barely triggered any further STAT3 phosphorylation at all. Despite a slight induction of p-STAT3 after SF and IL-6, STAT3 activation still differs significantly from activation with IL-6 alone.

Since the anti-inflammatory cytokine IL-10 is known to be an inducer of p-STAT3 (Lang et al., 2002), and it has furthermore been reported that IL-10 is present in the SF of RA patients (de

Jager et al., 2007) the potential of IL-10 to activate STAT3 was compared to that of IL-6. According to figure 3-27 B, stimulation of PBMCs with IL-10 resulted in an amount of phosphorylated STAT3 comparable to that induced by IL-6.

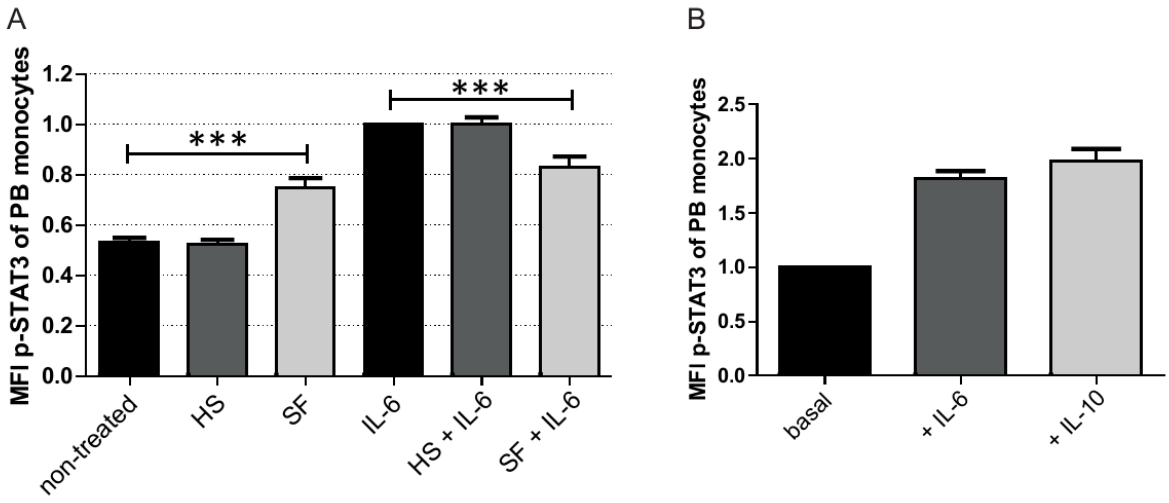

Figure 3-27: Influence of SF and IL-10 on STAT3 phosphorylation.
FACS analysis of p-STAT3 (2.2.2.4.2). Cells were stained with antibodies against p-STAT3 and CD14 and MFI of p-STAT3 was determined within the $CD14^+$ population. A) HS or SF (10%, v/v) was added to PBMCs 20 min prior to the stimulation with IL-6 (20 ng/ml) for 10 min. MFI values of p-STAT3 measured for IL-6-treated cells were set to 1. Bars show mean plus SEM (n = 24); *** $p<0.001$ (two-tailed, paired t-test). B) PBMCs were stimulated with IL-6 or IL-10 (both 20 ng/ml) for 10 or 20 min. Bars represent mean plus SEM (n = 4).

In line with the reduced expression of the IL-6 receptor complex on SF monocytes, preliminary data showed a diminished capacity of these cells to activate STAT3 in response to IL-6 compared to PB monocytes. Levels of basal STAT3 phosphorylation, however, were increased in SF monocytes from JIA patients, compared to PB monocytes. This increase of STAT3 activation could again be well mimicked by adding SF to PB monocytes. Further induction of p-STAT3 after incubation with SF by IL-6 stimulation was only marginal. IL-10 was able to induce STAT3 phosphorylation in PB monocytes to a level comparable to that induced by IL-6.

4 DISCUSSION

IL-6 signaling plays an important role in different immune reactions. Several regulatory mechanisms exist to avoid an overshooting response of cells to IL-6. It is becoming increasingly clear that apart from classical regulation, certain cytokines exert inhibitory effects on IL-6 signaling (Garbers et al., 2012).

The aim of the first part of this study was to investigate whether crosstalk regulation of IL-6 signaling takes place in human monocytes. IL-1β was chosen as pro-inflammatory stimulus and stimulation with this cytokine restricted IL-6 signaling (3.1.2) by downregulation of gp130 surface expression (3.1.1). As hypothesized from previous studies in other cell types, these effects depended on the MAPK p38 (3.1.3). In hepatocytes the phosphorylation of serine 782 within the cytoplasmic tail of gp130 was responsible for internalization of the receptor in response to pro-inflammatory stimuli (Radtke et al., 2010). As expected, the stimulation of monocytes with IL-1β resulted in increased phosphorylation of this particular residue (3.1.4).

The analogous serine and the upstream serine residue in the mouse were used to generate transgenic mice in the second part of this study. Two different constructs were cloned successfully and two transgenic strains were established (3.2) – one overexpressing gp130-wt and one overexpressing a mutated version of gp130 with non-phosphorylatable serine 778/780. Despite breeding problems, mice were partially characterized. Gp130 expression was differentially regulated by IL-1β on splenocyte subsets in the two strains (3.2.2). Our hypothesis that the serine mutation in gp130 would alter cell surface expression and downstream signaling was further supported by different migratory behavior of myeloid cells after zymosan-induced peritonitis in gp130-mut compared to gp130-wt mice (3.2.3).

In the third part of the study regulation of gp130 signaling was investigated in chronic inflammatory disorders. Two different diseases were taken into consideration: IBD and JIA. Both conditions are accompanied by increased serum levels of IL-6, IL-1β and TNF-α. The hypothesis that gp130 surface expression and downstream signaling might be altered was confirmed for PB monocytes in IBD patients compared to healthy controls (3.3.1.1). The changes observed in PB monocytes of IBD patients were successfully transferred to a murine model of chronic colitis (3.3.1.2). Differences in gp130 expression were furthermore identified in SF monocytes of JIA patients compared to PB monocytes of the same patient (3.3.2.1). Stimulation of PBMCs with SF from JIA patients resulted in a MAPK p38-dependent downregulation of gp130 expression comparable to the situation in the inflamed joint (3.3.2.1).

4.1 Crosstalk regulation of IL-6 signaling in human monocytes

4.1.1 Internalization of gp130

Data from the first part of this study indicate that IL-1β induces a downregulation of gp130 surface expression on monocytes. Figure 3-2 A and B show that in the presence of IL-1β enhanced internalization of gp130 occurs. Even in the absence of IL-1β internalization was apparent to a certain degree. Constitutive turnover of gp130 was observed earlier in other cell types (Thiel et al., 1998b) and it turned out to be true for primary human monocytes as well. The effect of IL-1β on gp130 surface expression was illustrated more clearly by confocal microscopy than by flow cytometry (figure 3-2). One main difference in sample preparation between the two methods was the order of stimulation and staining. For flow cytometry cells were stimulated with IL-1β, washed and subsequently incubated with antibodies on ice to prevent further internalization. After another washing step cells were directly analyzed by flow cytometry. For live-cell imaging cells were incubated with antibodies on ice, washed to remove non-bound antibodies and subsequently analyzed in the presence or absence of IL-1β at 37°C. Thus, during the period of stimulation no antibodies were bound to gp130 in the preparation for FACS analysis in contrast to sample preparation for microscopy. It may therefore be supposed that the antibody bound to the gp130 epitope exerted a stimulatory effect on gp130 internalization. Although it is known that after ligand binding the IL-6 receptor complex is internalized, a process depending on the di-leucine motif in the cytoplasmic tail of gp130, it has also been shown that JAK activation is not necessary for this process (Dittrich et al., 1994; Thiel et al., 1998a). Furthermore, the antibody used here was found to act antagonistically on gp130 activation (Wijdenes et al., 1995). Another potentially important difference between sample preparations for flow cytometry and microscopy concerns the purity of monocytes. For the FACS analysis shown in figure 3-2 C, PBMCs were stimulated and $CD14^-$ cells were excluded by gating. However, for microscopy, monocytes were enriched by allowing them to settle down, followed by stringent washing. Consequently, the numbers of lymphocytes were probably reduced in microscopy assays compared to flow cytometry. To what extent this might have influenced internalization of gp130 is not known. To exclude potential effects of lymphocytes on monocytic gp130 surface expression, pure monocyte populations should be used. Enrichment of monocytes by adherence was not only well suited but also necessary for microscopy because adherence of cells is a prerequisite for focusing on the correct layer. For flow cytometric analyses, however, this method would be less suitable, since cells would need to be removed from plastic dishes prior to preparation for FACS. Another aspect of the enrichment of monocytes by adherence used for

microscopy is the fact that adherence to plastic partially activates the cells (de Almeida et al., 2000). It cannot be excluded that this cell activation had an influence on internalization.
One commonly used method of monitoring internalization of cell surface proteins by flow cytometry is to label the respective protein with an antibody and to incubate the cells with the stimulus expected to induce internalization. Subsequently, antibodies bound to the cell surface are removed by an acid wash and cells are subjected to flow cytometry to visualize only internalized antibodies. The problem with these internalization assays is that surface-bound antibodies are not always removed efficiently (Helchowski et al., 2009). Furthermore, although such assays may be suitable for relatively robust cell lines, primary monocytes are quite sensitive and no longer usable for flow cytometry after an acid wash (own observations). An alternative, as yet untested, approach to illustrating internalization of gp130 more clearly would be the fractionation of cell membranes from cytoplasm after IL-1β stimulation. Gp130 could be visualized in a western blot in both compartments and compared to untreated cells. However, this is a quite laborious and time-consuming method and it seems questionable whether the sensitivity would be sufficient to detect small changes in expression.

4.1.2 Crosstalk inhibition of STAT3 phosphorylation

The reduced gp130 surface expression in response to IL-1β was expected to impair downstream signaling. STAT3 phosphorylation was determined as readout for IL-6 signaling. STAT3 is known to be phosphorylated after a few min in response to IL-6 with a peak around 15-30 min (Kortylewski et al., 1999). Indeed, after 10 min of IL-6 stimulation about 9-fold levels of p-STAT3 compared to untreated PBMCs were detected in a western blot (figure 3-3 A). After pre-stimulation with IL-1β levels of p-STAT3 increased only about 3-fold compared to untreated cells. These results confirmed our expectations and were reproduced by a flow cytometric approach (figure 3-3 B). Since these experiments were performed with PBMCs, rather than with isolated monocytes, neither method excludes co-stimulatory effects of lymphocytes. Whereas in the FACS analysis a gate was set on $CD14^+$ cells to examine only the monocyte population, the western blot includes lymphocytes. Monocytes account for approximately 10% of PBMCs. Thus, it might be concluded that the effects observed in the western blot are primarily due to lymphocytes and that in this cell population IL-1β restricts IL-6 signaling as well. However, expression of IL-6R on PBMCs is largely restricted to monocytes and some subsets of T and B cells (Jones et al., 2001) suggesting that stimulation with IL-6 alone would activate STAT3 predominantly in these cells, among which monocytes represent the strongest fraction.

To exclude co-stimulatory effects of lymphocytes on gp130 surface expression or IL-6 signaling in monocytes, Percoll gradients were used to isolate monocytes from PBMCs. Restriction of IL-6 signaling by pre-stimulation with IL-1β in isolated monocytes was comparable to PBMCs gated on $CD14^+$ cells (figure 3-3 B and C) showing that lymphocytes are dispensable for crosstalk regulation in monocytes.

One of the most potent mechanisms for shutting off STAT3 activation is the inactivation of JAKs by the feedback inhibitor SOCS3. Expression of SOCS3 rises rapidly after IL-6 stimulation and a stabilization of *SOCS3* mRNA by IL-1β has been described for hepatocytes (Heinrich et al., 2003; Yang et al., 2004). The question whether reduction of IL-6-induced STAT3 phosphorylation by IL-1β was dependent on SOCS proteins was therefore examined. By pre-incubation of the cells with actinomycin D, which intercalates with DNA and thus inhibits the synthesis of mRNA, transcription was blocked. The inhibitory effect of IL-1β on IL-6-induced STAT3 activation was unchanged in the absence of protein synthesis (figure 3-4 A) showing that it was independent of SOCS3. Although the use of actinomycin D as an inhibitor of protein synthesis is well-established, it cannot be inferred from this experiment that transcription was successfully blocked. To confirm the efficacy of actinomycin D, cells should be stimulated with IL-6 after pre-treatment with the inhibitor or the vehicle DMSO. Subsequently, expression of SOCS3 should be determined either by quantitative RT-PCR or by western blotting or FACS analysis at the protein level. Figure 3-4 B shows quantitative RT-PCR data, from which it was concluded that *SOCS3* expression was induced only marginally after 10 min of IL-6 stimulation and that this induction was not significantly increased by co-stimulation with IL-1β. Still there was a slight induction of *SOCS3* expression after IL-6 and after IL-1β stimulation compared to untreated cells. These effects seemed to be additive, since the combined stimulation with both cytokines further increased the induction minimally. These results demonstrate that in monocytes expression of *SOCS3* induced by IL-6 seems to be very rapid and that IL-1β has the potential to induce *SOCS3* expression. It has been shown before that stimulation of macrophages with IL-1β results in the induction of *SOCS3* (Ahmed and Ivashkiv, 2000). Since IL-1β alone was able to slightly induce *SOCS3* expression, this effect probably differs from the mRNA stabilization observed by Yang *et al*. However, it cannot be completely excluded that minimal basal levels of *SOCS3* mRNA are present in the cell and that IL-1β inhibited their degradation. Still, we concluded from these results that the inhibitory effect of IL-1β on IL-6-induced STAT3 phosphorylation was not primarily due to the action of SOCS3.

4.1.3 Involvement of p38

Crosstalk inhibition of IL-6 signaling in macrophages and hepatocytes has been shown to be dependent on p38 (Ahmed et al., 2002; Radtke et al., 2010). For this reason we hypothesized that p38 might be an important element in the signaling cascade induced by IL-1β leading to reduced gp130 surface expression on monocytes. Figure 3-5 shows that IL-1β induces phosphorylation of p38 in monocytes. This is consistent with earlier studies, which identified IL-1β and TNF-α as potent inducers of p38 (Raingeaud et al., 1995). The inhibition of p38 restored gp130 surface expression after stimulation with IL-1β (figure 3-6 A), thus demonstrating the involvement of the MAPK in downregulation of gp130. This was reflected in the level of downstream signaling, i.e. treatment with SB202190 reconstituted IL-6-induced STAT3 phosphorylation after IL-1β stimulation (figure 3-6 B). The incubation of cells with the inhibitor alone resulted in a minimal increase in gp130 surface expression, which again was reflected in the level of downstream signaling. IL-6-induced STAT3 phosphorylation was slightly stronger after pre-incubation with SB202190 compared to cells pre-incubated with DMSO (figure 3-6 B). These findings indicate that a certain basal activation of p38 might occur in the absence of IL-1β stimulation. Since p38 is a stress-activated MAPK, it may be induced by various stimuli. A similar picture was observed in hepatocytes (Radtke et al., 2010). Reduced STAT3 phosphorylation after pre-stimulation with IL-1β was reconstituted to levels observed without SB202190 treatment, however, a complete restoration to levels observed after p38 inhibition was not achieved (figure 3-6 B). One explanation could be the slight induction of SOCS3 by IL-1β (figure 3-4 B), which may have contributed to the inhibitory effect of IL-1β on IL-6-induced STAT3 activation.

The kinase MK2, which is activated by p38, was responsible for the phosphorylation of serine 782 in the cytoplasmic domain of gp130 in hepatocytes (Radtke et al., 2010). Serine 782 is part of a consensus sequence for MK2 and is located close to the di-leucine internalization motif of gp130. Phosphorylation of this residue was slightly increased in monocytes by stimulation with IL-1β (figure 3-7). However, the phosphorylation in untreated cells was also quite pronounced and differed from that found in hepatocytes, which might indicate unspecific binding of the used antibody. A control with an irrelevant antibody of matching isotype could be included to rule out the possibility of an unspecific cross reaction with that particular isotype. On the other hand, to our knowledge this is the first study examining phosphorylation of serine 782 in primary monocytes and it may be that phosphorylation levels differ from those observed in hepatocytes. Whether this basal phosphorylation leads to internalization and high turnover is inherent to monocytes is not clear. Stress due to isolation

procedures might have led to increased phosphorylation via p38 and as a consequence further phosphorylation by the additional stimulus IL-1β was weak. To confirm that the phosphorylation of serine 782 occurs via p38 and MK2, inhibitors of the kinases should be included in the analysis. In practice, the visualization of endogenous gp130 in primary monocytes is challenging. High numbers of cells are required to provide sufficient protein amounts for immunoprecipitation. Furthermore, the isolation of monocytes by Percoll gradients resulted in variable yield and purities, probably depending on quality of buffy coats. Isolation of monocytes by magnetic beads would represent an alternative approach, however, negative selection is very expensive due to the rather small fraction of PBMCs accounting for monocytes and positive selection has been shown to activate monocytes comparable to purification by adherence (Seager Danciger et al., 2004).

4.1.4 Physiological relevance

The crosstalk regulation of IL-6 signaling presented by IL-1β is most likely to be of particular relevance in physiological situations where cells need to react to a complex network of stimuli represented by many different cytokines. Pro- and anti-inflammatory properties have been described for IL-6. It seems that the overall role of the cytokine depends critically on the cell type affected, but also on modulatory actions on signal transduction. It is known that differential signaling thresholds are required for the induction of target genes (Ernst and Jenkins, 2004). This is exemplified by the transcription factor STAT3, which is activated not only by IL-6-type cytokines, but also by other cytokines including IL-10. IL-10 is a typical anti-inflammatory cytokine and often opposes the actions of IL-6 (Fiorentino et al., 1991). These converse functions of p-STAT3 are due to differential durations of signaling, which are controlled by SOCS3. Essentially, SOCS3 exerts feedback inhibition on gp130-mediated signaling, whereas IL-10 signaling remains unaffected. In macrophages lacking the Socs3 gene the actions of IL-6 resemble those of IL-10 (Yasukawa et al., 2003). Interestingly, mice carrying a mutation in the cytoplasmic domain of gp130, abolishing binding of SOCS3 and SHP2, show hyperactivation of STAT3, which is associated with defects in hematopoiesis (Jenkins et al., 2005). Subtle differences in expression levels of p-STAT3 due to the generation of these mice with murine or a partial human cDNA result in phenotypic variations (Ernst and Jenkins, 2004). This clearly indicates the significance of STAT3 signaling strength for biological outcome. Hence, the crosstalk mechanism presented herein could serve to modulate the threshold of STAT3 signaling and contribute critically to the biologic response of the cell. IL-1β and IL-6 are often co-expressed at sites of inflammation. By reducing IL-6-induced STAT3 activation, IL-1β could counterbalance potential additive

pro-inflammatory effects of both cytokines and thus prevent an overshooting inflammatory reaction. On the other hand, since IL-6 displays anti-inflammatory effects, especially on myeloid cells (Tilg et al., 1994), IL-1β might intensify inflammation by downregulation of gp130 expression. Taking into account the fact that prolonged STAT3 activation in macrophages elicits rather anti-inflammatory, IL-10-like responses, it seems conceivable that IL-1β, by supporting the termination of IL-6-induced STAT3 activation, could strengthen pro-inflammatory actions of IL-6. The use of STAT3 as transcription factor by more than one cytokine makes it difficult to distinguish the contribution of each cytokine *in vivo*. Gp130-mediated STAT3 phosphorylation can be triggered not only by IL-6 but also by 8 other cytokines belonging to the IL-6 family (Heinrich et al., 1998). Signaling of these cytokines could likewise be affected by IL-1β-mediated downregulation of gp130 expression. The modulation of p-STAT3 signaling strength by IL-1β is illustrated in figure 4-1.

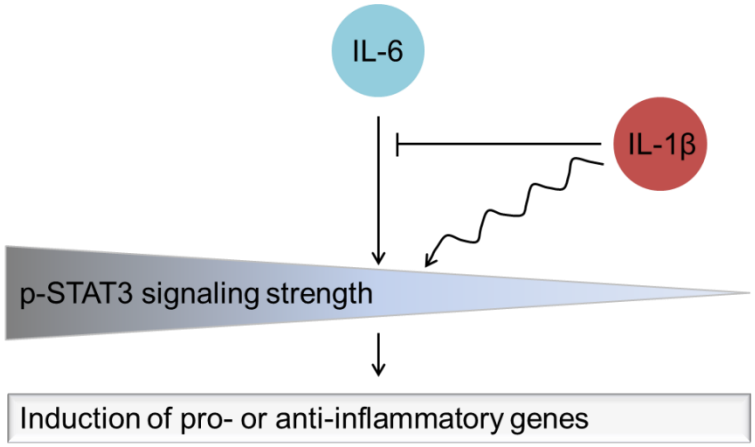

Figure 4-1: Modulation of p-STAT3 signaling strength by IL-1β.
Depending on the signaling threshold of p-STAT3, pro- or anti-inflammatory genes can be induced. By exerting an inhibitory effect on IL-6 signaling, IL-1β can modulate the signaling strength and thus the biological response of a cell.

4.2 Mouse model of crosstalk regulation

To study crosstalk regulation *in vivo*, transgenic mice were generated. We decided to overexpress gp130 in the complete hematopoietic compartment under the control of the vav promoter. To create a version of gp130 that would prevent potential crosstalk mechanisms mediated by serine phosphorylation and internalization, two serine residues were mutated to alanines. In addition to serine 780, which is analogous to human serine 782, serine 778, analogous to human serine 780, was mutated (figure 3-9). Serine 782 is potentially involved in crosstalk regulation in human monocytes (3.1.4) and serves as a stress sensor limiting gp130-mediated signaling by internalization (Gibson et al., 2000; Radtke et al., 2010). An

earlier study using human cell lines demonstrated an influence of serine 780 on receptor internalization (Dittrich et al., 1996). Later on it was proposed that the residue crucial for internalization is serine 782, but that serine 780 is required for its phosphorylation (Gibson et al., 2000). The cytoplasmic tail of gp130 is highly conserved between humans and mice (figure 3-9). So far, to our knowledge the only study that has been conducted in murine cells concerning the role of serine phosphorylation in receptor internalization is that of Radtke *et al*. In murine embryonal fibroblasts (MEFs), stimulation with IL-1β results in serine phosphorylation and downregulation of gp130, both of which depends on p38 and MK2 (Radtke et al., 2010). Furthermore, studies with primary murine macrophages support the finding that crosstalk regulation of gp130-mediated signaling by pro-inflammatory stimuli occurs in mouse cells (Kiu et al., 2007). We therefore generated gp130-mut mice, overexpressing a version of gp130, which is non-phosphorylatable at the two mentioned serine residues. A second mouse strain was generated, which overexpresses gp130-wt as reference for gp130-mut mice. After successful cloning of the different constructs (figure 3-8), the respective mouse strains were generated by pronuclear injection.

To detect the inserted gene, a PCR reaction was established and the mice identified as carrying the transgene were characterized. Quantitative RT-PCR of splenocytes showed enhanced *gp130* expression in both mouse strains compared to mice without transgene (figure 3-10). Expression in gp130-wt was slightly stronger than in gp130-mut splenocytes. The gp130 mRNA levels were not expected to differ between gp130-wt and gp130-mut mice, since the SS/AA mutation was assumed to influence cell surface expression but not basal expression levels. Through pronuclear injection transgenes are randomly integrated into the genome, rather than being targeted to a specific site. Furthermore, the number of copies cannot be influenced (Beard et al., 2006). Thus, gp130-wt mice might have integrated more copies of the transgene compared to gp130-mut.

4.2.1 Surface expression of gp130

To avoid interference with normal physiology, the inserted gp130 was not marked by a tag. Thus, discrimination between transgene and endogenous gp130 on the protein level was not possible.

In terms of gp130 surface expression differences between the two strains were detected on leukocytes from PB, which were most pronounced in B cells (figure 3-11). On splenocytes gp130 surface expression levels were comparable between gp130-wt and gp130-mut mice (figure 3-12) and thus not in line with data from quantitative RT-PCR suggesting lower gp130 expression in gp130-mut compared to gp130-wt mice. However, mRNA expression will not

necessarily be reflected in surface expression, since post-translational modifications or altered turnover can lead to differences. Assuming that gp130-mut splenocytes express lower levels of gp130 protein than gp130-wt splenocytes, but that both strains show similar levels of surface expression, this could indicate an increased stability of the gp130-mut protein on the cell surface. To clarify whether total gp130 protein levels differ between gp130-wt and gp130-mut splenocytes, gp130 protein amounts could be determined by western blotting or intracellular FACS analysis.

The mutation of serine 778 and 780 was hypothesized to increase the stability of gp130 surface expression and it was assumed that this increased stability would become apparent after stimulation of the cells with pro-inflammatory cytokines. The incubation of splenocytes with IL-1β resulted in a slight downregulation of gp130 surface expression on gp130-wt B cells and myeloid cells (figure 3-14 C-D). Although this change of surface expression was very small, it was still significantly different from expression on the respective cell population from gp130-mut mice after IL-1β stimulation. In the latter, no changes of gp130 surface expression by IL-1β were observed on B cells and even a slight increase could be detected on $CD11b^+$ cells (figure 3-14 C-D). These results provide first hints that the findings from human monocytes may be transferable to the murine system and that mutation of serine 778/780 may affect internalization in response to IL-1β.

4.2.2 Activation of STAT3

Although basal gp130 surface expression on gp130-wt T cells did not differ from gp130-mut T cells, differential STAT3 activation was observed. In response to IL-6, significantly more p-STAT3 could be detected in gp130-mut compared to gp130-wt T cells (figure 3-13 B). Since this enhanced response to IL-6 could not be due to higher levels of available gp130 molecules at the cell surface, remaining possibilities include an increased expression of IL-6R or an altered signal transduction. There is no obvious reason why the expression of IL-6R should have been enhanced on gp130-mut T cells, however, it was not tested and therefore cannot be completely excluded. Serine residues 778/780 are located between the two STAT3 binding sites tyrosine 765 and tyrosine 812. Other studies, which have worked with human gp130 mutated at one or two of the equivalent serine residues, have not investigated downstream signaling compared to non-mutated gp130 (Dittrich et al., 1996; Radtke et al., 2010). Still it seems unlikely that the exchange of serine to alanine had an effect on STAT3 binding, and this is supported by the fact that no changes in IL-6 responsiveness were observed for other splenocytes subsets (figure 3-13 C-D). The factors accounting for the increased IL-6-induced STAT3 activation in the T cell fraction of

gp130-mut splenocytes are not clear.

Consistent with the finding that IL-1β had no influence on gp130 surface expression of gp130-wt or gp130-mut T cells, stimulation with IL-1β did not change IL-6-induced STAT3 phosphorylation in the T cell subset of either of the mouse strains (figure 3-15 B). In contrast, in B cells and myeloid cells slight changes of IL-6-induced STAT3 phosphorylation by IL-1β were observed. In myeloid cells this tendency was in line with gp130 surface expression: IL-1β downregulated gp130 surface expression (figure 3-14 D) and IL-6-induced STAT3 phosphorylation in gp130-wt $CD11b^+$ cells, but not, or to a lesser extent, in gp130-mut cells (figure 3-15 D). Thus, it seems possible that results from human monocytes are transferable to some extent to $CD11b^+$ splenocytes. In contrast to myeloid cells, in B cells the changes of gp130 surface expression after IL-1β stimulation were not reflected in the level of STAT3 phosphorylation (figure 3-14 C and figure 3-15 C). Since differences detected for IL-6-induced STAT3 activation after incubation with IL-1β were not significant in either of the investigated cell types, it cannot be excluded that they represent normal levels of variation.

Because of breeding problems in both strains at different time points, the number of animals included in our analyses is quite low. It is possible that the observed tendencies would become more apparent in a larger population sample. Furthermore, other pro-inflammatory stimuli such as TNF-α or LPS might have stronger effects in the murine system than IL-1β. In a study with primary macrophages, differentiated from bone marrow, inhibitory effects of TNF-α and LPS on IL-6-induced STAT3 phosphorylation have been described (Kiu et al., 2007). It is also conceivable that another cell type is a more suitable system in which to explore crosstalk mechanisms. Since the inserted gp130 was not distinguishable from endogenous gp130, it remains unclear to what extent endogenous gp130 might have weakened the observed differences between the two mouse strains.

4.2.3 Migration of leukocytes

Data from zymosan-induced peritonitis, a model for leukocyte migration into the peritoneal cavity, showed increased leukocyte migration in gp130-mut mice in comparison to gp130-wt animals (figure 3-16). IL-6-mediated signals influence migration of leukocytes by different mechanisms. In epithelial cells in particular, IL-6 trans-signaling has been described as an important mechanism to induce chemokine secretion resulting in leukocyte recruitment (Hurst et al., 2001). Direct effects of IL-6 on the migratory potential of human T cells and monocytes have been shown as well (Clahsen and Schaper, 2008; Weissenbach et al., 2004) and similar findings have been obtained in murine macrophages (Koon et al., 2009). Mice with gp130-deficient macrophages and neutrophils show decreased migration in a

model of peritonitis compared to their wildtype littermates (Sander et al., 2008), which further supports the notion of IL-6 acting directly as a migration factor on myeloid cells. It is thus conceivable that increased stability of gp130 surface expression in gp130-mut mice leads to an enhanced migratory potential of myeloid cells.

4.3 Regulation of gp130 signaling in chronic disease

4.3.1 IBD

Pediatric patients with IBD displayed increased levels of gp130 surface expression on monocytes compared to healthy controls (figure 3-17 A-B). Expression levels of IL-6R, however, were not changed (figure 3-17 C). The upregulation of gp130 alone seemed to be sufficient to lead to an increased STAT3 activation (figure 3-18). This might be due to a milieu where high levels of IL-6 and sIL-6R are present (Mudter and Neurath, 2007). Trans-signaling could have contributed to enhanced STAT3 phosphorylation in monocytes with increased expression levels of gp130. This is consistent with studies on cell types expressing both, gp130 and IL-6R where gp130 expression was reported to be generally higher than that of IL-6R (Jones et al., 2011). However, it might also be possible that the expression of IL-6R on monocytes was high enough to bind many IL-6 molecules and to build an increased number of complexes with gp130. Both scenarios lead to the conclusion that the expression of gp130 rather than the expression of IL-6R for downstream signaling is likely to be the limiting factor. This highlights the importance of a strictly regulated gp130 cell surface expression. However, it cannot be excluded from the experiments performed here that other factors were responsible for the increased amount of p-STAT3 in monocytes of IBD patients. The anti-inflammatory cytokine IL-10 is known to be a potent inducer of STAT3 activation. However, the high serum levels of IL-6 in IBD patients make it tempting to hypothesize that increased STAT3 activation was induced by IL-6.

Considering the fact that the IL-6 receptor complex is internalized after ligand binding and that gp130 expression underlies potential crosstalk regulation by other pro-inflammatory cytokines such as IL-1β or TNF-α, which are abundantly present in serum of IBD patients, the observed increase in gp130 surface expression was unexpected. In this context it is interesting that exon 17 of gp130 was examined for mutations or polymorphisms in patients with IBD. One could speculate that mutations of the internalization motif might explain the observed effects and play a role in IBD pathophysiology. However, the study of Auernhammer *et al.* demonstrated that none of the tested patients carried a mutation or polymorphism in exon 17 of gp130 (Auernhammer et al., 2005), which accounts for most of

the intracellular domain and also includes the internalization motif and serine 782. It is unclear which factors resulted in upregulation of gp130 surface expression and STAT3 activation.

Intriguingly, it has been reported from *in vitro* studies that IL-6 enhances *gp130* mRNA in human monocytes and other cell types (Schoester et al., 1994; Schooltink et al., 1992). Furthermore, O'Brien et al. have proposed a STAT-binding element in the gp130 promoter (O'Brien and Manolagas, 1997). Whereas these studies have investigated mRNA expression, which is not necessarily an indicator of cell surface expression, it has also been reported that in mast cells gp130 surface expression is up-regulated by IL-10-induced STAT3 activation (Traum et al., 2012). These lines of evidence suggest that the observed increase in gp130 surface expression on monocytes from IBD patients might be induced by elevated p-STAT3 levels.

Interestingly, it was shown earlier that mRNA expression levels of the IL-6 receptor complex are increased in circulating lymphocytes of patients with IBD (Holub et al., 1998). Furthermore, Carey *et al.* reported that STAT3 phosphorylation is elevated in circulating neutrophils of pediatric IBD patients and suggested that this was IL-6-induced. The study additionally revealed a correlation between the frequency of neutrophils with activated STAT3 and mucosal inflammation (Carey et al., 2008).

What consequences might arise from increased gp130 surface expression and STAT3 phosphorylation in monocytes of IBD patients? The overall role of p-STAT3 in IBD is ambiguous and clearly depends on the cell type. The anti-inflammatory effects of p-STAT3 are often emphasized in macrophages. However, as mentioned earlier, STAT3 is also activated in response to IL-10 and the biological outcome seems to depend strictly on signaling strength and duration (4.1.4). The deficiency of gp130 in macrophages and neutrophils leads to reduction of DSS colitis in mice (Sander et al., 2008), obviously arguing against an anti-inflammatory role of gp130-mediated p-STAT3 in these cell types. The biologic effects of IL-6 on monocytes are even less clear. Since IL-6 acts as a direct migration factor on human monocytes, it is conceivable that the increased gp130-mediated signaling in monocytes of IBD patients leads to an upregulation of adhesion molecules. At the site of inflammation, in the lamina propria, IL-6 might act as chemotactic factor and attract monocytes to infiltrate the tissue.

The administration of infliximab, a monoclonal anti-TNF-α antibody, to children with IBD resulted in downregulation of gp130 (figure 3-19 A) and consistently also of p-STAT3

expression in monocytes (figure 3-19 B). Thus, the neutralization of TNF-α had an impact on gp130 surface expression and downstream signaling. The mechanism behind this observation is unclear, but it cannot be excluded that it might influence clinical efficacy. Interestingly, anti-TNF agents have been shown to bind to Fc receptors and thereby modulate their own inhibitory efficacy, as well as inducing Fc-mediated signaling. A recent study has reported that the capacity of infliximab to inhibit TNF-mediated responses in PBMCs from IBD patients is rather low (Wojtal et al., 2012). Furthermore, infliximab was shown to induce apoptosis in monocytes by a mechanism involving membrane-bound TNF-α (Lugering et al., 2001). Therefore, it is possible that the observed effects on gp130 surface expression and STAT3 phosphorylation were due to signaling via membrane-bound TNF-α or via Fc receptors instead of neutralization of TNF-α.

Since the small amount of blood obtained from IBD patients restricts the spectrum of possible analyses, chronic colitis was induced in mice. The aim was to determine possible parallels between the observations made in human IBD monocytes and the murine system. Indeed, in analogy to human IBD patients, mice suffering from DSS-induced colitis displayed an increased expression of gp130 on $CD11b^+$ cells at the end of the experiment compared to untreated mice (figure 3-21 A). This was reflected in the level of downstream signaling, i.e. DSS-treated mice showed increased STAT3 phosphorylation in $CD11b^+$ cells at day 37 compared to day 1 and to untreated mice (figure 3-21 B).

Many studies of murine colitis models have reported enhanced STAT3 phosphorylation in the colon (Lee et al., 2012; Suzuki et al., 2001). However, to our knowledge STAT3 activation in circulating leukocytes has not yet been investigated. As speculated concerning the human system, it could be that increased levels of gp130 surface expression and STAT3 phosphorylation contribute to an upregulation of adhesion molecules and act on the migration of myeloid cells.

Interestingly, the situation was reversed in mesenteric lymph nodes. $CD11b^+$ cells in this immune compartment of DSS-treated mice displayed lower levels of gp130 surface expression and STAT3 phosphorylation compared to control mice (figure 3-22). The mechanisms regulating increased gp130 surface expression and STAT3 phosphorylation in circulating myeloid cells and decreased gp130 surface expression and STAT3 phosphorylation in myeloid cells in the mesenteric lymph nodes are unclear. It is conceivable that cell-cell contacts or the close proximity to cells secreting soluble factors in the lymph nodes had a regulatory impact on gp130 surface expression.

4.3.2 JIA

Reduced surface expression of the IL-6 receptor complex was found on SF monocytes from patients with JIA compared to PB monocytes (figure 3-23). We hypothesized that soluble factors accounting for the highly inflammatory environment in the joint were responsible for the observed receptor downregulation by internalization. Indeed, gp130 expression was reconstituted after isolation of the cells from SF and after up to 1 hour of rest. In contrast, IL-6R levels remained constant (figure 3-24 A). The situation in the inflamed joint was mimicked by incubating PBMCs from healthy donors with SF. A rapid downregulation of both components of the IL-6 receptor complex was detected after 20 min of stimulation (figure 3-24 B-C). The loss of gp130 cell surface expression was slightly stronger compared to IL-6R.

Why gp130 re-appeared on the cell surface after 30 min of rest and IL-6R surface expression remained at very low levels, was not clarified. Normally, after endocytosis receptors are either sorted into recycling endosomes to be transported back to the plasma membrane or they are degraded by the lysosomal pathway (Sorkin, 2000). Internalization of the IL-6 receptor complex is ligand-induced. Re-appearance of IL-6 binding sites after ligand-induced internalization in hepatocytes requires >8 h and is sensitive to cyclohexamide, which indicates a dependence on new protein synthesis and thus lysosomal degradation (Zohlnhofer et al., 1992). However, considering that the internalization of IL-6R alone is highly inefficient and its cytoplasmic domain is not essential for internalization of the receptor complex (Dittrich et al., 1994), the findings from SF monocytes indicate that downregulation of IL-6R depended on gp130. This further suggests that complexes of IL-6R and gp130 must have formed previously. Whether such complexes of gp130 and IL-6R become separated in the endosomes in order to be subsequently sorted differentially, is not known. An alternative explanation might be different kinetics for re-synthesis of the two receptor components.

Association of gp130 and IL-6R normally occurs after binding of IL-6. Since high amounts of IL-6 are present in the SF, it may be hypothesized that the IL-6 receptor complex was internalized by a ligand-induced process and that this accounted for the observed reduced surface expression levels. Consistently, a recent study reported that gp130 and IL-6R expression on T cells was reduced by incubation with SF from RA patients and that this could be inhibited by an IL-6R blocking antibody (Hidalgo et al., 2011). However, levels were not completely restored after blockade of IL-6 signaling indicating an additional mechanism contributing to downregulation. This was supported by our own experiments in monocytes with the p38-specific inhibitor SB202190. Incubation of cells with SB202190 prior to the addition of SF partially restored surface expression of gp130 and IL-6R (figure 3-25). This

effect was again more pronounced for gp130 than for IL-6R. These results suggests that crosstalk mechanisms comparable to those observed in monocytes after IL-1β stimulation may be of importance in joint inflammation in patients with JIA.

To investigate whether downstream signaling is affected by diminished surface expression levels of gp130 and IL-6R, STAT3 phosphorylation was analyzed in SF monocytes and compared to that in PB monocytes. Surprisingly, basal STAT3 phosphorylation was stronger in SF than in PB monocytes (figure 3-26 A). Since reduced availability of gp130 or even both receptor components on the cell surface strongly implicates decreased IL-6 responsiveness, STAT3 phosphorylation was determined after IL-6 stimulation. In accordance with low receptor availability, SF monocytes were largely unresponsive to IL-6 in contrast to PB monocytes (figure 3-26 B). Thus, it can be concluded that increased amounts of p-STAT3 in SF monocytes are likely to be induced by factors other than IL-6. One possible candidate is the anti-inflammatory cytokine IL-10, which was shown to induce STAT3 phosphorylation to an extent comparable to IL-6, though after a longer incubation time (figure 3-27 B). Similar to the downregulation of gp130 and IL-6R surface expression following incubation of PBMCs with SF, STAT3 phosphorylation was induced by stimulation with SF (figure 3-27 A). The addition of IL-6 after pre-incubation with SF resulted in only a slight further induction of p-STAT3 compared to stimulation with SF alone. One obvious reason for this could be the decreased amount of IL-6 receptor complexes on the cell surface. An alternative explanation, which most likely contributes to the diminished p-STAT3 induction by IL-6, is the induction of SOCS3. The feedback inhibitor SOCS3 is expressed, irrespective of the factor by which STAT3 is activated.

As described in the section 4.1.4, the biological outcome of gp130-mediated signaling may be modulated by crosstalk inhibition. Whether the overall role of IL-6 is pro- or anti-inflammatory and how this is influenced by the decrease of gp130 and IL-6R surface expression can only be speculated. Actions of IL-6 on monocytes, which most likely contribute to a pro-inflammatory response in the inflamed joint, include the role of monocytes as osteoclast precursors. Normally, the action of bone-forming osteoblasts and bone-resorbing osteoclasts is determined by a strictly regulated balance (Kwan Tat et al., 2004). However, in inflammatory situations this balance might be disturbed. The destruction of articular cartilage and bone is a hallmark in JIA and RA (Gravallese et al., 1998). It has been shown that IL-6 together with M-CSF is capable of inducing differentiation of $CD14^+$ cells to osteoclasts (Kudo et al., 2003). The authors suggested that this mechanism may not be of relevance in normal bone physiology, but in pathological situations with increased amounts of cytokines. IL-6 was furthermore shown to up-regulate the expression of M-CSF receptors

on monocytes (Chomarat et al., 2000), which may amplify the induction of osteoclast formation by IL-6. Osteoclastogenesis moreover can be triggered by M-CSF in association with RANKL and IL-6 induces RANKL from T cells or synovial fibroblasts. The reduction of surface expression of the IL-6 receptor complex by soluble factors in the SF would, in this scenario, act as protective mechanism, averting an overwhelming pro-inflammatory reaction. Anti-inflammatory actions of IL-6 on monocytes include the induction of IL-1Ra. Increased amounts of IL-1Ra have been detected in SF of RA patients (Malyak et al., 1993). An overview of these mechanisms is given in figure 4-2.

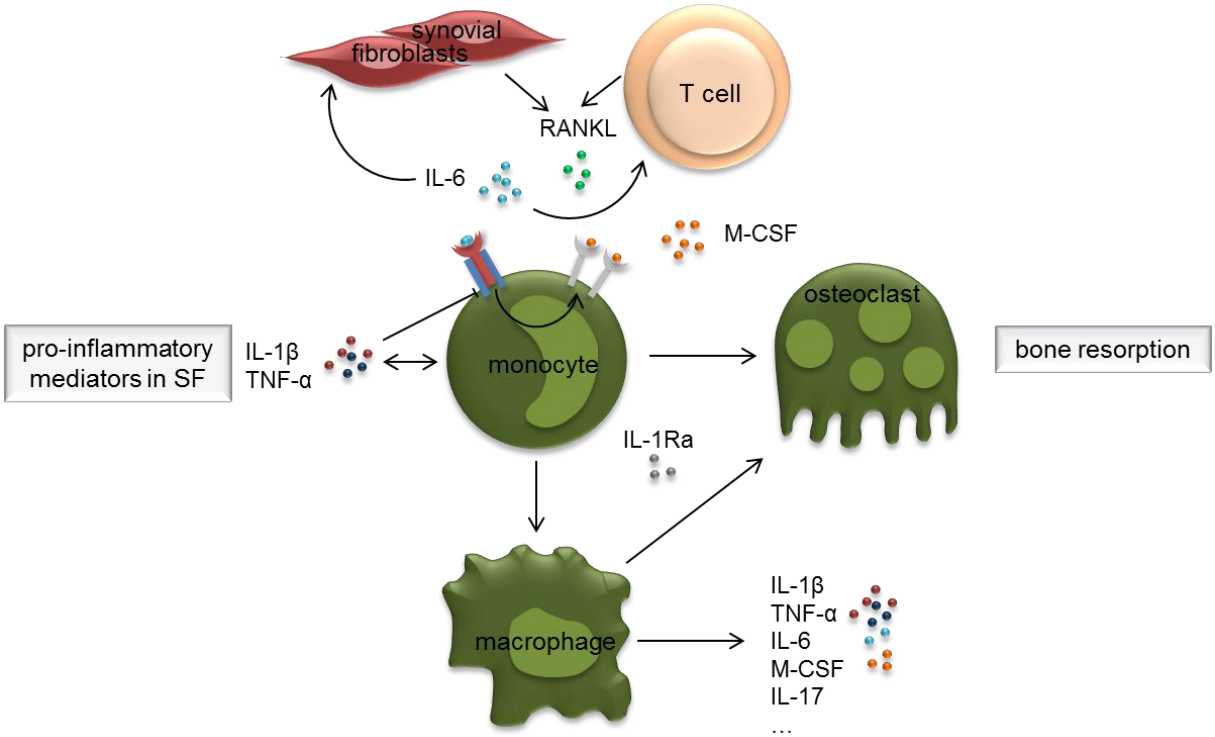

Figure 4-2: Possible pro- and anti-inflammatory actions of IL-6 signaling in monocytes in the synovial fluid.
IL-6 upregulates the expression of M-CSFR on monocytes and induces the secretion of RANKL from synovial fibroblasts and T cells. Either M-CSF and RANKL or M-CSF and IL-6 lead to the differentiation of monocytes or macrophages to bone resorbing osteoclasts. M-CSF can further support the differentiation of monocytes to macrophages, which are potent producers of pro-inflammatory cytokines. The anti-inflammatory actions of IL-6 signaling in monocytes are exemplified by the secretion of IL-1Ra. IL-1β or other pro-inflammatory mediators may modulate the different actions of IL-6 by downregulation of the IL-6 receptor.

5 OUTLOOK

This study has contributed to a better understanding of the regulation of gp130 surface expression, but questions remain unanswered and new questions have been raised by the results presented.
In future experiments it would be interesting to investigate the extent to which crosstalk regulation of IL-6 signaling is translated to the level of gene expression. Induction of p-STAT3 target genes could be determined by quantitative RT-PCR after IL-6 stimulation with or without IL-1β pre-incubation. This analysis could additionally be performed with SF instead of IL-1β to further elucidate the role of gp130-mediated signals in JIA.

In gp130 transgenic mice crosstalk should be investigated in other cell types and with different stimuli to explore whether the observed tendencies then become more apparent. Restriction of IL-6 signaling in murine macrophages by TNF-α and LPS has been shown before (Kiu et al., 2007). On the basis of these results it would be interesting to study crosstalk regulation in the two transgenic mouse strains in macrophages and to compare the impact of IL-1β to other pro-inflammatory stimuli.
Since T cells of gp130-mut splenocytes showed an enhanced capacity to activate STAT3 in response to IL-6 in comparison to gp130-wt splenocytes (figure 3-13 B), it would be interesting to investigate differentiation of T cells derived from both strains towards the Th17 lineage. Differentiation of Th17 cells depends on IL-6 and TGF-β. A possibly increased potential to differentiate into Th17 cells might be of importance for models of inflammation. Th17 cells are known to be involved in RA and other inflammatory conditions.

In future, a model of arthritis and DSS colitis in transgenic mice will be used to further explore the impact of crosstalk regulation in chronic inflammatory conditions. Results from JIA patients and *in vitro* stimulation of PBMCs with SF (3.3.2.1) strongly suggest that crosstalk mechanisms may be of relevance in the inflamed joint. Furthermore, the differential regulation of gp130 expression and STAT3 phosphorylation in monocytes from IBD patients (figure 3-17 and figure 3-18) and $CD11b^+$ cells from wt mice with chronic DSS colitis (figure 3-21) provide evidence that regulation of gp130 surface expression is of relevance in the disease. Since CD11b is not an exclusive marker of monocytes, it will be necessary to discriminate between monocytes and other myeloid cells such as neutrophils in future experiments.

It would also be interesting to include adult IBD patients in future analyses to investigate potential differences between adult and pediatric forms of IBD in terms of gp130 and

p-STAT3 expression. This idea is supported by the fact that Musso *et al.* did not discover increased p-STAT3 levels in PBMCs of adult IBD patients, which is in contrast to the results shown in this study and the one of Carey *et al.* (Carey et al., 2008; Musso et al., 2005). To support the hypothesis that increased STAT3 phosphorylation in monocytes from IBD patients arises from elevated gp130 expression and high levels of IL-6 and/or sIL-6R-IL-6 complexes, IL-6 responsiveness should be investigated as in the experiments performed with PB and SF monocytes from JIA patients (figure 3-26 B). Furthermore, it would be interesting to elucidate the mechanism by which infliximab influences gp130 surface expression and STAT3 activation. The observed parallels in the murine system also provide a basis for the study of potential effects of infliximab in the mouse. It would be of further interest to isolate lamina propria cells in the final stages of chronic DSS colitis and to investigate gp130 surface expression and STAT3 phosphorylation in these cells. As with the changed gp130 expression on SF monocytes compared to PB monocytes in JIA patients, it seems conceivable that similar mechanisms are present at the site of inflammation in IBD.

Further experiments with PBMCs stimulated with SF should elucidate mechanisms of gp130 downregulation in more detail. Phosphorylation of p38 and serine 782, for example, can be determined in monocytes after stimulation with SF. The anti-IL-6R antibody tocilizumab can be used to evaluate the impact on ligand-induced internalization of gp130 and IL-6R. Furthermore, the reason for increased levels of STAT3 phosphorylation in SF monocytes compared to PB monocytes (figure 3-26 A) will be investigated. Concretely, PBMCs will be stimulated with SF after pre-incubation of different blocking antibodies. By inhibition of protein synthesis, the extent to which SOCS3 contributes to the unresponsiveness of monocytes to IL-6 after pre-stimulation with SF (figure 3-27 A) could also be determined.

Future analyses of gp130 regulation and associated changes will contribute to a better understanding of the sometimes contradictory effects of IL-6 in inflammatory conditions.

6 REFERENCES

Afford, S.C., Pongracz, J., Stockley, R.A., Crocker, J., and Burnett, D. (1992). The induction by human interleukin-6 of apoptosis in the promonocytic cell line U937 and human neutrophils. J Biol Chem *267*, 21612-21616.

Ahmed, S.T., and Ivashkiv, L.B. (2000). Inhibition of IL-6 and IL-10 signaling and Stat activation by inflammatory and stress pathways. J Immunol *165*, 5227-5237.

Ahmed, S.T., Mayer, A., Ji, J.D., and Ivashkiv, L.B. (2002). Inhibition of IL-6 signaling by a p38-dependent pathway occurs in the absence of new protein synthesis. J Leukoc Biol *72*, 154-162.

Andus, T., Geiger, T., Hirano, T., Kishimoto, T., and Heinrich, P.C. (1988). Action of recombinant human interleukin 6, interleukin 1 beta and tumor necrosis factor alpha on the mRNA induction of acute-phase proteins. Eur J Immunol *18*, 739-746.

Atreya, R., Mudter, J., Finotto, S., Mullberg, J., Jostock, T., Wirtz, S., Schutz, M., Bartsch, B., Holtmann, M., Becker, C.*, et al.* (2000). Blockade of interleukin 6 trans signaling suppresses T-cell resistance against apoptosis in chronic intestinal inflammation: evidence in crohn disease and experimental colitis in vivo. Nat Med *6*, 583-588.

Atsumi, T., Ishihara, K., Kamimura, D., Ikushima, H., Ohtani, T., Hirota, S., Kobayashi, H., Park, S.J., Saeki, Y., Kitamura, Y., and Hirano, T. (2002). A point mutation of Tyr-759 in interleukin 6 family cytokine receptor subunit gp130 causes autoimmune arthritis. J Exp Med *196*, 979-990.

Auernhammer, C.J., Zitzmann, K., Schnitzler, F., Seiderer, J., Lohse, P., Vlotides, G., Engelhardt, D., Sackmann, M., Goke, B., and Ochsenkuhn, T. (2005). Role of the intracellular receptor domain of gp130 (exon 17) in human inflammatory bowel disease. World J Gastroenterol *11*, 1196-1199.

Axelsson, L.G., Landstrom, E., Goldschmidt, T.J., Gronberg, A., and Bylund-Fellenius, A.C. (1996). Dextran sulfate sodium (DSS) induced experimental colitis in immunodeficient mice: effects in CD4(+) -cell depleted, athymic and NK-cell depleted SCID mice. Inflamm Res *45*, 181-191.

Barton, B.E., and Jackson, J.V. (1993). Protective role of interleukin 6 in the lipopolysaccharide-galactosamine septic shock model. Infect Immun *61*, 1496-1499.

Beard, C., Hochedlinger, K., Plath, K., Wutz, A., and Jaenisch, R. (2006). Efficient method to generate single-copy transgenic mice by site-specific integration in embryonic stem cells. Genesis *44*, 23-28.

Bettelli, E., Carrier, Y., Gao, W., Korn, T., Strom, T.B., Oukka, M., Weiner, H.L., and Kuchroo, V.K. (2006). Reciprocal developmental pathways for the generation of pathogenic effector TH17 and regulatory T cells. Nature *441*, 235-238.

Betz, U.A., Bloch, W., van den Broek, M., Yoshida, K., Taga, T., Kishimoto, T., Addicks, K., Rajewsky, K., and Muller, W. (1998). Postnatally induced inactivation of gp130 in mice results in neurological, cardiac, hematopoietic, immunological, hepatic, and pulmonary defects. J Exp Med *188*, 1955-1965.

Bode, J.G., Albrecht, U., Haussinger, D., Heinrich, P.C., and Schaper, F. (2012). Hepatic acute phase proteins--regulation by IL-6- and IL-1-type cytokines involving STAT3 and its crosstalk with NF-kappaB-dependent signaling. Eur J Cell Biol *91*, 496-505.

Bode, J.G., Nimmesgern, A., Schmitz, J., Schaper, F., Schmitt, M., Frisch, W., Haussinger, D., Heinrich, P.C., and Graeve, L. (1999). LPS and TNFalpha induce SOCS3 mRNA and inhibit IL-6-induced activation of STAT3 in macrophages. FEBS Lett *463*, 365-370.

Bode, J.G., Schweigart, J., Kehrmann, J., Ehlting, C., Schaper, F., Heinrich, P.C., and Haussinger, D. (2003). TNF-alpha induces tyrosine phosphorylation and recruitment of the Src homology protein-tyrosine phosphatase 2 to the gp130 signal-transducing subunit of the IL-6 receptor complex. J Immunol *171*, 257-266.

Bradford, M.M. (1976). A rapid and sensitive method for the quantitation of microgram quantities of protein utilizing the principle of protein-dye binding. Anal Biochem *72*, 248-254.

Carey, R., Jurickova, I., Ballard, E., Bonkowski, E., Han, X., Xu, H., and Denson, L.A. (2008). Activation of an IL-6:STAT3-dependent transcriptome in pediatric-onset inflammatory bowel disease. Inflamm Bowel Dis *14*, 446-457.

Cash, J.L., White, G.E., and Greaves, D.R. (2009). Chapter 17. Zymosan-induced peritonitis as a simple experimental system for the study of inflammation. Methods Enzymol *461*, 379-396.

Chomarat, P., Banchereau, J., Davoust, J., and Palucka, A.K. (2000). IL-6 switches the differentiation of monocytes from dendritic cells to macrophages. Nat Immunol *1*, 510-514.

Choy, E. (2012). Understanding the dynamics: pathways involved in the pathogenesis of rheumatoid arthritis. Rheumatology (Oxford) *51 Suppl 5*, v3-11.
Chung, C.D., Liao, J., Liu, B., Rao, X., Jay, P., Berta, P., and Shuai, K. (1997). Specific inhibition of Stat3 signal transduction by PIAS3. Science *278*, 1803-1805.
Clahsen, T., and Schaper, F. (2008). Interleukin-6 acts in the fashion of a classical chemokine on monocytic cells by inducing integrin activation, cell adhesion, actin polymerization, chemotaxis, and transmigration. J Leukoc Biol *84*, 1521-1529.
de Almeida, M.C., Silva, A.C., Barral, A., and Barral Netto, M. (2000). A simple method for human peripheral blood monocyte isolation. Mem Inst Oswaldo Cruz *95*, 221-223.
de Jager, W., Hoppenreijs, E.P., Wulffraat, N.M., Wedderburn, L.R., Kuis, W., and Prakken, B.J. (2007). Blood and synovial fluid cytokine signatures in patients with juvenile idiopathic arthritis: a cross-sectional study. Ann Rheum Dis *66*, 589-598.
Dittrich, E., Haft, C.R., Muys, L., Heinrich, P.C., and Graeve, L. (1996). A di-leucine motif and an upstream serine in the interleukin-6 (IL-6) signal transducer gp130 mediate ligand-induced endocytosis and down-regulation of the IL-6 receptor. J Biol Chem *271*, 5487-5494.
Dittrich, E., Rose-John, S., Gerhartz, C., Mullberg, J., Stoyan, T., Yasukawa, K., Heinrich, P.C., and Graeve, L. (1994). Identification of a region within the cytoplasmic domain of the interleukin-6 (IL-6) signal transducer gp130 important for ligand-induced endocytosis of the IL-6 receptor. J Biol Chem *269*, 19014-19020.
Diveu, C., Lak-Hal, A.H., Froger, J., Ravon, E., Grimaud, L., Barbier, F., Hermann, J., Gascan, H., and Chevalier, S. (2004). Predominant expression of the long isoform of GP130-like (GPL) receptor is required for interleukin-31 signaling. Eur Cytokine Netw *15*, 291-302.
Ehlting, C., Lai, W.S., Schaper, F., Brenndorfer, E.D., Matthes, R.J., Heinrich, P.C., Ludwig, S., Blackshear, P.J., Gaestel, M., Haussinger, D., and Bode, J.G. (2007). Regulation of suppressor of cytokine signaling 3 (SOCS3) mRNA stability by TNF-alpha involves activation of the MKK6/p38MAPK/MK2 cascade. J Immunol *178*, 2813-2826.
Ernst, M., Inglese, M., Waring, P., Campbell, I.K., Bao, S., Clay, F.J., Alexander, W.S., Wicks, I.P., Tarlinton, D.M., Novak, U.*, et al.* (2001). Defective gp130-mediated signal transducer and activator of transcription (STAT) signaling results in degenerative joint disease, gastrointestinal ulceration, and failure of uterine implantation. J Exp Med *194*, 189-203.
Ernst, M., and Jenkins, B.J. (2004). Acquiring signalling specificity from the cytokine receptor gp130. Trends Genet *20*, 23-32.
Eulenfeld, R., Dittrich, A., Khouri, C., Muller, P.J., Mutze, B., Wolf, A., and Schaper, F. (2012). Interleukin-6 signalling: more than Jaks and STATs. Eur J Cell Biol *91*, 486-495.
Fiorentino, D.F., Zlotnik, A., Mosmann, T.R., Howard, M., and O'Garra, A. (1991). IL-10 inhibits cytokine production by activated macrophages. J Immunol *147*, 3815-3822.
Gabay, C., and Kushner, I. (1999). Acute-phase proteins and other systemic responses to inflammation. N Engl J Med *340*, 448-454.
Garbers, C., Hermanns, H.M., Schaper, F., Muller-Newen, G., Grotzinger, J., Rose-John, S., and Scheller, J. (2012). Plasticity and cross-talk of interleukin 6-type cytokines. Cytokine Growth Factor Rev *23*, 85-97.
Gibson, R.M., Schiemann, W.P., Prichard, L.B., Reno, J.M., Ericsson, L.H., and Nathanson, N.M. (2000). Phosphorylation of human gp130 at Ser-782 adjacent to the Di-leucine internalization motif. Effects on expression and signaling. J Biol Chem *275*, 22574-22582.
Gravallese, E.M., Harada, Y., Wang, J.T., Gorn, A.H., Thornhill, T.S., and Goldring, S.R. (1998). Identification of cell types responsible for bone resorption in rheumatoid arthritis and juvenile rheumatoid arthritis. Am J Pathol *152*, 943-951.
Grivennikov, S., Karin, E., Terzic, J., Mucida, D., Yu, G.Y., Vallabhapurapu, S., Scheller, J., Rose-John, S., Cheroutre, H., Eckmann, L., and Karin, M. (2009). IL-6 and Stat3 are required for survival of intestinal epithelial cells and development of colitis-associated cancer. Cancer Cell *15*, 103-113.
Haufe, S., Haug, M., Schepp, C., Kuemmerle-Deschner, J., Hansmann, S., Rieber, N., Tzaribachev, N., Hospach, T., Maier, J., Dannecker, G.E., and Holzer, U. (2011). Impaired suppression of synovial fluid CD4+CD25- T cells from patients with juvenile idiopathic arthritis by CD4+CD25+ Treg cells. Arthritis Rheum *63*, 3153-3162.
Heinrich, P.C., Behrmann, I., Haan, S., Hermanns, H.M., Muller-Newen, G., and Schaper, F. (2003). Principles of interleukin (IL)-6-type cytokine signalling and its regulation. Biochem J *374*, 1-20.
Heinrich, P.C., Behrmann, I., Muller-Newen, G., Schaper, F., and Graeve, L. (1998). Interleukin-6-type cytokine signalling through the gp130/Jak/STAT pathway. Biochem J *334 (Pt 2)*, 297-314.

Helchowski, C.M., Minea, R.O., Swenson, S.D., and Markland, F.S., Jr. (2009). The use of pepsin in receptor internalization assays. Biochem Biophys Res Commun *388*, 240-246.

Hidalgo, E., Essex, S.J., Yeo, L., Curnow, S.J., Filer, A., Cooper, M.S., Thomas, A.M., McGettrick, H.M., Salmon, M., Buckley, C.D.*, et al.* (2011). The response of T cells to interleukin-6 is differentially regulated by the microenvironment of the rheumatoid synovial fluid and tissue. Arthritis Rheum *63*, 3284-3293.

Holub, M.C., Mako, E., Devay, T., Dank, M., Szalai, C., Fenyvesi, A., and Falus, A. (1998). Increased interleukin-6 levels, interleukin-6 receptor and gp130 expression in peripheral lymphocytes of patients with inflammatory bowel disease. Scand J Gastroenterol Suppl *228*, 47-50.

Honda, M., Yamamoto, S., Cheng, M., Yasukawa, K., Suzuki, H., Saito, T., Osugi, Y., Tokunaga, T., and Kishimoto, T. (1992). Human soluble IL-6 receptor: its detection and enhanced release by HIV infection. J Immunol *148*, 2175-2180.

Horiuchi, T., Mitoma, H., Harashima, S., Tsukamoto, H., and Shimoda, T. (2010). Transmembrane TNF-alpha: structure, function and interaction with anti-TNF agents. Rheumatology (Oxford) *49*, 1215-1228.

Hurst, S.M., Wilkinson, T.S., McLoughlin, R.M., Jones, S., Horiuchi, S., Yamamoto, N., Rose-John, S., Fuller, G.M., Topley, N., and Jones, S.A. (2001). Il-6 and its soluble receptor orchestrate a temporal switch in the pattern of leukocyte recruitment seen during acute inflammation. Immunity *14*, 705-714.

Ito, H., Takazoe, M., Fukuda, Y., Hibi, T., Kusugami, K., Andoh, A., Matsumoto, T., Yamamura, T., Azuma, J., Nishimoto, N.*, et al.* (2004). A pilot randomized trial of a human anti-interleukin-6 receptor monoclonal antibody in active Crohn's disease. Gastroenterology *126*, 989-996; discussion 947.

Jenkins, B.J., Roberts, A.W., Najdovska, M., Grail, D., and Ernst, M. (2005). The threshold of gp130-dependent STAT3 signaling is critical for normal regulation of hematopoiesis. Blood *105*, 3512-3520.

Jones, S.A. (2005). Directing transition from innate to acquired immunity: defining a role for IL-6. J Immunol *175*, 3463-3468.

Jones, S.A., Horiuchi, S., Topley, N., Yamamoto, N., and Fuller, G.M. (2001). The soluble interleukin 6 receptor: mechanisms of production and implications in disease. FASEB J *15*, 43-58.

Jones, S.A., Scheller, J., and Rose-John, S. (2011). Therapeutic strategies for the clinical blockade of IL-6/gp130 signaling. J Clin Invest *121*, 3375-3383.

Jostock, T., Mullberg, J., Ozbek, S., Atreya, R., Blinn, G., Voltz, N., Fischer, M., Neurath, M.F., and Rose-John, S. (2001). Soluble gp130 is the natural inhibitor of soluble interleukin-6 receptor transsignaling responses. Eur J Biochem *268*, 160-167.

Kiu, H., Hilton, D.J., Nicola, N.A., Ernst, M., Marquez, R., Alexander, W.S., Roberts, A.W., and McManus, E.J. (2007). Mechanism of crosstalk inhibition of IL-6 signaling in response to LPS and TNFalpha. Growth Factors *25*, 319-328.

Klein, C., Wustefeld, T., Assmus, U., Roskams, T., Rose-John, S., Muller, M., Manns, M.P., Ernst, M., and Trautwein, C. (2005). The IL-6-gp130-STAT3 pathway in hepatocytes triggers liver protection in T cell-mediated liver injury. J Clin Invest *115*, 860-869.

Koon, H.W., Kim, Y.S., Xu, H., Kumar, A., Zhao, D., Karagiannides, I., Dobner, P.R., and Pothoulakis, C. (2009). Neurotensin induces IL-6 secretion in mouse preadipocytes and adipose tissues during 2,4,6,-trinitrobenzensulphonic acid-induced colitis. Proc Natl Acad Sci U S A *106*, 8766-8771.

Kopf, M., Baumann, H., Freer, G., Freudenberg, M., Lamers, M., Kishimoto, T., Zinkernagel, R., Bluethmann, H., and Kohler, G. (1994). Impaired immune and acute-phase responses in interleukin-6-deficient mice. Nature *368*, 339-342.

Kortylewski, M., Heinrich, P.C., Mackiewicz, A., Schniertshauer, U., Klingmuller, U., Nakajima, K., Hirano, T., Horn, F., and Behrmann, I. (1999). Interleukin-6 and oncostatin M-induced growth inhibition of human A375 melanoma cells is STAT-dependent and involves upregulation of the cyclin-dependent kinase inhibitor p27/Kip1. Oncogene *18*, 3742-3753.

Krause, A., Scaletta, N., Ji, J.D., and Ivashkiv, L.B. (2002). Rheumatoid arthritis synoviocyte survival is dependent on Stat3. J Immunol *169*, 6610-6616.

Kudo, O., Sabokbar, A., Pocock, A., Itonaga, I., Fujikawa, Y., and Athanasou, N.A. (2003). Interleukin-6 and interleukin-11 support human osteoclast formation by a RANKL-independent mechanism. Bone *32*, 1-7.

Kutukculer, N., Caglayan, S., and Aydogdu, F. (1998). Study of pro-inflammatory (TNF-alpha, IL-1alpha, IL-6) and T-cell-derived (IL-2, IL-4) cytokines in plasma and synovial fluid of patients with

juvenile chronic arthritis: correlations with clinical and laboratory parameters. Clin Rheumatol *17*, 288-292.

Kwan Tat, S., Padrines, M., Theoleyre, S., Heymann, D., and Fortun, Y. (2004). IL-6, RANKL, TNF-alpha/IL-1: interrelations in bone resorption pathophysiology. Cytokine Growth Factor Rev *15*, 49-60.

Laemmli, U.K. (1970). Cleavage of structural proteins during the assembly of the head of bacteriophage T4. Nature *227*, 680-685.

Lang, R., Patel, D., Morris, J.J., Rutschman, R.L., and Murray, P.J. (2002). Shaping gene expression in activated and resting primary macrophages by IL-10. J Immunol *169*, 2253-2263.

Lee, M.J., Lee, J.K., Choi, J.W., Lee, C.S., Sim, J.H., Cho, C.H., Lee, K.H., Cho, I.H., Chung, M.H., Kim, H.R., and Ye, S.K. (2012). Interleukin-6 induces S100A9 expression in colonic epithelial cells through STAT3 activation in experimental ulcerative colitis. PLoS One *7*, e38801.

Lehmann, U., Schmitz, J., Weissenbach, M., Sobota, R.M., Hortner, M., Friederichs, K., Behrmann, I., Tsiaris, W., Sasaki, A., Schneider-Mergener, J.*, et al.* (2003). SHP2 and SOCS3 contribute to Tyr-759-dependent attenuation of interleukin-6 signaling through gp130. J Biol Chem *278*, 661-671.

Li, Y., de Haar, C., Peppelenbosch, M.P., and van der Woude, C.J. (2012). SOCS3 in immune regulation of inflammatory bowel disease and inflammatory bowel disease-related cancer. Cytokine Growth Factor Rev *23*, 127-138.

Lugering, A., Schmidt, M., Lugering, N., Pauels, H.G., Domschke, W., and Kucharzik, T. (2001). Infliximab induces apoptosis in monocytes from patients with chronic active Crohn's disease by using a caspase-dependent pathway. Gastroenterology *121*, 1145-1157.

Malyak, M., Swaney, R.E., and Arend, W.P. (1993). Levels of synovial fluid interleukin-1 receptor antagonist in rheumatoid arthritis and other arthropathies. Potential contribution from synovial fluid neutrophils. Arthritis Rheum *36*, 781-789.

McGovern, J.L., Nguyen, D.X., Notley, C.A., Mauri, C., Isenberg, D.A., and Ehrenstein, M.R. (2012). Th17 cells are restrained by Treg cells via the inhibition of interleukin-6 in patients with rheumatoid arthritis responding to anti-tumor necrosis factor antibody therapy. Arthritis Rheum *64*, 3129-3138.

McInnes, I.B., and Schett, G. (2007). Cytokines in the pathogenesis of rheumatoid arthritis. Nat Rev Immunol *7*, 429-442.

McInnes, I.B., and Schett, G. (2011). The pathogenesis of rheumatoid arthritis. N Engl J Med *365*, 2205-2219.

Mitsuyama, K., Sata, M., and Rose-John, S. (2006). Interleukin-6 trans-signaling in inflammatory bowel disease. Cytokine Growth Factor Rev *17*, 451-461.

Mitsuyama, K., Sata, M., and Tanikawa, K. (1991). Significance of interleukin-6 in patients with inflammatory bowel disease. Gastroenterol Jpn *26*, 20-28.

Mudter, J., and Neurath, M.F. (2007). Il-6 signaling in inflammatory bowel disease: pathophysiological role and clinical relevance. Inflamm Bowel Dis *13*, 1016-1023.

Mudter, J., Weigmann, B., Bartsch, B., Kiesslich, R., Strand, D., Galle, P.R., Lehr, H.A., Schmidt, J., and Neurath, M.F. (2005). Activation pattern of signal transducers and activators of transcription (STAT) factors in inflammatory bowel diseases. Am J Gastroenterol *100*, 64-72.

Murphy, S.F., Kwon, J.H., and Boone, D.L. (2012). Novel players in inflammatory bowel disease pathogenesis. Curr Gastroenterol Rep *14*, 146-152.

Musso, A., Dentelli, P., Carlino, A., Chiusa, L., Repici, A., Sturm, A., Fiocchi, C., Rizzetto, M., Pegoraro, L., Sategna-Guidetti, C., and Brizzi, M.F. (2005). Signal transducers and activators of transcription 3 signaling pathway: an essential mediator of inflammatory bowel disease and other forms of intestinal inflammation. Inflamm Bowel Dis *11*, 91-98.

Naka, T., Nishimoto, N., and Kishimoto, T. (2002). The paradigm of IL-6: from basic science to medicine. Arthritis Res *4 Suppl 3*, S233-242.

Neufert, C., Pickert, G., Zheng, Y., Wittkopf, N., Warntjen, M., Nikolaev, A., Ouyang, W., Neurath, M.F., and Becker, C. (2010). Activation of epithelial STAT3 regulates intestinal homeostasis. Cell Cycle *9*, 652-655.

Nicholson, G.C., Malakellis, M., Collier, F.M., Cameron, P.U., Holloway, W.R., Gough, T.J., Gregorio-King, C., Kirkland, M.A., and Myers, D.E. (2000). Induction of osteoclasts from CD14-positive human peripheral blood mononuclear cells by receptor activator of nuclear factor kappaB ligand (RANKL). Clin Sci (Lond) *99*, 133-140.

Niedbala, W., Cai, B., Wei, X., Patakas, A., Leung, B.P., McInnes, I.B., and Liew, F.Y. (2008). Interleukin 27 attenuates collagen-induced arthritis. Ann Rheum Dis *67*, 1474-1479.

Nowell, M.A., Richards, P.J., Horiuchi, S., Yamamoto, N., Rose-John, S., Topley, N., Williams, A.S., and Jones, S.A. (2003). Soluble IL-6 receptor governs IL-6 activity in experimental arthritis: blockade of arthritis severity by soluble glycoprotein 130. J Immunol *171*, 3202-3209.

O'Brien, C.A., Gubrij, I., Lin, S.C., Saylors, R.L., and Manolagas, S.C. (1999). STAT3 activation in stromal/osteoblastic cells is required for induction of the receptor activator of NF-kappaB ligand and stimulation of osteoclastogenesis by gp130-utilizing cytokines or interleukin-1 but not 1,25-dihydroxyvitamin D3 or parathyroid hormone. J Biol Chem *274*, 19301-19308.

O'Brien, C.A., and Manolagas, S.C. (1997). Isolation and characterization of the human gp130 promoter. Regulation by STATS. J Biol Chem *272*, 15003-15010.

Oberg, H.H., Wesch, D., Grussel, S., Rose-John, S., and Kabelitz, D. (2006). Differential expression of CD126 and CD130 mediates different STAT-3 phosphorylation in CD4+CD25- and CD25high regulatory T cells. Int Immunol *18*, 555-563.

Ogilvy, S., Metcalf, D., Gibson, L., Bath, M.L., Harris, A.W., and Adams, J.M. (1999). Promoter elements of vav drive transgene expression in vivo throughout the hematopoietic compartment. Blood *94*, 1855-1863.

Ohshima, S., Saeki, Y., Mima, T., Sasai, M., Nishioka, K., Nomura, S., Kopf, M., Katada, Y., Tanaka, T., Suemura, M., and Kishimoto, T. (1998). Interleukin 6 plays a key role in the development of antigen-induced arthritis. Proc Natl Acad Sci U S A *95*, 8222-8226.

Quinn, J.M., Elliott, J., Gillespie, M.T., and Martin, T.J. (1998). A combination of osteoclast differentiation factor and macrophage-colony stimulating factor is sufficient for both human and mouse osteoclast formation in vitro. Endocrinology *139*, 4424-4427.

Radtke, S., Wuller, S., Yang, X.P., Lippok, B.E., Mutze, B., Mais, C., de Leur, H.S., Bode, J.G., Gaestel, M., Heinrich, P.C.*, et al.* (2010). Cross-regulation of cytokine signalling: pro-inflammatory cytokines restrict IL-6 signalling through receptor internalisation and degradation. J Cell Sci *123*, 947-959.

Raingeaud, J., Gupta, S., Rogers, J.S., Dickens, M., Han, J., Ulevitch, R.J., and Davis, R.J. (1995). Pro-inflammatory cytokines and environmental stress cause p38 mitogen-activated protein kinase activation by dual phosphorylation on tyrosine and threonine. J Biol Chem *270*, 7420-7426.

Ravelli, A., and Martini, A. (2007). Juvenile idiopathic arthritis. Lancet *369*, 767-778.

Repnik, U., Knezevic, M., and Jeras, M. (2003). Simple and cost-effective isolation of monocytes from buffy coats. J Immunol Methods *278*, 283-292.

Romano, M., Sironi, M., Toniatti, C., Polentarutti, N., Fruscella, P., Ghezzi, P., Faggioni, R., Luini, W., van Hinsbergh, V., Sozzani, S.*, et al.* (1997). Role of IL-6 and its soluble receptor in induction of chemokines and leukocyte recruitment. Immunity *6*, 315-325.

Rose-John, S. (2012). IL-6 trans-signaling via the soluble IL-6 receptor: importance for the pro-inflammatory activities of IL-6. Int J Biol Sci *8*, 1237-1247.

Rose-John, S., and Heinrich, P.C. (1994). Soluble receptors for cytokines and growth factors: generation and biological function. Biochem J *300 (Pt 2)*, 281-290.

Sambrook, J., Fritsch, E.F., and Maniatis, T. (1989). Molecular cloning: a laboratory manual. Cold Spring Harbor, N.Y., Laboratory Press.

Sander, L.E., Obermeier, F., Dierssen, U., Kroy, D.C., Singh, A.K., Seidler, U., Streetz, K.L., Lutz, H.H., Muller, W., Tacke, F., and Trautwein, C. (2008). Gp130 signaling promotes development of acute experimental colitis by facilitating early neutrophil/macrophage recruitment and activation. J Immunol *181*, 3586-3594.

Sasaki, A., Yasukawa, H., Shouda, T., Kitamura, T., Dikic, I., and Yoshimura, A. (2000). CIS3/SOCS-3 suppresses erythropoietin (EPO) signaling by binding the EPO receptor and JAK2. J Biol Chem *275*, 29338-29347.

Scheller, J., Chalaris, A., Schmidt-Arras, D., and Rose-John, S. (2011). The pro- and anti-inflammatory properties of the cytokine interleukin-6. Biochim Biophys Acta *1813*, 878-888.

Schoester, M., Heinrich, P.C., and Graeve, L. (1994). Regulation of interleukin-6 receptor expression by interleukin-6 in human monocytes--a re-examination. FEBS Lett *345*, 131-134.

Schooltink, H., Schmitz-Van de Leur, H., Heinrich, P.C., and Rose-John, S. (1992). Up-regulation of the interleukin-6-signal transducing protein (gp130) by interleukin-6 and dexamethasone in HepG2 cells. FEBS Lett *297*, 263-265.

Seager Danciger, J., Lutz, M., Hama, S., Cruz, D., Castrillo, A., Lazaro, J., Phillips, R., Premack, B., and Berliner, J. (2004). Method for large scale isolation, culture and cryopreservation of human monocytes suitable for chemotaxis, cellular adhesion assays, macrophage and dendritic cell differentiation. J Immunol Methods *288*, 123-134.

Shouda, T., Yoshida, T., Hanada, T., Wakioka, T., Oishi, M., Miyoshi, K., Komiya, S., Kosai, K., Hanakawa, Y., Hashimoto, K.*, et al.* (2001). Induction of the cytokine signal regulator SOCS3/CIS3 as a therapeutic strategy for treating inflammatory arthritis. J Clin Invest *108*, 1781-1788.
Solomon, L., Mansor, M., Mallon, P., and Donnelly, E. (2010). The dextran sulphate sodium (DSS) model of colitis: an overview. Comp Clin Pathol *19*, 235–239.
Sorkin, A. (2000). The endocytosis machinery. J Cell Sci *113 Pt 24*, 4375-4376.
Stahl, N., Boulton, T.G., Farruggella, T., Ip, N.Y., Davis, S., Witthuhn, B.A., Quelle, F.W., Silvennoinen, O., Barbieri, G., Pellegrini, S., and et al. (1994). Association and activation of Jak-Tyk kinases by CNTF-LIF-OSM-IL-6 beta receptor components. Science *263*, 92-95.
Suzuki, A., Hanada, T., Mitsuyama, K., Yoshida, T., Kamizono, S., Hoshino, T., Kubo, M., Yamashita, A., Okabe, M., Takeda, K.*, et al.* (2001). CIS3/SOCS3/SSI3 plays a negative regulatory role in STAT3 activation and intestinal inflammation. J Exp Med *193*, 471-481.
Takeda, K., Clausen, B.E., Kaisho, T., Tsujimura, T., Terada, N., Forster, I., and Akira, S. (1999). Enhanced Th1 activity and development of chronic enterocolitis in mice devoid of Stat3 in macrophages and neutrophils. Immunity *10*, 39-49.
Tanaka, Y., Maeshima, K., and Yamaoka, K. (2012). In vitro and in vivo analysis of a JAK inhibitor in rheumatoid arthritis. Ann Rheum Dis *71 Suppl 2*, i70-74.
Tanuma, N., Shima, H., Nakamura, K., and Kikuchi, K. (2001). Protein tyrosine phosphatase epsilonC selectively inhibits interleukin-6- and interleukin- 10-induced JAK-STAT signaling. Blood *98*, 3030-3034.
Teague, T.K., Marrack, P., Kappler, J.W., and Vella, A.T. (1997). IL-6 rescues resting mouse T cells from apoptosis. J Immunol *158*, 5791-5796.
Tebbutt, N.C., Giraud, A.S., Inglese, M., Jenkins, B., Waring, P., Clay, F.J., Malki, S., Alderman, B.M., Grail, D., Hollande, F.*, et al.* (2002). Reciprocal regulation of gastrointestinal homeostasis by SHP2 and STAT-mediated trefoil gene activation in gp130 mutant mice. Nat Med *8*, 1089-1097.
Thiel, S., Behrmann, I., Dittrich, E., Muys, L., Tavernier, J., Wijdenes, J., Heinrich, P.C., and Graeve, L. (1998a). Internalization of the interleukin 6 signal transducer gp130 does not require activation of the Jak/STAT pathway. Biochem J *330 (Pt 1)*, 47-54.
Thiel, S., Dahmen, H., Martens, A., Muller-Newen, G., Schaper, F., Heinrich, P.C., and Graeve, L. (1998b). Constitutive internalization and association with adaptor protein-2 of the interleukin-6 signal transducer gp130. FEBS Lett *441*, 231-234.
Tilg, H., Trehu, E., Atkins, M.B., Dinarello, C.A., and Mier, J.W. (1994). Interleukin-6 (IL-6) as an anti-inflammatory cytokine: induction of circulating IL-1 receptor antagonist and soluble tumor necrosis factor receptor p55. Blood *83*, 113-118.
Traum, D., Timothee, P., Silver, J., Rose-John, S., Ernst, M., and LaRosa, D.F. (2012). IL-10-induced gp130 expression in mouse mast cells permits IL-6 trans-signaling. J Leukoc Biol *91*, 427-435.
van Amelsfort, J.M., Jacobs, K.M., Bijlsma, J.W., Lafeber, F.P., and Taams, L.S. (2004). CD4(+)CD25(+) regulatory T cells in rheumatoid arthritis: differences in the presence, phenotype, and function between peripheral blood and synovial fluid. Arthritis Rheum *50*, 2775-2785.
Weissenbach, M., Clahsen, T., Weber, C., Spitzer, D., Wirth, D., Vestweber, D., Heinrich, P.C., and Schaper, F. (2004). Interleukin-6 is a direct mediator of T cell migration. Eur J Immunol *34*, 2895-2906.
Wijdenes, J., Heinrich, P.C., Muller-Newen, G., Roche, C., Gu, Z.J., Clement, C., and Klein, B. (1995). Interleukin-6 signal transducer gp130 has specific binding sites for different cytokines as determined by antagonistic and agonistic anti-gp130 monoclonal antibodies. Eur J Immunol *25*, 3474-3481.
Wojtal, K.A., Rogler, G., Scharl, M., Biedermann, L., Frei, P., Fried, M., Weber, A., Eloranta, J.J., Kullak-Ublick, G.A., and Vavricka, S.R. (2012). Fc gamma receptor CD64 modulates the inhibitory activity of infliximab. PLoS One *7*, e43361.
Wong, P.K., Egan, P.J., Croker, B.A., O'Donnell, K., Sims, N.A., Drake, S., Kiu, H., McManus, E.J., Alexander, W.S., Roberts, A.W., and Wicks, I.P. (2006a). SOCS-3 negatively regulates innate and adaptive immune mechanisms in acute IL-1-dependent inflammatory arthritis. J Clin Invest *116*, 1571-1581.
Wong, P.K., Quinn, J.M., Sims, N.A., van Nieuwenhuijze, A., Campbell, I.K., and Wicks, I.P. (2006b). Interleukin-6 modulates production of T lymphocyte-derived cytokines in antigen-induced arthritis and drives inflammation-induced osteoclastogenesis. Arthritis Rheum *54*, 158-168.
Wormald, S., and Hilton, D.J. (2004). Inhibitors of cytokine signal transduction. J Biol Chem *279*, 821-824.

Yang, L.S., Alex, G., and Catto-Smith, A.G. (2012). The use of biologic agents in pediatric inflammatory bowel disease. Curr Opin Pediatr *24*, 609-614.

Yang, X.P., Albrecht, U., Zakowski, V., Sobota, R.M., Haussinger, D., Heinrich, P.C., Ludwig, S., Bode, J.G., and Schaper, F. (2004). Dual function of interleukin-1beta for the regulation of interleukin-6-induced suppressor of cytokine signaling 3 expression. J Biol Chem *279*, 45279-45289.

Yasukawa, H., Ohishi, M., Mori, H., Murakami, M., Chinen, T., Aki, D., Hanada, T., Takeda, K., Akira, S., Hoshijima, M.*, et al.* (2003). IL-6 induces an anti-inflammatory response in the absence of SOCS3 in macrophages. Nat Immunol *4*, 551-556.

Yoshida, K., Taga, T., Saito, M., Suematsu, S., Kumanogoh, A., Tanaka, T., Fujiwara, H., Hirata, M., Yamagami, T., Nakahata, T.*, et al.* (1996). Targeted disruption of gp130, a common signal transducer for the interleukin 6 family of cytokines, leads to myocardial and hematological disorders. Proc Natl Acad Sci U S A *93*, 407-411.

Yoshida, Y., Kumar, A., Koyama, Y., Peng, H., Arman, A., Boch, J.A., and Auron, P.E. (2004). Interleukin 1 activates STAT3/nuclear factor-kappaB cross-talk via a unique TRAF6- and p65-dependent mechanism. J Biol Chem *279*, 1768-1776.

Zhang, J.G., Farley, A., Nicholson, S.E., Willson, T.A., Zugaro, L.M., Simpson, R.J., Moritz, R.L., Cary, D., Richardson, R., Hausmann, G.*, et al.* (1999). The conserved SOCS box motif in suppressors of cytokine signaling binds to elongins B and C and may couple bound proteins to proteasomal degradation. Proc Natl Acad Sci U S A *96*, 2071-2076.

Zohlnhofer, D., Graeve, L., Rose-John, S., Schooltink, H., Dittrich, E., and Heinrich, P.C. (1992). The hepatic interleukin-6 receptor. Down-regulation of the interleukin-6 binding subunit (gp80) by its ligand. FEBS Lett *306*, 219-222.

7 ATTACHMENT

7.1 List of figures

7.2 List of tables

7.3 Curriculum vitae

Persönliches

Name	Nora Honke
Geboren	04.06.1983 in Herdecke
Familienstand	ledig
Staatsangehörigkeit	deutsch

Ausbildung

Universitätsklinikum der RWTH Aachen **Aachen, Deutschland**
Promotionsstudium *seit 10/2009*

- Promotion im Forschungslabor der Klinik für Kinder- und Jugendmedizin
- Titel der Doktorarbeit: „The regulation of gp130 surface expression on monocytes – implications in chronic inflammation"

RWTH Aachen **Aachen, Deutschland**
Studium der Biologie *10/2005 – 08/2009*

- Abschluss: Diplom Biologin
- Titel der Diplomarbeit: ,,Substrate von PARP10: Die Regulation des NF-κB-Signalwegs"

University of Reading **Reading, England**
Auslandsstudium *10/2004 – 03/2005*

Heinrich-Heine-Universität Düsseldorf **Düsseldorf, Deutschland**
Studium der Biologie *10/2002 – 09/2005*

- Abschluss des Vordiploms

Carl-Fuhlrott-Gymnasium **Wuppertal, Deutschland**
Schulausbildung *08/1993 – 06/2002*

- Erlangen der Allgemeinen Hochschulreife

7.4 Publications

Parts of this study were accepted for publication:

Honke N, Ohl K, Wiener A, Peitz J, Di Fiore S, Fischer R, Wagner N, Wüller S, Tenbrock K
The p38-mediated rapid downregulation of cell surface gp130 expression impairs IL-6 signaling in the synovial fluid of childhood arthritis patients. (2013) Arthritis & Rheumatism

Other publications:

Lippe R, Ohl K, Varga G, Rauen T, Crispin JC, Juang YT, Kuerten S, Tacke F, Wolf M, Roebrock K, Vogl T, Verjans E, Honke N, Ehrchen J, Foell D, Skryabin B, Wagner N, Tsokos GC, Roth J, Tenbrock K.
CREMα overexpression decreases IL-2 production, induces a TH17 phenotype and accelerates autoimmunity. (2012) J Mol Cell Biol

Eberhardt C, Haas J, Girschick H, Schwarz T, Morbach H, Rösen-Wolff A, Foell D, Dannecker G, Schepp C, Ganser G, Honke N, Eggermann T, Müller-Berghaus J, Wagner N, Tenbrock K
Association of IL-12p40 pro 1.1 polymorphism with clinical subtypes of JIA. (2013) Arthritis Research & Therapy (submitted)

7.5 Acknowledgement

First of all, I want to thank PD Dr. med. Klaus Tenbrock for giving me the opportunity to carry out my PhD thesis at the department of pediatrics and for his supervision. He was always accessible for my concerns and supported me with helpful discussions and numerous ideas.

I would like to thank Prof. Dr. Rainer Fischer, who kindly agreed to be my second reviewer. This gave me the opportunity to carry out my PhD thesis in cooperation with the medical faculty. Special thanks also for the offer to make use of the imaging facility of the Fraunhofer institute.

Many thanks go to Stefano Di Fiore for his competent support in the imaging sessions.

I would also like to thank Hildegard Schmitz-van de Leur for excellent technical assistance in all cloning procedures. Thanks to Dr. med. Stefan Wüller for giving me the opportunity to work at this interesting project.

Furthermore, I would like to thank the whole laboratory team of the department of pediatrics for their support and the nice working atmosphere. This includes: Dr. rer. nat. Kim Ohl, Anastasia Wiener, Jeff Bierwagen, Dr. rer. nat. Stephan Dreschers, Dr. rer nat. Angela Schippers and Dr. rer. nat. Thomas Clahsen.

I thank my family and my friends, who supported me during the complete time of this thesis. Very special thanks to my boyfriend Thomas for all his patience and for his optimistic character always encouraging me to stay focused.